



THE HONG KONG
POLYTECHNIC UNIVERSITY

香港理工大學

Pao Yue-kong Library

包玉剛圖書館

Copyright Undertaking

This thesis is protected by copyright, with all rights reserved.

By reading and using the thesis, the reader understands and agrees to the following terms:

1. The reader will abide by the rules and legal ordinances governing copyright regarding the use of the thesis.
2. The reader will use the thesis for the purpose of research or private study only and not for distribution or further reproduction or any other purpose.
3. The reader agrees to indemnify and hold the University harmless from and against any loss, damage, cost, liability or expenses arising from copyright infringement or unauthorized usage.

IMPORTANT

If you have reasons to believe that any materials in this thesis are deemed not suitable to be distributed in this form, or a copyright owner having difficulty with the material being included in our database, please contact lbsys@polyu.edu.hk providing details. The Library will look into your claim and consider taking remedial action upon receipt of the written requests.

**STUDIES OF SHAPE MEMORY
POLYMERS WITH NOVEL FUNCTIONS**

WU YOU

Ph.D

The Hong Kong Polytechnic University

2015

CERTIFICATE OF ORIGINALITY

THE HONG KONG POLYTECHNIC UNIVERSITY

INSTITUTE OF TEXTILES AND CLOTHING

**STUDIES OF SHAPE MEMORY
POLYMERS WITH NOVEL FUNCTIONS**

WU YOU

A THESIS SUBMITTED

IN PARTIAL FULFILMENT OF THE REQUIREMENTS

FOR THE DEGREE OF DOCTOR OF PHILOSOPHY

December 2014

CERTIFICATE OF ORIGINALITY

I hereby declare that the thesis entitled “**Studies of Shape Memory Polymers with Novel Functions**” which is submitted to The Hong Kong Polytechnic University, Hong Kong for the award of Doctor of Philosophy is my own work and that, to the best of my knowledge and belief, it reproduces no material previously published or written, except where due acknowledgement has been made in the text. The matter embodied in this dissertation has not been submitted for the award of any other degree or diploma.

(Signature)

WU You _____ (Name of student)

ABSTRACT

Shape memory polymers (SMPs) are a class of smart materials whose shape could change with external stimuli. They have been widely used in terms of form, stimuli, structure and applications. Recently, developing SMPs with additional functions has drawn increasing attention. This project is focused on the research of functional SMPs with novel molecular strategies, including multi-responsive chromic behavior, stress-free two way shape memory effect, light/heat dual sensitive triple shape memory effect and supra-SMPs with moisture management applications.

A new multi-functional SMP which can memorize both shapes and colors responsive to different stimuli by was fabricated by covalently connecting the aggregation induced emission (AIE)-active dye to a polymer. The color of the polymer is responsive to its memory properties such as the original and temporary shapes, shape recovery, associated stimuli including solvent and transition temperature. The outcome polymer displayed excellent shape memory effect and fluorescent response to mechanical stress, temperature and solvent.

Furthermore, a new molecular strategy for two-way shape memory polymers (TWSMPs) was studied. TWSMPs or reversible shape memory polymers are one of the most promising smart materials because of their potential applications as artificial muscle, actuators, sensors etc. None of current methods could realize reversible shrinkage without external tensile at ambient temperature. It is hoped that the issue can be solved by a simple method, which is employing an interpenetrating polymeric network (IPN) with elastomeric network and crystalline network. Thus, a series of polymers with UV-

crosslinked crystalline segment and thermal-crosslinked elastomeric segment as IPNs were constructed and their possibilities for two-way shape memory effect were further explored. This work demonstrated a simple way of fabricating stress-free TWSMPs with T_{trans} around 40 °C and a maximum shape changing ratio around 6% (close to shape memory alloy).

In addition, a facile approach was employed to fabricate Light/heat dual-responsive triple shape memory polymer (SMP) by simply mixing $\text{Zn}(\text{Mebip})_2(\text{NTf}_2)_2$, a metallosupramolecular unit formed by coordinate 2,6-bis(N-methyl benzimidazolyl)-pyridine (Mebip) ligands to Zinc di[bis(trifluoromethylsulfonyl)-imide] ($\text{Zn}(\text{NTf}_2)_2$), or Gold Nanoparticles (AuNPs) into one part of epoxy resin. Also thanks to the light-heat transfer nature of $\text{Zn}(\text{Mebip})_2(\text{NTf}_2)_2$ and segmented material structure, the outcome polymer displayed UV sensitivity to composite part, while leaving the shape of neat SMP part unchanged under UV source (solely thermal sensitive).

Later, a series of SMPs with supra-molecular switches were fabricated by employing pyridine into polymer backbone as proton acceptors. Various proton donors, like the neat SMPs and poly(4-vinylphenol) were blended into the supra-SMPs. Unlike previously reported thermal responsive water vapor permeability, the current work was focused on the moisture responsive water vapor permeability. The out-come Supra-SMP displayed RH-dependent WVP behavior, which is, at low RH, the Supra-molecular switches are closed, leading to a low WVP. When at high RH (say, higher than 65%), the WVP of the supra-SMPs increased dramatically. The mechanism of moisture sensitive WVP was further proved by FTIR. Such RH dependent WVP displayed the potential

applications as moisture management materials in packaging and textiles
industrials.

PUBLICATIONS**REFERRED JOURNAL PAPERS**

1. You WU, Jinlian HU*, Jianping HAN et al. Two-way Shape Memory Polymer with “Switch–Spring” Composition by Interpenetrating Polymer Network. **Journal of Materials Chemistry A**, 2014, 2, 18816.
2. You WU, Jinlian HU, Huahua HUANG et al. Memory Chromic Polyurethane with Tetraphenylethylene. **Journal of Polymer Science, Part B: Polymer Physics**. 2014, 52, 104-110.
3. You WU, Jinlian HU*, Cuili ZHANG et al. A Facile Approach to UV/Heat Dual-Responsive Triple Shape Memory Polymer. **Journal of Materials Chemistry A**, 2015 (In press)
4. Cuili ZHANG, Jinlian HU* and You WU. Theoretical studies on hydrogen-bonding interactions in hard segments of shape memory polyurethane-III: Isophorone diisocyanate. **Journal of Molecular Structure**, 2014, 1072, 13.
5. Cuili ZHANG, Jinlian HU* and You WU. Hydrogen-Bonding Interactions in Hard Segments of Shape Memory Polyurethane: Toluene Diisocyanates and 1,6-Hexamethylene Diisocyanate – A Theoretical and Comparative Study. **The Journal of Physical Chemistry A**. (In press)
6. You WU, Jinlian HU* and Cuili ZHANG. Moisture Management of Supramolecular Shape Memory Polyurethane. (Submitted)

PATENTS

1. Jinlian HU, You WU. A Two-Way Shape Memory Polymer by Interpenetrating Polymer Network. China Patent, Application No.

201410234045.5.

2. Jinlian HU, You WU. Two-Way Shape Memory Polymer Composite Material And Preparation Method Thereof. US Patent. Application No. 14/453,687.

CONFERENCE PAPER

1. You WU, Jinlian HU,* Huahua HUANG et al. Construction of Stress-Free Two Way Shape Memory Polymer by Interpenetrating Polymer Network. 6th ECCOMAS Conference on Smart Structures and Materials, SMART2013, Politecnico di Torino, Italy 24-26 June 2013. Oral Presentation.
2. You WU, Jinlian HU,* Cuili ZHANG. Two-Way Shape Memory Polymer with “Switch-Spring” Composition by Interpenetrating Polymer Network. Cross-Straits Conference on Textiles 17-19 Dec 2014, Hong Kong. Oral Presentation.
3. Y. WU, J. HU* and Y. ZHU. Memory Chromic Polyurethane with Tetraphenylethylene. Cross-Straits Conference on Textiles 17-19 Dec 2014, Hong Kong. Oral Presentation.

ACKNOWLEDGEMENT

I am greatly indebted to my chief supervisor Professor Jinlian Hu, Institute of Textiles and Clothing, The Hong Kong Polytechnic University. It is impossible to finish this doctoral dissertation in time without her support, valuable guidance and insightful suggestions. Working under her guidance has enriched both of my academic and industrial experience and it will always be an unforgettable memory for the rest of my life. I am always inspired by her encouragement, support, direction, inspiration, enlightening guidance and kindness. I would also express my acknowledgement to my co-supervisor, Prof. Benzhong Tang, Department of Chemistry, The University of Science and Technology of Hong Kong, for his generous support and suggestion on my work.

I would like to acknowledge the labmates that worked in Prof. Hu's group with me during past 4 years. Special thanks go to Dr. Yong Zhu, Dr. Huahua Huang, Mr. Jianping Han, Dr. Bipin Kumar, Dr. Cuili Zhang, Ms. Susanna Li, Mr. Lin Tan, Dr. Jing Lv, Dr. Kenneth Yeung, Dr. Pengqing Liu, Dr. Yan Pang, Dr. Hongsheng Luo, Mr. Wenguo Li, Mr. Harish Kumar, Ms. Ruiqi Xie, Ms. Chenyan Shen, Ms. Jun Zhang, Ms. Chang Gao, Mr. Jianming Chen, Mr. Yifu Wang, Dr. Xueliang Xiao, Dr. Yanxiong Pan, Mr. Ziqing Cai and Dr. Yijun Liu for their unconditional help and unforgettable memories we shared. I want to extend my thanks to other group members not mentioned here. I will cherish the study and working experience together with faithful friendship forever. I will express my acknowledgement to my roommates Wenjun Xu,

Dalu Fang, Junlong Zhang, Linrong Liao, with whom I shared unforgettable memories.

Special thanks will go to my grandparents and parents for their selfless support and understanding which lead me to finish all my degrees.

TABLE OF CONTENTS

LIST OF ABBREVIATIONS	X
CHAPTER 1 INTRODUCTION.....	1
1.1. General Introduction of SMPs.....	1
1.2. General Introduction of Functional SMPs	3
1.2.1. Memory Chromic SMPs	3
1.2.2. Two-Way SMPs.....	5
1.2.3. Light induced SMPs.....	8
1.2.3. Water induced SMPs.....	11
1.2.4. Water Vapor Permeability of SMPs	12
1.3. Objectives of the Project	14
1.3.1. Chromic SMP with novel AIE dyes.....	15
1.3.2. Stress-free two-way shape memory polymer by interpenetrating polymeric network	15
1.3.3. Light induced shape memory polymer	16
1.3.4. Shape memory polymer with supra-molecular switches	16
1.4. Significance.....	16
CHAPTER 2 LITERATURE REVIEW.....	21
2.1. Introduction to the shape memory polymers	21
2.2. Molecular Mechanism of Shape Memory Polymers.....	23
2.2.1. One-way Dual-Shape Memory Polymer.....	24
2.2.2. Two-way Dual-Shape Memory Polymers	25
2.2.3. Triple Shape Memory Polymers	33
2.2.4 Multiple Shape Memory Effects.....	41
2.3. Functional Shape Memory Polymers	42
2.3.1. Stress-Free/Free Stand Type 2WSMP	43
2.3.2. Tunable Transparency.....	49
2.3.3. Tunable Water Vapor Permeability	51
2.3.4. Tunable Stiffness	52
2.4. Supra-molecular Shape Memory Polymers.....	67
CHAPTER 3 EXPERIMENTAL	74
3.2 Preparation of Functional SMPs	77
3.2.1 Synthesis of Memory Chromic SMPUs Films	77
3.2.2 Preparation of stand-free two-way shape memory polymers by interpenetration network	79
3.2.3 Preparation of Light/Heat dual sensitive SMP nanocomposites.....	81
3.2.4 Preparation of SMPUs with supra-molecular switches for moisture management	83
3.3 Characterization techniques	85
3.3.1 Molecular weight test.....	85
3.3.2 FTIR spectrometry	85
3.3.3 Melt flow index.....	86
3.3.4 Mechanical property test.....	86
3.3.5 Shape memory effect test of SMPs.....	87

PL spectra were recorded on a SLM 8000C spectrofluorometer. Laser pulses of 343 nm were employed as the excitation light source for the PL

measurements. The time-resolved PL measurements was carried out according to the literature[127].....	88
3.3.7 Shape recovery stress test	88
3.3.8 Differential scanning calorimetry	89
3.3.9 X-ray diffraction	89
3.3.10 Dynamic mechanical analysis.....	89
3.3.11 Atomic force microscopy.....	90
3.3.12 Polarizing optical microscopy.....	90
3.3.13 Scanning electron microscopy	91
3.3.15 Cytotoxicity test.....	91
3.3.16 Water vapor permeability	92
CHAPTER 4 MEMORY CHROMIC POLY-URETHANE WITH TETRAPHENYLETHYLENE.....	93
4.1. Introduction.....	93
4.2. Polymer Design.....	95
4.3. Results and discussion.	96
4.4. Summary.....	110
CHAPTER 5 TWO-WAY SHAPE MEMORY POLYMER BY INTERPENETRATING POLYMER NETWORK.....	112
5.1. Introduction.....	112
5.2. Statement of problem and polymer design.....	113
5.3. Results and discussions.....	117
5.4 Summary.....	128
CHAPTER 6 A FACILE APPROACH TO LIGHT/HEAT DUAL SENSITIVE TRIPLE SHAPE MEMORY POLYMER	129
6.1 Introduction.....	129
6.2 Polymer design	132
6.3 Results and discussions.....	134
6.4 Summary.....	143
CHAPTER 7 SUPRA-MOLECULAR SHAPE MEMORY POLYMER FILM FOR MOISTURE MANAGEMENT.....	145
7.1 Introduction.....	145
7.2 Polymer design	149
7.3 Results and discussions.....	150
7.4 Summary.....	158
CHAPTER 8 CONCLUSIONS AND SUGGESTIONS FOR FUTURE WORK	160
8.1 Conclusions.....	160
8.1.1. General functional SMPs	160
8.1.2. Memory chromic SMPs	160
8.1.3. Two-way SMPs by interpenetrating polymeric network	161
8.1.4. Light/heat dual sensitive triple shape memory polymer	162
8.1.5. Supra-molecular shape memory polymer for moisture management	163
8.2. Suggestions for future work.....	163
8.2.1. Memory chromic SMPs	163
8.2.2. Two-way shape memory fibers.....	164
8.2.3. Supra-molecular shape memory polymers.....	164

LIST OF ABBREVIATIONS

AFM	Atomic force microscopy
BDO	1,4-butanediol
DMA	Dynamic mechanical analysis
DMAc	N,N-dimethylacetamide
DMF	N,N-dimethylformamide
DSC	Differential scanning calorimetry
FTIR	Fourier transform infrared spectroscopy
FWHM	Full width at half maximum
HPLC	High performance liquid chromatography
IPDI	Isophorone diisocyanate
IPN	Interpenetrating polymer network
MDI	4,4-diphenylmethane diisocyanate
MFI	Melt flow index
PCL	Poly(ϵ -caprolactone)
PEG	Polyethylene glycol
POM	Polarizing optical microscopy
PTMEG	Poly(oxytetramethylene)glycol
SAXS	Small-angle X-ray scattering
SEM	Scanning electron microscopy
SMA	Shape memory metallic alloy
SME	Shape memory effect
SMP	Shape memory polymer
SMPU	Shape memory polyurethane
TEM	Transmission electron microscopy
WVP	Water vapor permeability
XRD	X-ray diffraction

LIST OF SYMBOLS

Symbol	Definition	Unit
ΔH	Enthalpy data	J/g
2θ	Bragg's angle	°
E'	Elastic modulus	Pa, cN/dtex
M_n	Number average molecular weight	Dalton
M_w	Weight average molecular weight	Dalton
$R_f(N)$	Fixity ratio at the N^{th} cycle	%
$R_r(N)$	Recovery ratio at the N^{th} cycle	%
$R_{r\text{-tot}}$	Total recovery ratio after the N^{th} cycle	%
$\text{Tan } \delta$	Loss tangent	
T_c	Crystallizing temperature	°C
T_g	Glass transition temperature	°C
T_{low}	A temperature below T_{trans}	°C
T_m	Melting transition temperate	°C
T_{trans}	A lower phase transition temperature	°C
ϵ_m	The maximum strain in the cyclic tensile tests	%
$\epsilon_p(N)$	The residual strain after recovery in the N^{th} cycle	%
ϵ_u	The strain after unloading at T_{low}	%
σ_m	The maximum stress at the maximum strain ϵ_m .	MPa, cN/dtex
τ	Apparent shear stress	Pa

LIST OF FIGURES

Figure 1.1. General shape memory effect. (http://ashbygroup.web.unc.edu/shape-memory/)	2
Figure 1.2. General molecular mechanism of shape memory effect [1].....	2
Figure 1.3. Category of polymeric shape memory effect. (Ref: Hu JL, et. Progress in Polymer Science 37 (2012) 1720–1763).....	3
Figure 1.4. Aggregation induced emission effect of TPE.[2].....	5
Figure 1.5. Illustration of mechanism of TWSMPs. (from top to bottom, LCEs, lamination structure and semi-crystalline switch)	7
Figure 1.6 A film of grafted polymer BHCA	9
Figure 1.7. Snap shots of infrared light-induced shape recovery of SMP nanocomposite incorporated with 4 wt.% boron nitride and 4 wt.% CNTs.	11
Figure 1.8. The shape <u>memory</u> effect of SM-PVA in water at room temperature. (I) The permanent shape “SMP”, (II) the deformed shape, (III) the shape recovery in water.	12
Figure 1.9. Change™ functions similarly to a pine, spruce or fir cone. (http://www.textileworld.com/Articles/2006/October/Quality_Fabric_Of_The_Month/Climate_Change-An_Open_And_Shut_Case)	13
Figure 2.1. Figure of different applications of shape memory polymers in textiles, biomedical and aerospace applications. 1) A fabric modified by shape memory polyurethane, the upper is permanent shape, the middle is deformed shape and the under is recovered shape upon stimulus. 2) Biodegradable suture based on SMPs, the suture shrink upon heating to proper temperature. 3) Model for cardiovascular stents based on biodegradable SMPs, the stent recover to its origin shape after 100s at proper temperature. 4) Catheter based on SMPs.[1, 24-26].....	21
Figure 2.2. General molecular mechanism of shape memory effect, the figure is the basic unit of SMPs, the purple spot display as net-point and the black box means variety of switch.[1]	23
Figure 2.3. Illustration of SMPs according to their memory properties	24
Figure 2.4. Photo-induced two-way SME observed in azobenzene- containing LCEs [43].....	30
Figure 2.5. Two-way SME observed in SMPU laminated composites[13]32	
Figure 2.6. Illumination of different category of currently reported triple- shape memory polymers [57-61]	34
Figure 2.7. Polymeric network architecture of (a) MACL, (b) CLEG, and (c) PDCL network (Color codingsin MACL and CLEG networks are as follows: green, PCHMA segments; red, PCL segments; blue, PEG side chains; gray, cross-links. In PDCL network: green, PPD segments; yellow, PCL segments)[3, 61]	35
Figure 2.8. Series of photographs of the polymer sample showing a photoinduced multifunctional shape memory. The permanent shape A was irradiated by UV light at $\lambda=280-450$ nm for 20 s to form shape B. Upon being deformed by an external load to the screw shape at 70 oC and cooled/fixd at room temperature, shape C was fixed. Shape D, which is the same as shape B, was recovered by heating again to 70oC.	

Shape A was recovered by irradiation with a low-pressure Hg lamp at $\lambda=250$ nm for 180 minutes. [74]	39
Figure 2.9. (A) Illustration of composition of SMPs and shape recovery routes (from shape #1 to the permanent shape). (B) Molecular structure of $\text{Zn}(\text{Mebip})_2(\text{NTf}_2)_2$. (C) Differential scanning calorimetry results of the second heating curve of each part of the SMP. (D) Temperature–time relationship of each region under UV irradiation. [73]	40
Figure 2.10. Quadruple-shape memory properties of PFSA (a. Visual demonstration. S0: permanent shape; S1: first temporary shape (T_{d1} :140°C); S2: second temporary shape (T_{d1} :107°C); S3: third temporary shape (T_{d3} : 68°C). b. Quantitative thermal mechanical cycle)[77]	42
Figure 2.11 Schematic illustration of mechanism of free stand 2WSME..	43
Figure 2.12. Schematic illustration of free-stand 2WSME by Lendlein. [16]	45
Figure 2.13. Interplay of reversible and irreversible shape-memory processes. [85].....	47
Figure 2.14. Molecular illustration of stress-free 2WSME by new molecular strategy, which is an interpenetrating network (IPN) with elastomeric and crystalline components leading to a "switch-spring" composition [86]	48
Figure 2.15. Illustration of in situ wide-angle X-ray scattering gave evidence for progressive growth of oriented crystallites during cooling and second heating curve of sample in DSC. [87].....	49
Figure 2.16. optical tests for the fluorogels of different compositions. Samples of 1 mm thickness were prepared for all the optical measurements. c) Demonstration of the shape-memory behavior of PFOEA-95: 1 and 2) converting a rigid film (white) to a soft and flexible (transparent) film upon heating with a heat gun; 3 and 4) twisting a soft film and keeping the shape when cooling down; 5 and 6) recovering the original shape upon heating. (copy write permission from [88]).....	50
Figure 2.17. Water vapor permeability of SMPU coated fabrics. (copyright permission from [89])	52
Figure 2.18. Relationship between the elastic modulus and the temperature of the SMP. [90].....	53
Figure 2.19. Application of blood to bare and FC-70-swollen PFOEA-50 fluorogels: time lapse images show blood sliding on swollen fluorogels and pinning and streaking on bare fluorogels. [88]	55
Figure 2.20. Schematic of a mixed state of Wenzel and Cassie–Baxter. [93]	56
Figure 2.21. Wettability of SMP pillar arrays. (a) Static water contact angles of straight pillars (circles for square array and squares for hexagonal array) and deformed pillars (diamonds for $AR = 2$ and triangles for $AR = 3$) and theoretical prediction (lines) by the Cassie–Baxter and Wenzel models. (b) Experimental sliding angles (circles) vs. the theoretical ones according to Equation 7 (---) Equation 9 (...) and Equation 10 (—), respectively. (c) Anisotropic wetting on the deformed sample 5, from left to right: top-view optical image of the	

deformed pillar array with illustration of the direction the droplet being viewed on the deformed pillars; droplet viewed perpendicularly to the deformed pillars; water viewed in parallel to the deformed pillars; the droplet on the original SMP pillars. [92]	57
Figure 2.22. Simplified working principle of thermo-reversible color changes in microencapsulated T-PIGs: the polymeric microcapsules remain in a colored state as long as the solvent does not inhibit electronic interaction between color former and developer. Multifunctional QR code carriers at 23 °C (a), 60 °C (b) and 23 °C (c). The QR codes were consistently machine-readable below CST (a and c) and unreadable above CST (b). [95]	59
Figure 2.23. A model to illustrate the molecular mechanism during, stretch-recovery process (1), heating-cooling process (2), solvent-dry process (3), and solvent induced shape recovery process (4).	60
Figure 2.24. (a) Schematic illustration of the setup for localized light exposure. Diameter of the hole in the mask is 5 μm. (b–d) Optical images of SMP-AuNR (SMP-4) micropillars at different stages. (b) Pristine pillars. (c) The right half of the sample was deformed and became opaque. (d) SMP sample in (c) after laser exposure. The white circle indicates the exposed region. [98]	61
Figure 2.25. Shape deformation and recovery of an SMP hologram. Optical images of the a) original, b) deformed, and c) recovered hologram under white light illumination. Topographic AFM images of the d) original, e) deformed, and f) recovered holographic structure. The corresponding height profiles are shown below (g–i). [101]	63
Figure 2.26. Scheme of the protocol followed for the grating imprint on the PDDC-HD elastomer surface (a) and study of its programmable shape-memory properties either varying the lattice parameter (b) or erasing the surface nanotopography (c). [102]	64
Figure 2.27 Synthesis routine of SMP containing UPy side-groups. [111]	70
Figure 2.28. Molecular model of SMPU with UPy switch [112]	71
Figure 2.29 Triple-shape memory polymer containing UPy unit. [113] ..	72
Figure 2.30. Schematic representation of the proposed chain structures...	73
Figure 3.1. Illustration of general synthesis procedure of SMPUs	78
Figure 3.2. Illustration for the polymerization of SMPUs with covalently connected TPE units.	79
Figure 3.3. Illustration of synthesis procedure of stand-free two-way shape memory polymers	81
Figure 3.4. Fabrication method of light/heat dual sensitive triple shape memory polymer.	83
Figure 3.5. Polymer structure of Supra-SMPs.	84
Figure 4.1. Chemical structure of tetraphenylethylene (The red part) unit used in Memory chromic Polyurethane	96
Figure 4.2. Second heating curve of differential scanning calorimetry (DSC) of the outcome polymer	98
Figure 4.3. Dynamic mechanic analysis of SMPU	98
Figure 4.4. Photoluminescent of TPE-diol crystalline.....	99
Figure 4.5. PL emission (excited at 343 nm) spectra of SMPU film with 0.1% wt TPE at different state (black line--original state, red line--stretched state and blue line--subsequently recovered state); demo of	

one film with 0.1%wt TPE under 365 nm UV lamp at different state.	101
Figure 4.6. Ultra-fast time-resolved fluorescent spectrometry.	101
Figure 4.7. PL emission spectra of SMPU films of SMPU and TPE as function of drawing ratio in stretched films.....	103
Figure 4.8. Emission intensity of SMPU with 0.1%wt TPE film (excited by 343 nm) at 479 nm at different shape fixity.....	103
Figure 4.9. Illustration of temperature dependent photoluminescent. All the samples are excited at 343nm UV light and recorded their emission intensity at 479nm for PL test.....	105
Figure 4.10. Intensity-Temperature relationship of SMPU.	105
Figure 4.11. Demonstration of temperature dependent photoluminescent. Related demos were recorded by immersing the polymer film into silica oil with different temperature under a UV lamp (excited by 365nm UV lamp).	106
Figure 4.12. Chemical sensitive photoluminescent. All the samples are excited at 343nm UV light and recorded their emission intensity at 479nm for PL test.....	107
Figure 4.13. Chemical sensitive photoluminescent of different cycles. ..	107
Figure 4.14. Demonstration of solvent induced shape recovery and chromic behavior. The polymer film 1 was first stretched 2 and then immersed into acetone 3 and then took out from solvent and wait till dry 4 at room temperature. The demos were recorded under a UV lamp (excited by 365nm UV lamp).	108
Figure 4.15. PL of SMPU immersed into acetone as a function of time.	108
Figure 4.16. Cytotoxicity test of SMPU.	109
Figure 4.17. A model to illustrate the molecular mechanism during, stretch- recovery process (1), heating-cooling process (2), solvent-dry process (3) and solvent induced shape recovery process (4).	110
Figure 5.1. Illustration of the synthesis and mechanism of the polymer network and two-way shape memory effect.	115
Figure 5.2. The general synthesis and programming process of IPNs.....	118
Figure 5.3. The demo of two-way shape memory effect of the polymer at different temperature.....	119
Figure 5.4. Differential scanning calorimetry of out-come samples.	121
Figure 5.5. The dynamic mechanical analysis (SS control) of different samples. The green lines represent the temperature, the blue lines represent the constant load (2mN) and the orange lines represent the thermomechanical analysis (change of the strain).....	125
Figure 5.6. The 1D-XRD of Sample C-1(left) and Sample 5(right).	127
Figure 5.7. Illustration of 2DXRD of the IPNs (S5 for example), the intensity at 21.4° vs. the azimuthal angle with Debye Scherrer reflections.....	127
Figure 5.8. Potential application of out-come polymer as artificial tendon.	127
Figure 6.1. Illustration of composition of SMP, shape recovery routes (from shape #1 to the permanent shape).	132
Figure 6.2. Molecular structure of Zn(Mebip) ₂ (NTf ₂) ₂	132
Figure 6.3. Differential scanning calorimetry of the second heating curve of each parts of the SMP.....	135

Figure 6.4. Temperature-time relationship of the each region under UV irradiation.....	136
Figure 6.5. Dynamic mechanical analysis and demonstration of triple-shape effect. (A) and (B) illustrated the elastic modulus and $\tan\delta$ of each SMP part.	137
Figure 6.6. The deformed sample (C_1) was exposed to UV source and heat sequentially, leading to temporary shape 2 (C_3) and permanent shape (C_4). C_2 is the IR image taken by a FLIR E55 IR camera from above of the sample when it was exposing to UV source.	138
Figure 6.7. SEM images of the SMP composites. A) SEM image of $Zn(Mebimpy)_2(NTf_2)_2$ -SMP at $\times 10000$ magnification.	139
Figure 6.8. TEM image of $Zn(Mebimpy)_2(NTf_2)_2$ -SMP.	139
Figure 6.9. EDX image of composite.	140
Figure 6.10. Illustration of molecular structure of AuNPs composites ...	141
Figure 6.11. The temperature-time relationship the SMP composite.	142
Figure 6.12. TEM of AuNPs part of composite.	142
Figure 6.13. The demonstration of a practical application of the outcome SMP as robot hands.	143
Figure 7.1. Schematic illustration of proposed supra-molecular SMP film as RH sensitive material and the molecular structure.	149
Figure 7.2. Demonstration of moisture induced shape memory effect....	151
Figure 7.3. WVP of Supra-SMP1 with different hard segment content (left) and different content of PVP (right).	153
Figure 7.4. WVP vs RH of Supra-SMP2 with (a) different ratio of proton donor, (b, c) different thickness of Supra-SMP2 and (d) with different type of proton donor at low thickness.	153
Figure 7.5. Illustration of change of hydrogen bonding in Supra-SMP2 by FTIR at low RH and high RH state.	155
Figure 7.6. Positron annihilation lifetime (τ_3) and intensity (I_3) of Supra-SMP2.	156
Figure 7.7. Modeling of hydrogen competition and proposed mechanism of RH sensitive WVP.	158
Figure 7.8. Schematic illustration of practical application of Supra-SMP2 as moisture management material in textile industrials.	158

LIST OF TABLES

Table 3.1 Raw materials used in the synthesis of SMPUs.....	74
Table 3.2 The main equipment used in the project.....	76
Table 3.3. Receptie of Supra-SMPs	84
Table 5.1. Recipes of IPNs with different ratio of PCL and PTMEG content.....	119
Table 5.2. The deformation rates from different temperature points.....	124
Table 7.1. Recipes of Supra-SMP 1 &2.....	150

CHAPTER 1 INTRODUCTION

1.1. General Introduction of SMPs

Study on shape memory polymers (SMPs) has been actively conducted for more than three decades. In recent years, the interest in this area has been intensified. Traditional thermal induced one-way two shape memory effect depends on the formation of well separated hard phase and soft phase with different transition temperature in the elastic network (see **Figure.1.1**). Generally, the transition temperature of switch (T_{C2}) is lower than that of net-point (T_{C1}). Thus the hard phases can act as net-points which determine the permanent shape and provide the inner force for recovery, while the soft phases act as the switches and reversibly immobilize the temporary shape. When the SMPs are deformed above T_{C2} and then cool down, the network will be fixed and the internal stresses are saved. Upon heating to T_{C2} or above, the internal stress will be released and enable the recovery of the polymer to the origin shape (or permanent shape). Indicated by **Figure 1.2**, either physical cross-linking or chemical cross-linking can act as net-point while the oligomers with proper glass transition, crystallization, liquid crystallization, supra-molecular hydrogen bonding, light-induced reversible network and percolating network in nano-composites can act as switches.

The technical significance of SMPs is becoming increasingly apparent in the application including packaging materials, assembling devices, textiles, membranes, biomedical materials as well as aerospace applications. To satisfy different requirements of variety applications, many research congregated

around the developing different functions like stimulus mechanism of shape memory effect, two-way shape memory polymers, triple-shape or multi-shape memory polymers and multifunctional shape memory polymers. Recently, different combinations of functionalities with shape memory properties were reported.

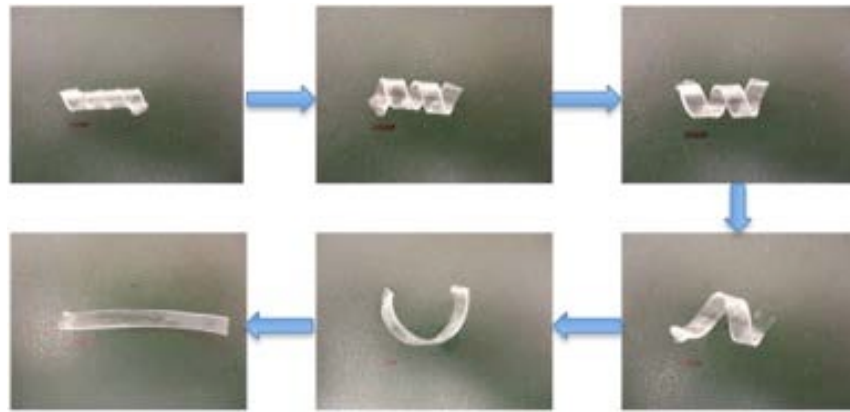


Figure 1.1. General shape memory effect.

(<http://ashbygroup.web.unc.edu/shape-memory/>)

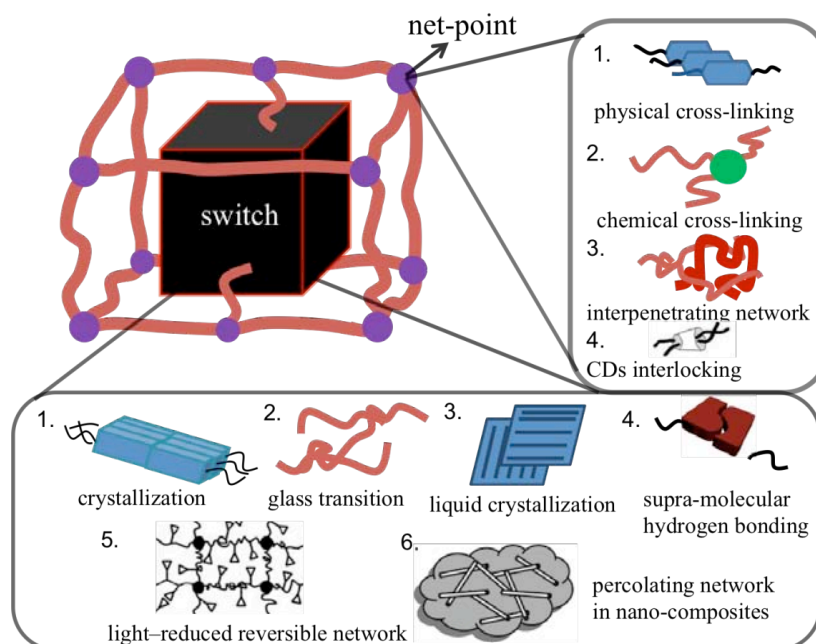


Figure 1.2. General molecular mechanism of shape memory effect [1]

1.2. General Introduction of Functional SMPs

Despite the intrinsic shape memory function of SMPs, the addition of extra function(s) to SMPs has drawn increasing research interest. Typical examples include biodegradability, luminescent, drug release, electronic sensitive, light sensitive, water sensitive, reversible SME, tunable transparency, multi-shape memory, stimuli-chromic and solvent sensitive et al. (see **Figure 1.3**) These functions can be related to its SME or be independent.



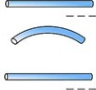
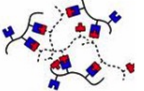

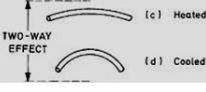
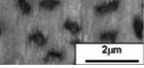
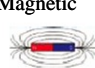


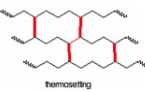


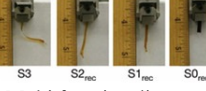
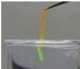
Polymerization & Crosslink	Composition & structure	Stimulus	Shape memory function
Polyaddition •Urea/urethane •Acrylate/acrylic	Block-copolymer 	Temperature 	One way SME 
Polycondensation •esterification1	Supramolecular polymer 	Electricity 	Two way SME 
Free-radical polymerization	Polymer blend / composite 	Magnetic 	1) Thermal sensitive
Photochemical polymerization	Polymer IPN/semi IPN 	Water sensitive 	2) Water sensitive
Radiation crosslink	Crosslinked Homopolymer 	Light/radiation 	3) Light sensitive
Acyclic diene metathesis polymerization		Oxidation-reduction 	4) Redox sensitive
Ring Opening Polymerization			Multi shape SME 
			Multi functionality 

Figure 1.3. Category of polymeric shape memory effect. (Ref: Hu JL, et. Progress in Polymer Science 37 (2012) 1720–1763)

1.2.1. Memory Chromic SMPs

As title suggested, memory chromic SMPs refer to a kind of polymer with chromic function and this function is associated with shape memory behavior,

say, shape change, shape fix and stimuli induced recovery. As far as we know, most report on memory chromic materials are based on cyano-(p-phenylenevinylene) derivatives by either physical mix or chemical connection with variety polymer matrix like linear low density polyethylene, poly(ethylene terephthalate), Thermoplastic polyurethanes, polycyclooctene, etc. Although such system exhibit relatively good effect as mechanosensor, the degree of elongation can not be detected quantitative in a large range.

Recently developed tetraphenylethene (TPE) and hexaphenylsilole (HPS) are a kind of building block for aggregation induced emission (AIE) effect. Unlike other fluorophores which suffer from aggregation-caused quenching (ACQ), the AIE units are non-emissive in solution and highly luminescent as aggregates. As shown in **Figure 1.4.** (a) & (b), PL spectra of diphenylated TPE (10 μM) in acetonitrile and water/acetonitrile mixtures (left picture) and plots of fluorescence quantum yields of TPE and diphenylated TPE vs compositions of the water/acetonitrile mixtures. (right picture) By increasing the water fracture into the solvent system, the TPE molecule begin to precipitate as nano or micro aggregation, thus emit strong light. Tang etc. demonstrate their viewpoint of this phenomenon as the phenyl rotators (whose free rotation could release the energy) are hindered in aggregation state by formation of π - π interaction. Such abnormal AIE effect have utilized in many fields like chemical sensor, explosive detection and biosensor, etc.

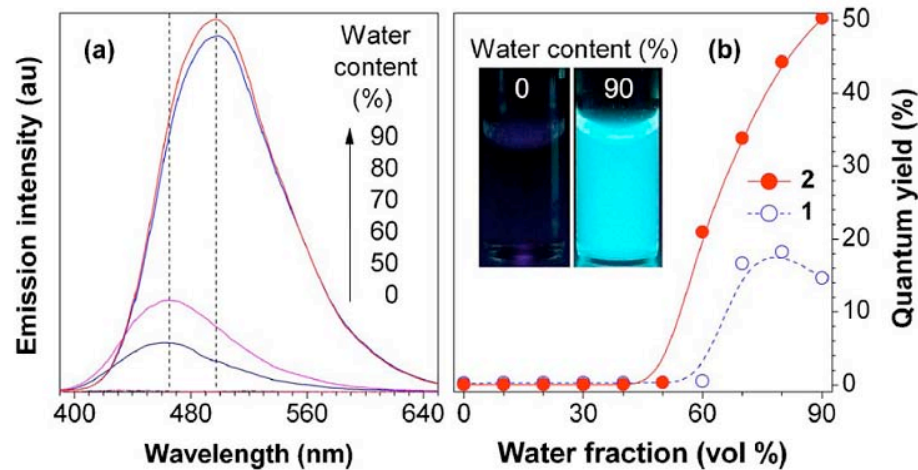


Figure 1.4. Aggregation induced emission effect of TPE.[2]

1.2.2. Two-Way SMPs

Two-way shape memory polymers (TWSMPs), or reversible shape memory polymers are one of the most promising smart materials because of their potential applications as artificial muscle, actuators, sensors etc.[3] When the SMPs are deformed above T_{trans} and then cool down, the soft-segment will be fixed and the internal stress is saved. Upon re-heating to T_{trans} or above, the internal stress will be released and enable the recovery of the polymer to its origin shape. [3-10] This shape will stay unchanged when dropping the temperature below transition temperature. However, TWSMPs could switch to previous shape when stimulus is over/reverse stimulus is applied. Currently there are three types of TWSMPs, liquid crystalline elastomers (LCEs) type,[11] semi-crystalline switch type [12] and laminated structure type.[13] For the LCEs, the molecular chain of LCEs generally adopt a prolate shape in the nematic state. If the crosslinking process takes place without any external intervention, the alignment of the prolate molecule is random, thus resulting in

an overall non-orientation nematic state which is called polydomain LCEs. When stretching is applied during the crosslinking process, a monodomain LCEs can be obtained, in which the director is aligned along the stretching direction. Thus the directed molecular morphology change below & above T_c contributes to the overall geometry change of the LCEs.[14] For semi-crystalline type, the Two-way shape memory effect (TWSME) is based on the cooling-induced elongation (CIE) and the melt induced contraction (MIC) of the semi-crystalline switch under a tensile load. With constant tensile, the soft-segment (semi-crystalline type) will grow into crystallites oriented along the stretching direction when cooling. While entropy driven contraction will occur when the soft-segment was melt above the transition temperature.[15] For laminated structure type, the TW-SME was achieved by combining pre-stretched SMPU layer and elastomer layer with adhesives. The SMPU layer provides the force for bending upon heating while the elastomer layer provides the force for recovery when cooling.[13] However, Each of these approaches has disadvantages. For LCEs, a high transition temperature is required and the synthesis procedure is relatively complicated. While for SMPs with semi-crystalline switch, the external force is essential. At the same time, the laminated architecture can only realize bending, although applicable for other complicated deformation, it can not realize reversible shrinkage. To our best knowledge, so far none of above mentioned methods could realise reversible shrinkage without external tensile at ambient temperature. Recently, Lendlein et al solved this problem by employing two kind of crystalline soft-segments in one polymeric network with proper programming process, which convert a normal tripe-shape memory polymer to a two-way shape memory polymer. The

key concept of their work is the separation of the shifting geometry determining function from the actuator function on the level of phase morphology, the actuator domains expand during cooling and collapse during heating in the direction determined by the shifting-geometry determining domains.[16]

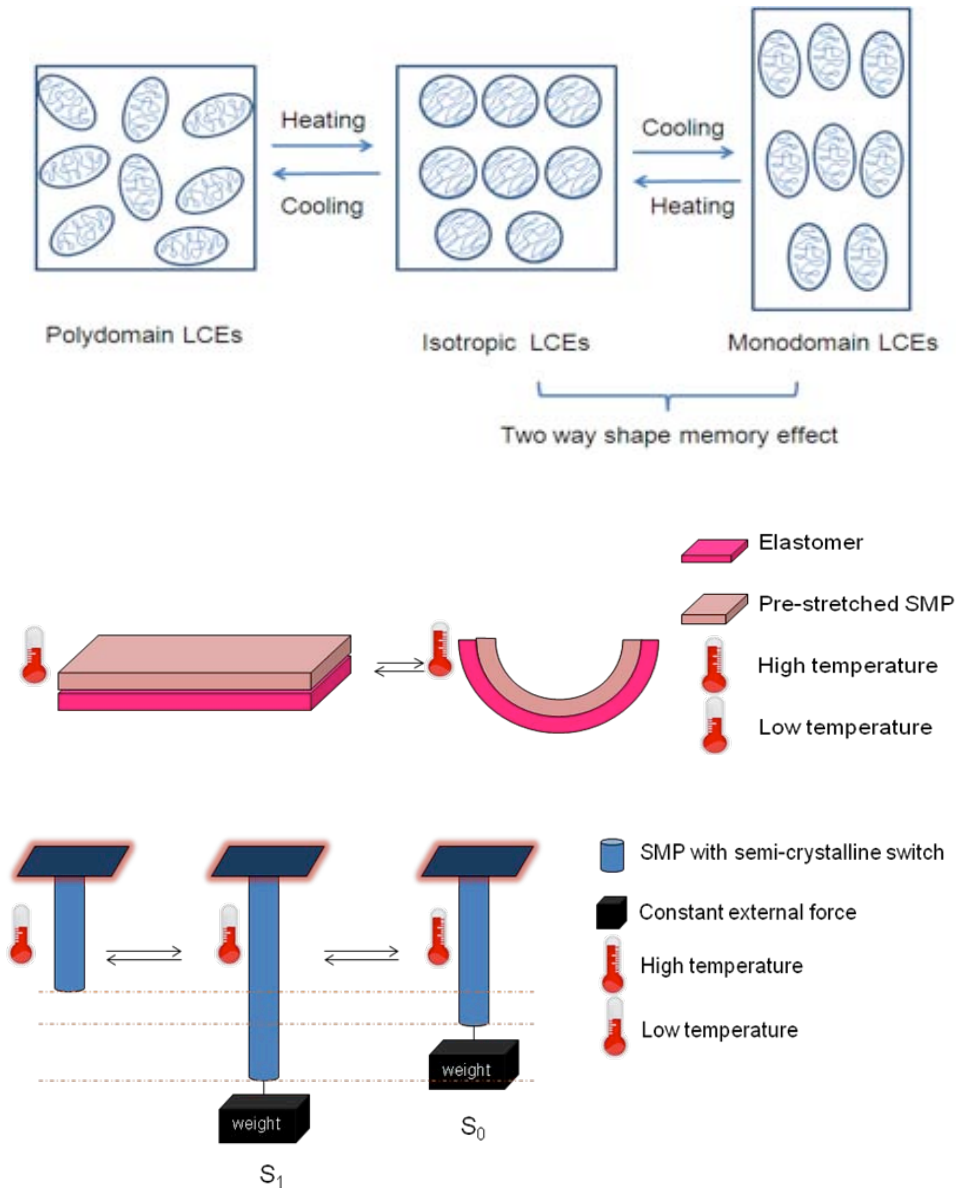


Figure 1.5. Illustration of mechanism of TWSMPs. (from top to bottom, LCEs, lamination structure and semi-crystalline switch)

1.2.3. Light induced SMPs

Photo-sensitive unit is the most popular molecular switch. Light is a clean energy and can be quickly, accurately and remotely activated. Therefore, photo-responsive shape memory polymers have attracted increasing interest. Lendlein et al.[17, 18] introduced the photosensitive cinnamic groups which serve as the molecular switches into polymer backbone and thus developed the light-sensitive SMPs (LSMPs) by. In this way, SMEs could be totally and independently induced from any temperature effect, rather through the use of light. Cinnamic groups are able to form covalent crosslinked bonds under a UV light of $\lambda > 260$ nm, however, these bonds could also be cleaved under different UV-light irradiations of $\lambda < 260$ nm[19]. These LSMPs displayed a high R_r but low R_f . The maximal R_f of the grafted polymers was only 52% when the strain was as high as 20%. The low R_f of LSMPs is attributed to the low efficiency of the cross-linked bondings from cinnamic units via light irradiation. Later after this work, a biodegradable LSMP composing of N,N-bis(2-hydroxyethyl) cinnamamide, Poly-(L-Lactic Acid) (PLLA) and PCL was synthesized by Wu et al. [20]. Compared to thermal-induced one-way dual shape SMPs, the strain fixity of light-responsive SMPs is relatively lower. However, the distinctive characteristics of LSMPs allow shape recovery at room temperature through remote activation, which should be more feasible for SMPs in medical and other real applications which high temperature is restricted.

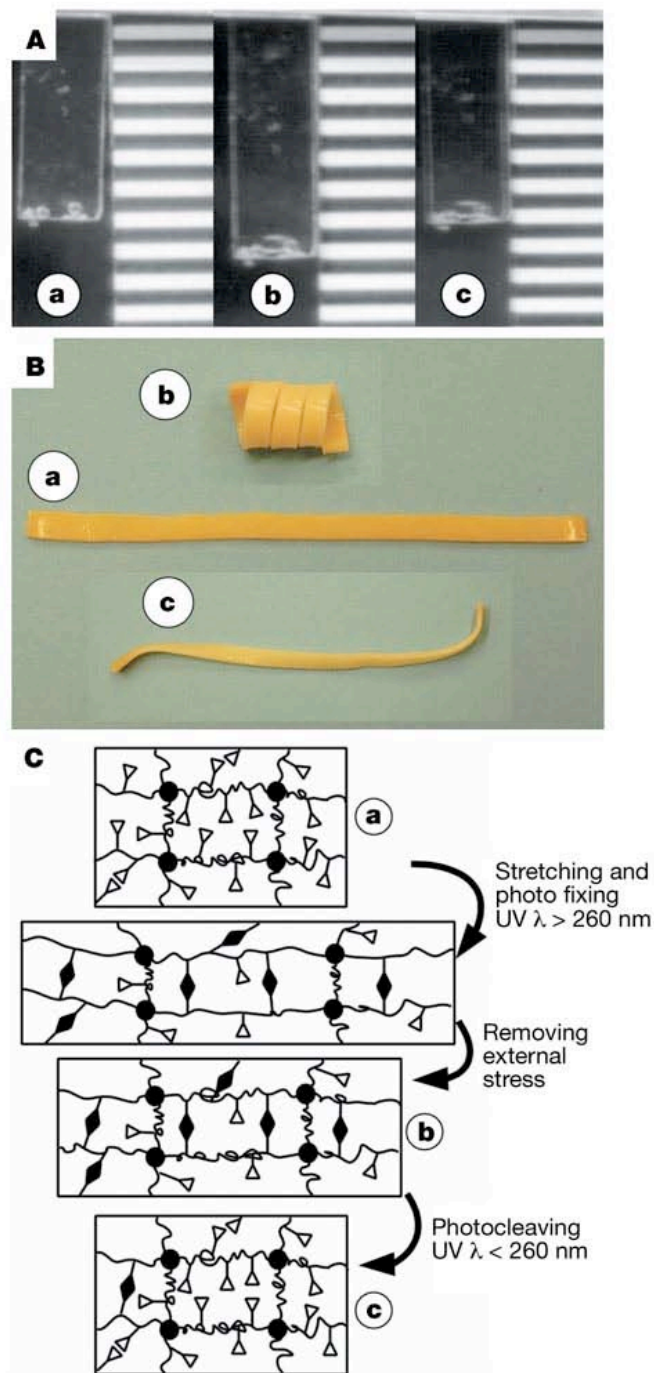


Figure 1.6 A film of grafted polymer BHCA .

a, Permanent shape (6 cm \times 1.2 cm \times 0.05 cm); b, temporary shape; c, recovered permanent shape. B, An IPN polymer film. a, Permanent shape (8 cm \times 0.4 cm \times 0.05 cm); b, corkscrew spiral temporary shape; c, recovered

shape obtained by irradiation with UV light of $\lambda < 260$ nm for 60 min. C, Molecular mechanism of shape-memory effect of the grafted polymer network: the chromophores (open triangles) are covalently grafted onto the permanent polymer network (filled circles, permanent crosslinks), forming photoreversible crosslinks (filled diamonds); fixation and recovery of the temporary shape are realized by UV light irradiation of suitable wavelengths.

Motivation of SMP nanocomposites in a remote way is attractive because of higher possibilities of application areas. Addition of CNTs or graphene into polymer matrix can be served as a facile approach to capture the infrared light for the composites, transferring the energy of the light into heat which further triggers the phase transitions of the polymers. Koerner et al. [21] dispersed CNTs (1-5 vol. %) into TPE uniformly, Upon exposure to the IR light, the internal temperature of the composites will be heated indirectly, leading to the melt of the polymer crystallites and thus remotely triggered the release of the shape recovery. Leng et al.[22] reported that a thermoset SMP filled with carbon nanoparticles and exhibited higher Rr and shape recovery speed as actuated by IR source in vacuum, compared to those SMPs without blendings. Similarly, Liang et al [23] employed graphene as optical-absorption and energy transfer unit and blended into a TPU matrix, resulted in an infrared-triggered actuation behavior. In their work, graphene/TPU nanocomposites with 1 wt.% sulfonated-graphene showed intriguing and repeatable IR-responsive actuation performance which could shrink and lift a 21.6 g weight 3.1 cm with 0.21 N of force upon exposure to IR light.

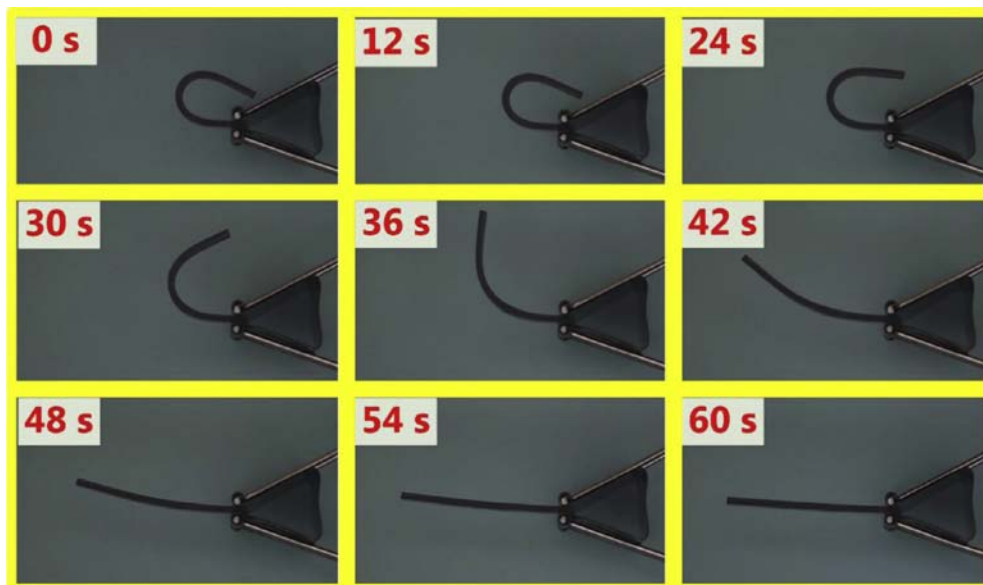


Figure 1.7. Snap shots of infrared light-induced shape recovery of SMP nanocomposite incorporated with 4 wt.% boron nitride and 4 wt.% CNTs.

1.2.3. Water induced SMPs.

Despite heat and other indirect heating method, water can also be a athermal trigger for shape memory effect. Huang et al. first reported the water responsive SMPs in 2005, later, water or solvent-induced shape recovery effects have been further reported in many SMPs with T_g-type switch. Generally, water or solvent molecules may penetrate into the amorphous areas of glass transition type SMPs as plasticizer and increase the flexibility of molecule chain. Once the immerse time is long enough, the glass transition temperature could drop to a temperature below the testing temperature, thus leading to the shape recovery. However, one of the drawback of this type of water induced SMPs is the responding time, which is too long for real application. To solve this problem, a hydrophilic or water soluble ingredient (for example, PEG400) was mixed in the backbone of SMPs. Another interesting work was done by Dr. Zhu, who introduced cellulose

nanowhisker into thermal-plastic polyurethane, and transferred the elastomer into the water-responsive SMPU. Most importantly, this method enabled the shape recovery within 3 mins after immerse into water.

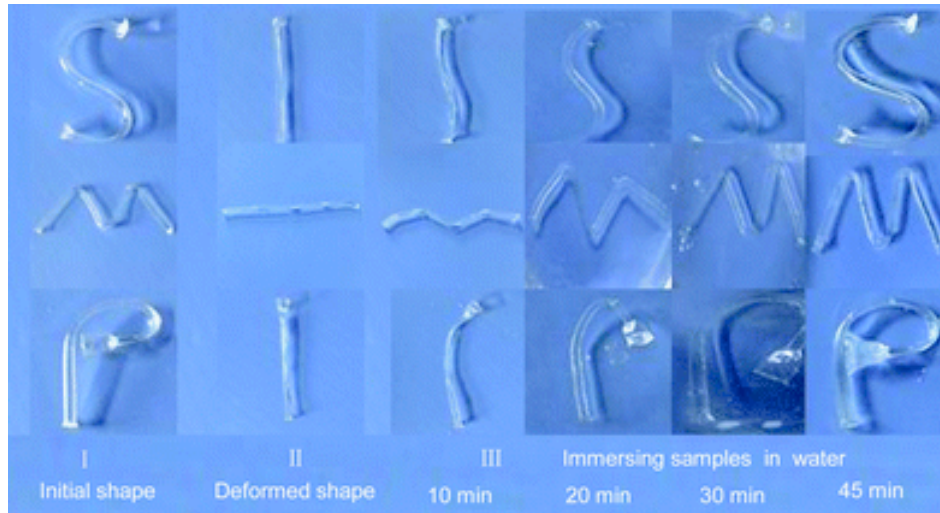


Figure 1.8. The shape memory effect of SM-PVA in water at room temperature. (I) The permanent shape “SMP”, (II) the deformed shape, (III) the shape recovery in water.

1.2.4. Water Vapor Permeability of SMPs

The water proof and breathable fabric are with increasing industrial interests, especially for out-door sportswear companies. Currently there are mainly two methods to realize such requirement, Gore-Tex and TPU film. The key factor in Gore-Tex technology is the porous Teflon film. The hydrophobic nature of Teflon guarantees the water proof property while the porous structure helps the penetration of moisture. Such porous structure also make Gore-Tex fabric indurable, the failure of pores may be harmful for the water proof property. Another technology is based on the dense TPU film with hydrophilic segment.

Thanks to the dense nature of TPU film, the durability is far more better than Gore-Tex product.

Recently researchers have found some unique phenomenon when employing SMPU as breathable material, whose water vapor permeability is temperature dependant. This phenomenon was explained as the change of the molecular chain mobility below and above the transition temperature of soft-segment of SMPU. The brown movement of the water molecule at high temperature is relatively high. Hu et al have studied a series of factors of SMPU on WVP, both on bulk film and fabric coating.

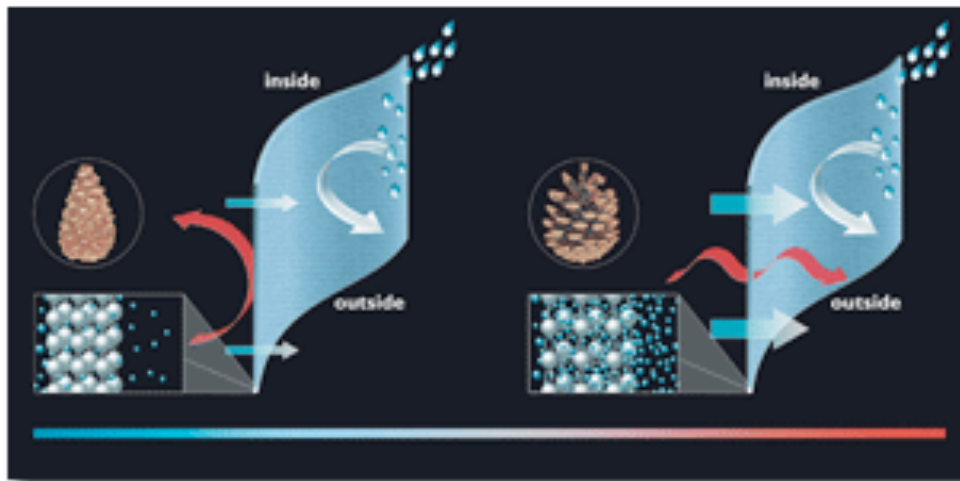


Figure 1.9. Change™ functions similarly to a pine, spruce or fir cone. (http://www.textileworld.com/Articles/2006/October/Quality_Fabric_Of_The_Month/Climate_Change-An_Open_And_Shut_Case)

Left: In cool temperatures and/or periods of low activity, the polymer structure is closed and allows very limited moisture vapor transport. The membrane holds in body heat while remaining breathable. Right: In warm temperatures and/or periods of high activity, the structure opens up, allowing significantly more

moisture vapor to pass through and releasing body heat. In all conditions, the membrane remains wind- and waterproof.

1.3. Objectives of the Project

Development of new SMPs and exploration of their high-tech applications as well as elucidation of the underlying mechanism and structure/property relationships have been our constant pursuit. Attracted by the splendid property and fascinating perspectives of the SMPs and coupled with our expertises in polymer chemistry, I have launched a program directed towards the development of novel SMPs structure, functionality and mechanisms. The four main objectives of this project are: 1) design and synthesis SMPs with multifunctionalities; 2) study the structure and properties of the new materials; 3) explore the practical applications of new SMPs; 4) reveal mechanistic understanding of SME. Although many research interests have been developed in the field, my work is mainly focused on the functionality of SMPs.

Generally, in this project, a series of functional SMPs are designed and synthesized. The design of monomer structure, optimization of polymerization conditions, structure characterization of the resultant polymers, investigation of their mechanical properties, thermal properties, luminescent properties, water sensitivity, light sensitivity, WVP and exploration of their high-tech applications as mechanosensor, actuator, breathable material, biomedical material constitute the major contents for each project. It is anticipated that by enthusiastic research efforts, a variety of SMPs will be generated, which will exhibit versatile properties that are not observed in traditional SMPs. It will greatly deepen the mechanism understanding and the development of SMPs. It

is hoped that this work could trigger new ideas and to accelerate the pace in the designing and synthesis of new SMPs with novel functions for high-tech innovations.

1.3.1. Chromic SMP with novel AIE dyes

The first project is to study the chromic behavior and SME by embracing TPU units covalently into backbone of SMPU. The shape memory behavior, including thermal induced shape recovery and solvent induced shape recovery, is studied and explained in molecular level. Then we further studied the chromic behavior caused by stress, heat and solvent. The intrinsic mechanism of chromic behavior is further studied by time-dependent photo-luminescent.

1.3.2. Stress-free two-way shape memory polymer by interpenetrating polymeric network

This project is to explore the possibility of fabricating a kind of TWSMP which could overcome the disadvantages of currently reported TWSMP. We chose two segment as different function, reversible recovery part and energy storage part. The shape changing ratio was studied and optimized by adjusting the ratio of two segments. The molecular mechanism was further proved by two-dimensional XRD.

1.3.3. Light induced shape memory polymer

This project is to study a facile approach to realize light-sensitivity for traditional thermal induced SMPs. Two kind of light-heat transfer unit were embedded into polymer matrix. Their shape memory behavior and micro-morphology of composite were further studied.

1.3.4. Shape memory polymer with supra-molecular switches

In this project, a series of shape memory polymer with supra-molecular switch were synthesized and their potential applications as water/moisture sensitive polymer, moisture management material were also studied.

1.4. Significance

SMPs are promising materials for their applications in the industry as they provide inspiration to create intelligent materials with self-regulating structure and performance in response to thermal and other stimulation. SMPs with novel properties such as mechanochromic, solvatochromic, thermalchromic, electro-active effect, moisture-regulating effect and body temperature transition can have more potential applications not only in textile areas but also in other areas like wound dressing, scaffolding materials, aerospace applications, biomedical applications, sensors, actuators, pressure garment, high performance sensors, actuators and microgrippers.

As far as we know, most reported work about mechanosensors are based on cyano-(p-phenylenevinylene) derivatives which are either physically mixed or chemically connected with a variety of polymer matrix like linear low density polyethylene, poly(ethylene terephthalate), thermoplastic polyurethanes, poly(cyclooctene), etc. Although such systems exhibit relatively good effect as mechanosensor, the degree of elongation can not be detected quantitative in a large range. The monitor of shape memory effect is a common issue in complicated circumstance like biomedical and aerospace applications where precisely controlled deployment or shrinkage is highly required. In this article, we try to solve this problem by employing TPE (see Fig. 3) units into shape memory polyurethane with biodegradable switch. The morphology, thermal mechanical properties and photo luminescent properties are also well explored.

Two-way shape memory polymers (TW-SMPs), or reversible shape memory polymers are one of the most promising smart materials as their potential application like artificial muscle, actuators, sensors etc. Current approach for fabricating TW-SMPs including combining liquid crystalline into polymer network, applying constant external stress to SMPs with semicrystalline switch or by simply laminated structures. However, they have different drawbacks. For LCEs, a high transition temperature is required and the synthesis procedure is much complicated. While for SMPs with semicrystalline switch, the external force is essential. At the same time, the laminated architecture can only realize bending, although applicable for other complicated deformation, but it can not realize shrinkage. We hope we can solve this issue by employing interpenetration network (IPN) (see fig.4.). Thus, we construct a kind of polymer network and explore if they could exhibit two-way shape memory

effects without external tensile at low transition temperature. Dynamic mechanic analysis (DMA) and differential scanning calorimetry (DSC) proved the reversible shrinkage with ambient transition temperature.

So far, the way to fabricate light-induced shape memory polymer is relatively limited. Most of convenient approaches are focusing on the addition of grapheme, carbon nanotube and other conjugated carbon structure, which are responsive to IR light. In our study, we further enriched light induced SMPs family by introducing other light-heat transfer unit with responsive region around UV and visible region.

The SMPs with supra-molecular switch is a big family of SMPs in terms of molecular structure. However, there are some disadvantages for this kind of SMPU, say the fabrication process is difficult and its functionality is relatively simple. In our project, we explored a facile approach to fabricate water sensitive shape memory supra-molecular polymer. Further we also studied their application on moisture management and moisture-dependent shape memory behavior.

1.6 Outline of the thesis

This thesis studies the properties and performances of the SMPs with novel functions, i.e., memory chromic effect, UV and visible light sensitivity, moisture management and water/moisture sensitive shape memory effect. The biological evaluation of the SMPs with a human body switching transition temperature is also conducted for potential biomedical applications.

In Chapter 1, the general background of shape memory materials and the research of shape memory materials for various applications such as sensor, actuator, breathable fabrics was introduced. Objectives and significance of the present study are presented.

In Chapter 2, comprehensive literature review on SMPs of different functions is generally presented. The research on reversible SMPs, multi-shape SMPs, sensitivity to athermal source, multifunctional and supra-molecular SMPs is described.

Chapter 3 includes sample preparations and characterizations of the corresponding samples. SMPs are synthesized by solution and bulk polymerization and the preparation of other related samples are presented in the chapter such as epoxy resin, light-heat transfer unit, AIE unit. The characterization techniques used in this study are illustrated.

In Chapter 4, the properties of the prepared memory chromic SMPU are studied. The preparation routine for the prepared SMPs with AIE units is presented. The physical properties, including thermal mechanical properties, shape memory effect and different stimuli respond luminescence emission were systematically studied. The mechanism was further explored.

In Chapter 5, we employed a novel approach to fabricate a free-stand two-way shape memory polymer with ambient transition temperature. The idea for fabricate such polymer was well examined by a series of polymer with different ratio of pre-macromonomers. The shape changing behavior and mechanism

were studied by dynamic mechanical analysis and two dimensional x-ray diffraction.

In Chapter 6, we explored a facile approach to realize UV/heat dual responsive triple shape polymer. The fabrication method of both organic-metal compound and polymer were introduced. The physical properties and selective shape recovery were also studied.

Chapter 7 describes a shape memory polymer with supra-molecular switches for moisture management. Molecular design and synthesis routine were introduced. The RH-dependent water vapor permeability were also studied.

Chapter 8 presents the conclusions of the study followed by suggestions of future work.

CHAPTER 2 LITERATURE REVIEW

2.1. Introduction to the shape memory polymers

Study on shape memory polymers (SMPs) has been dynamically conducted for more than three decades. In recent years, the attention in this area has been intensified not only in fundamental research but also in their application. The technological superiority of SMPs became increasing obvious recently. Their technology significance and superiority have drawn increasing attention in various application like textiles, packaging materials, biomedical applications, electronic devices and aerospace applications. (see **Figure 2.1.**)

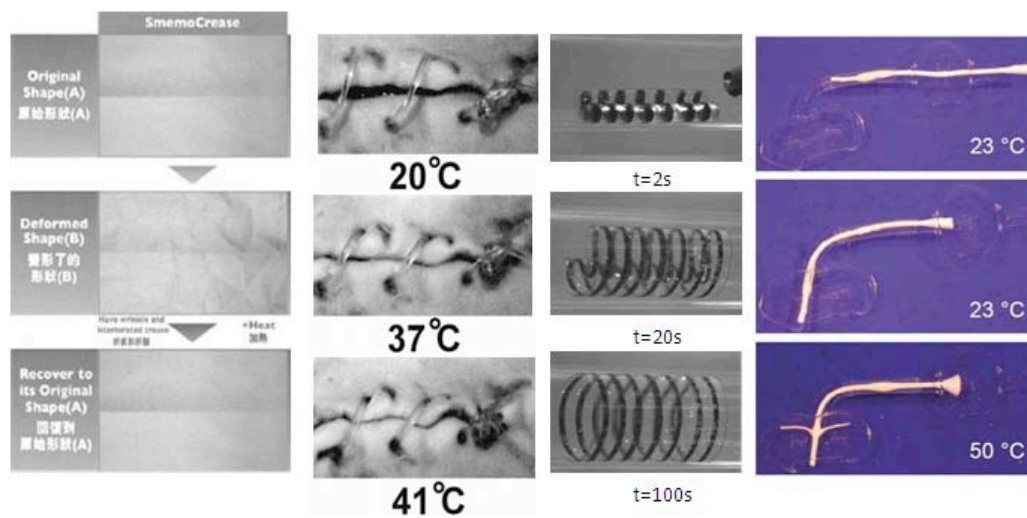


Figure 2.1. Figure of different applications of shape memory polymers in textiles, biomedical and aerospace applications. 1) A fabric modified by shape memory polyurethane, the upper is permanent shape, the middle is deformed shape and the under is recovered shape upon stimulus. 2) Biodegradable suture based on SMPs, the suture shrink upon heating to proper temperature. 3) Model for cardiovascular stents based on biodegradable SMPs, the stent recover to its origin shape after 100s at proper temperature. 4) Catheter based on SMPs.[1, 24-26]

The conception of shape memory effect is first raised in inorganic chemistry, call shape memory alloy (SMA). As to shape memory polymer, their molecular mechanism is different. Typical shape memory polymer can recover to its well-defined permanent shape upon proper external stimulus. However, most of shape memory effects in polymer are essentially entropy driven, which may lead to a misunderstanding that shape memory property is a common property in polymer science. Take polyurethane as example, the expression of shape memory effect is by at least two steps, programming and shape recovery. In the programming process, we may need to stretch the polyurethane film to a certain length above the transition temperature (T_c) and then cool down below the T_c to settle the temporary shape. It is common that both of SMPs and polymer are thermodynamic unstable but kinetic stable below T_c . However, when heating above to T_c and maintain a constant external tensile (programming process), the SMPs is still thermodynamic unstable and kinetic stable, but the normal polymer will tend to thermodynamic stable and kinetic stable state. For a polyurethane with proper amount of hard segment (maybe around 30%), the interaction between $(\text{MDI-BDO})_n$ unit is strong enough to act as physical crosslink point even in the programming process, when cooling down, the inner tensile was fully stored. While in a polyurethane with low hard segment (less than 5%), the interaction between $(\text{MDI-BDO})_n$ is weak and even not existed. Upon programming, the intermolecular slippage within polymer may occur, thus leading to the decay of inner tensile. Similar phenomenal will also be observed in the recovery process, when high temperature is required, SMPs will maintain memory effect within a couple round with slightly decay, while for common polymer, a much faster decay will be observed.

2.2. Molecular Mechanism of Shape Memory Polymers

Traditional thermal induced one-way two shape memory effect depends on the formation of well separated hard phase and soft phase with different transition temperature in the elastic network[1] (See **Figure 2.2.**).

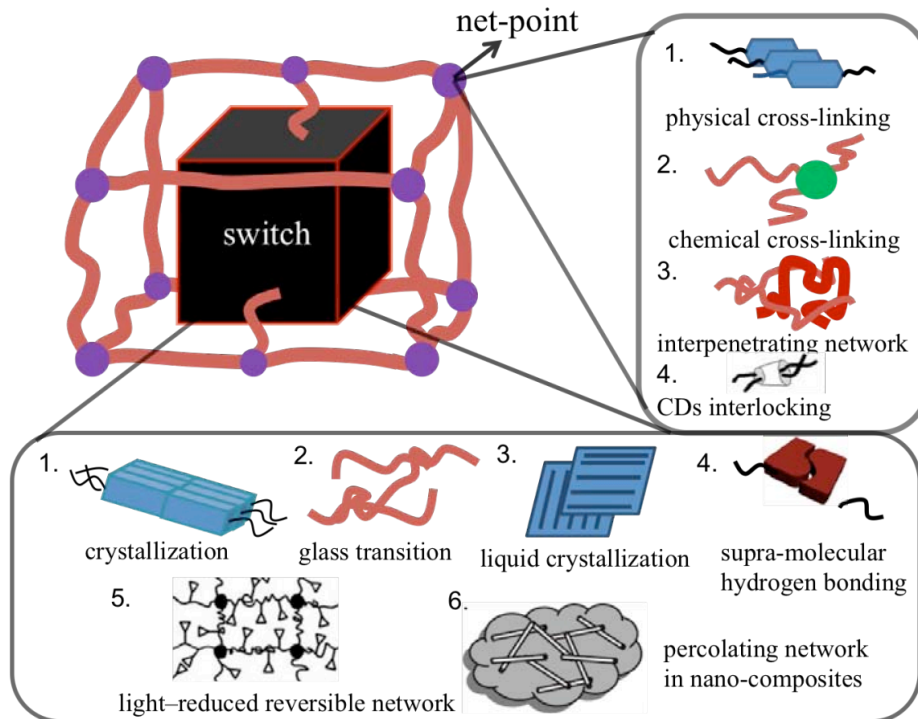


Figure 2.2. General molecular mechanism of shape memory effect, the figure is the basic unit of SMPs, the purple spot display as net-point and the black box means variety of switch.[1]

Generally, the transition temperature of switch (T_{C2}) is lower than net-point (T_{C1}). The hard phases act as net-point which determine the permanent shape and provide the inner force for recovery, while the soft phases act as the switch and immobilize the temporary shape. When the SMPs are deformed above T_{C2} and then cool down, the network will be fixed and the internal stress is saved. Upon heating to T_{C2} or above, the internal stress will be released and enable the

recovery of the polymer to the origin shape. Generally, either physical cross-linking or chemical cross-linking can act as net-point while the realization of switch can attribute to their glass transition, crystallization, liquid crystallization, supra-molecular hydrogen bonding, light-induced reversible network or percolating network in nano-composites.[3]

2.2.1. One-way Dual-Shape Memory Polymer

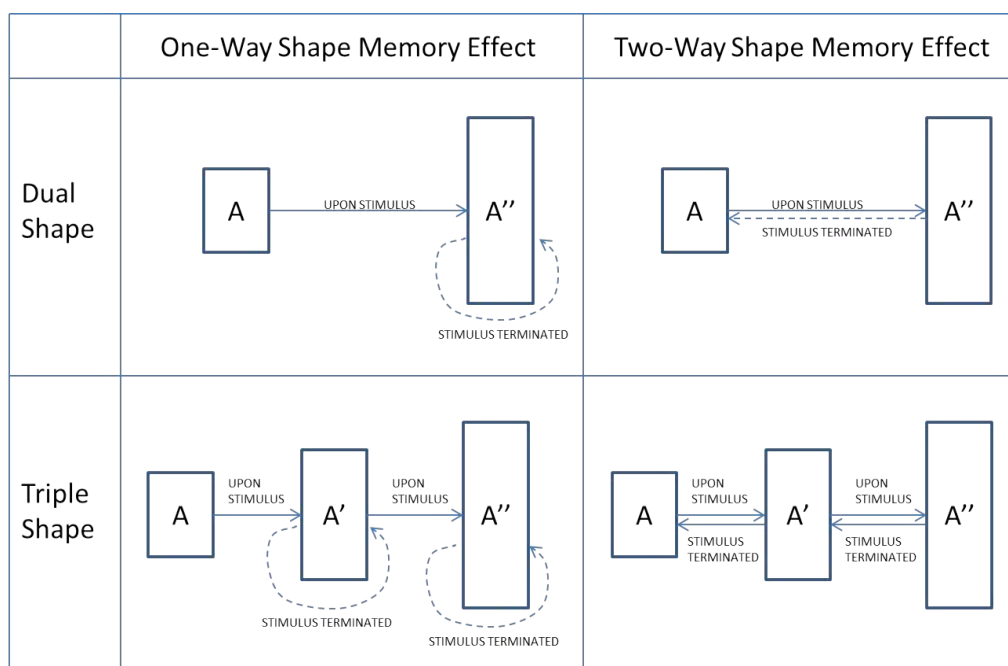


Figure 2.3. Illustration of SMPs according to their memory properties

Generally, there are four types of shape memory polymer in category of their memory effect, one-way dual shape memory effect, two-way dual shape memory effect, one-way triple-shape memory effect and recently developed two-way triple-shape memory effect. Their relationship is shown in **Figure 2.3**. One-way dual shape memory effect can be defined as: in a certain stimulus category, there is only one transition condition which leads to irreversible

recovery to the original geometry, the irreversible recovery means that when the certain stimulus condition is terminated, the shape will not change to the temporary shape without external energy input.

Typical one-way dual shape memory polymers are elastomers under the certain condition. When such elastomers are deformed under proper routine and then freeze the elastomeric recovery under another condition, this process is called programming. The most commonly studied thermal induced one-way dual shape memory polymer consists of net-point and switch. As described before, either chemical crosslinking or physical crosslinking can act as net-point, which determines the fixation of permanent shape. In experimental level, the crosslinker or the oligomer with strong intermolecular interaction (e.g. hydrogen bonds, crystalline regions, ionic clusters or phase-separated microdomains) can act as net-point. Oligomers with proper transition temperature like glass transition temperature or melt temperature are suitable candidate as switch for thermal induced SMPs.[3]

2.2.2. Two-way Dual-Shape Memory Polymers

Two-way shape memory polymer change their shape, e.g., shrink or bend, as long as they are exposed to a suitable stimulus. The original shape is recovered as soon as the stimulation is terminated. The geometry, how such workpiece is moving, is determined by its original three-dimensional shape. While the geometry of the shape change cannot be varied for two-way shape memory polymer, the process of stimulated deformation with subsequent recovery can be

repeated several times. Heat, light, and electro-magnetic fields have been reported as stimuli for TW-SMPs.[3, 27]

2.2.2.1. Liquid Crystalline Elastomers

The first reported TW-SMP are liquid crystalline elastomers (LCEs), which employing liquid crystalline units into a polymeric crosslinking network. The soft elasticity and their reversible strain actuation make LCE candidates for actuators and artificial muscles.

The mechanism of the two-way shape-memory effect intrinsic in LCEs stems is from their anisotropic polymer-chain conformation. The constituent polymer chains are prolate in the direction of the liquid-crystalline director for temperatures in the liquid-crystalline state, while in the isotropic phase the polymer chains are spherical, existing as Gaussian coils. Traversing the clearing transition from the liquid-crystalline phase to the isotropic rubber phase, the polymer chains can spontaneously contract from a prolate to a spherical configuration. The reverse is true upon cooling. In the case of monodomain LCEs, this microscopic deformation can accumulate into a macroscopic one in the direction of the liquid-crystalline director.

Compared with two-way shape-memory alloys, LCEs are capable of much larger recoverable strains, up to 300%. In 2001, by the hydrosilation reaction between poly(methyl-hydrogensiloxane), vinyl functionalized liquid-crystalline mesogen, and cross-linker, a class of monodomain nematic LCEs were prepared by Finkelmann's group. Under a small preload stress of 6 kPa, a recoverable strain as high as 300% was observed through the nematic–isotropic transition

(T_{NI}). Furthermore, more than 90% of the total strain sharply recovered in a narrow temperature range of $0.95 < T_{red} < 1$, where T_{red} is defined as T/T_{NI} . Indeed, in such a sharp transition, the rate of recovery/deformation is determined more by thermal conductivity than other factors. In the case of thin samples, the response rate of this kind of nematic LCEs can match that of natural muscles.[3, 28]

2.2.2.2. Two-way SMPs with Semi-crystalline switch

Another important approach for fabricating Two-way shape memory polymer is combining semi-crystalline units into a polymer network under external stress. The basic principle for such TWSME is based on the melt-induced contraction (MIC) and cooling induced elongation (CIE). Generally, a dual-shape polymer having a crystallizable switching segment was deformed at T_{high} to an elongation ϵ_m resulting in shape (C_{rev}). [12, 29] During cooling to T_{low} under constant stress a crystallization induced elongation (CIE) occurred, attributed to a promoted formation of crystallites in the load direction. In general, the crystallization of entangled polymers from a melt is a two-step process. At first, polymer chains aggregate to granular crystal layers, which then merge into a lamellar crystal below the melting peak temperature. The applied stress to the polymer network at T_{high} and the subsequent increase in strain leads to a situation similar to an anisotropic melt, where the chain segments are preferentially oriented and more extended (higher trans content) than in the isotropic case. During supercooling the most extended chain segments serve as row nuclei in the direction of the applied stress inducing subsequent epitaxial growth of extended chain lamellae.[30] When heated from T_{low} to T_{high} the

increased elongation caused by CIE can be reversed by melting-induced contraction (MIC). The melting of the crystallites enables the polymer chain segments to gain entropy by random coiling, whereby the sample contracts and reassumes the original elongation at T high under the applied stress. Recently, Lendlein reported their study about reversible triple shape polymer containing polypentadecalactone and poly(ϵ -caprolactone)-segment. Suitable values for the constant stress level and the cooling rate were found to ensure two substantial CIEs and two MICs with similar contribution from both segments.[3]

2.2.2.3. Photo Induced Two Way Shape Memory Effect

Photomechanical effects display the change in the shape of a material when it is exposed to light. Basically, photomechanical polymers thus can be thought as two-way SMPs. To date, Photo-mechanical effects have been observed in monolayers, gels and solid films [17, 31-33]. The first kind of photo-chromic amorphous systems capable of generating photo-deformation have resulted from their azobenzene chromophores. It is well known that upon alternate irradiation of UV and visible light, azobenzene undergoes reversible trans-cis isomerization accompanied by a significant change in molecular length from about 9.0 Å in the trans form to 5.5 Å in the cis form. Therefore, by incorporation of azobenzene chromophores into polymer backbones or side chains in monolayers, gels and solid films, irradiation at the two different wavelengths produce reversible contraction and expansion of the materials.[34] In this way, many kinds of polymers that contain azobenzene moieties in their main and/or side chains are expected to exhibit photo-deformation behavior. For instance, Keumet al. synthesized several kinds of PUs that contained push-pull

types of azobenzene moieties in their main and/or side chains, and photo-deformation was observed in this system [35].

Another mechanism for photo-deformation results from the different affinities of the trans and cis-azobenzene to the water surface. It was reported that the trans-azobenzene has a small dipole moment of less than 0.5 D while the dipole moment of the cisform is about 3.1 D. When the azobenzene units in monolayers are free from the water surface, the monolayers show the opposite photo-deformation behavior. They expand when exposed to UV light while shrinking when exposed to visible light. According to this principle, Seki et al. [36, 37] prepared poly(vinyl alcohol)s (PVAs) that contained azobenzene side chains, and reported that the monolayers formed at the air/water interface expanded upon irradiation with UV light, but shrank when exposed to visible light[38].

The most attractive light-induced two-way SMP systems are LCEs that contain azobenzenechromophores[39-41]. In these polymeric systems, the driving force for the shape deformation result from the variation of the alignment order. Upon exposure of UV light irradiation, the azobenzene LCs experience a reduction in alignment order, and even an isotropization phase transition as mentioned above. Usually, the rod-like trans-azobenzene units stabilize the LC alignment, whereas the bent cis forms reduce the LC order parameter (as seen in **Figure 2.4.**) [42]. Therefore, on a macroscopic level, reversible shape changing such as bending and reversible bending are achieved in the LCEs that contain azobenzenechromophore. Therefore, these types of LCEs have been extensively explored recently as highly functional and high-performance materials.

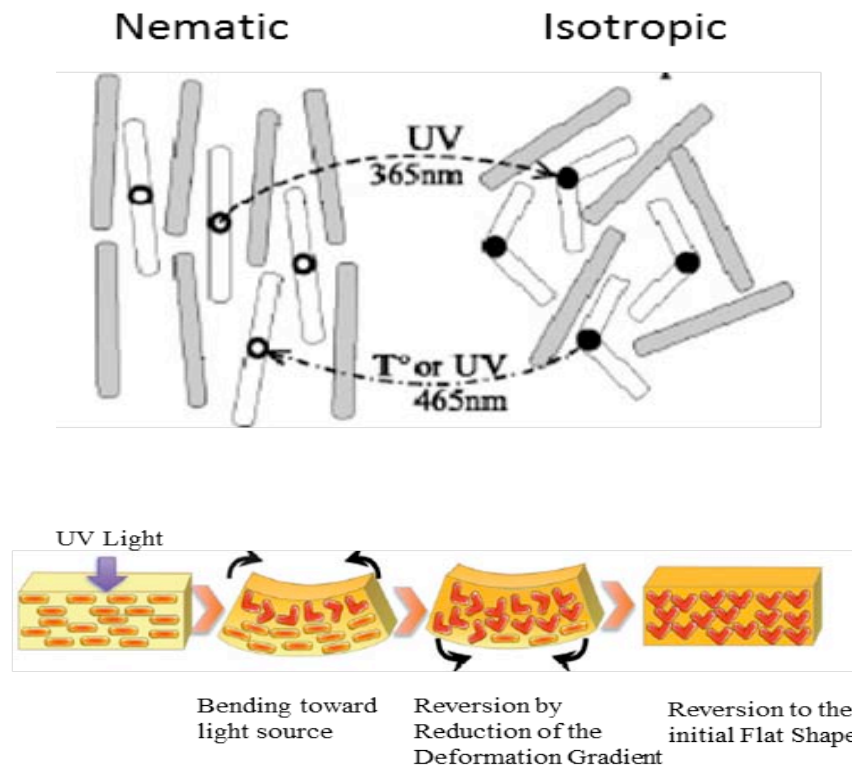


Figure 2.4. Photo-induced two-way SME observed in azobenzene-containing LCEs [43]

For instance, Ikeda et al. studied a wide range of such photosensitive nematic LCEs with photo-induced contraction/expansion effects [40, 41]. Yu et al. achieved photo-induced bending and even precise direction-controllable bending [44]. They also reported that azobenzene-doped LCE that was floating on water can swim away from light [45]. In addition, Zhao et al. prepared photoactive thermoplastic azobenzene-containing triblock LCE copolymers by using ATRP technology [46]. Ilnytskyi et al. reported photo-induced deformation behavior in azobenzene-containing side-chain LCEs [47]. Recently, Endo et al. also reported the anisotropic photomechanical response of stretched blend film made of polycaprolactone-polyvinyl ether with azobenzene group as the side chain [48]. Ikeda et al. systematically studied the effect of the

concentration of photoactive chromophores on the photomechanical properties of crosslinked azobenzene LCPs [42]. Thus, by using the deformations of photo deformable polymers, light energy can be directly converted into mechanical power. Moreover, since deformations driven by light require neither batteries nor controlling devices on the materials themselves, it should be simple to miniaturize them for micro- and nano-applications.[3]

2.2.2.4. Two-way Shape Memory Polymers Fabricated by Multi-component Systems

In addition to the abovementioned LCEs and photomechanical polymers having two-way SME, in the last decade, many instances of research work have concentrated on the development of two-way SMEs by utilizing composite technologies. The earlier two-way SMP laminated polymer composites mostly concentrated on SMA/polymer composites. For example, Winzek et al. developed a thin SMA/polymer-composite [49]. Recently, Tobushiet al. also developed SMA/SMP composites [50-53]. In this system, two-way bending deformation with an angle of 56 degrees was observed in the fabricated SMA/SMP composite belt. In fact, the SMA used in these laminated composites mainly shows the two-way SME. That is, the two-way SMEs of previous SMA/polymers or SMA/SMP composites was actually resulted from the SME and super-elasticity of the SMA tapes during heating and cooling. In this kind of SMA based laminated composite, good binding is usually required as there is less interaction between the SMA and polymer layer.

It was proposed that two-way SMPs can be prepared by multi-layer techniques (similar to bimetal) or interpenetrating networks. However, scientists have not

been able to adequately prepare a pure two-way SMP composite until Chen et al. who realized reversible bending/unbending performance in a pure SMP composites [54]. In this system, two-way SMP composites were prepared by using one-way SMPs without SMAs [55]. The obtained SMP composites (original shape a) bent to curve (shape b) with a bend angle of θ_1 when it was heated to temperature T_2 . While it cooled to temperature T_3 , shape b changed to shape c with another bend angle of θ_2 . The bend angles θ_1 , θ_2 mainly depend on the temperature. At different temperatures, the angle can be quite different. Upon heating, shape c bent into shape b; upon cooling, shape c bent back into shape b. Thus, different shapes can be obtained in different temperatures. More than two shapes can be memorized in these two-way SMP composites (shown in **Figure 2.5**).

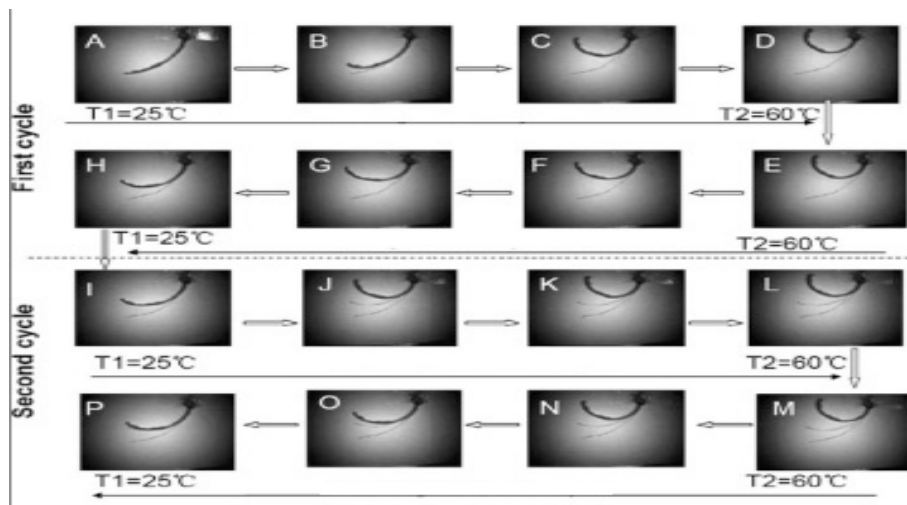


Figure 2.5. Two-way SME observed in SMPU laminated composites[13]

In fact, the driving force of this material results from a mixture of the recovery force of SMP layers through heating, and the elasticity or stiffness of other polymer layers. Recently, Qi et al. also fabricated a pure two-way SMP laminated composite by embedding pre-stretched two-way SMPs into an

elastomeric polymer matrix. Similarly, this composite also demonstrates two-way SMEs in response to changes in temperature without the prerequisite of a stable external force. A transversal actuation of 10% in length was achieved. Cyclic tests show that transversal actuation stabilizes after an initial training cycle and shows no significant decreases after four cycles [56]. Compared with two-way SMAs laminated materials, this kind of SMP composite is able to realize much larger recoverable strains, and its reversible deformation can be easily controlled by its hardness, thickness and deformation ratio of the SMP layer. In addition, this material has stronger bonding at the interface than that of the common SMA/polymer composite. Thus, this SMP composite is expected to be one of the most popular smart materials in the future.[3]

2.2.3. Triple Shape Memory Polymers

In addition to the one-way and two-way SMPs, triple SMPs have also been dramatically developed in recent years. Being little different to one-way SME and two-way SME, triple SME refers to the capability of a polymer to memorize two temporary shapes and subsequently recover them. Since Lendlein and Langer first exploited triple SMPs in 2006 [57], many polymer systems have been explored to exhibit triple SMEs. According to their components, triple SMPs are classified into two categories in this review. The first category is triple SMPs that possess mono-component systems, in which the triple SMEs are mainly related to the formation of at least two separated domains. The second category comprises those with multi-component systems.

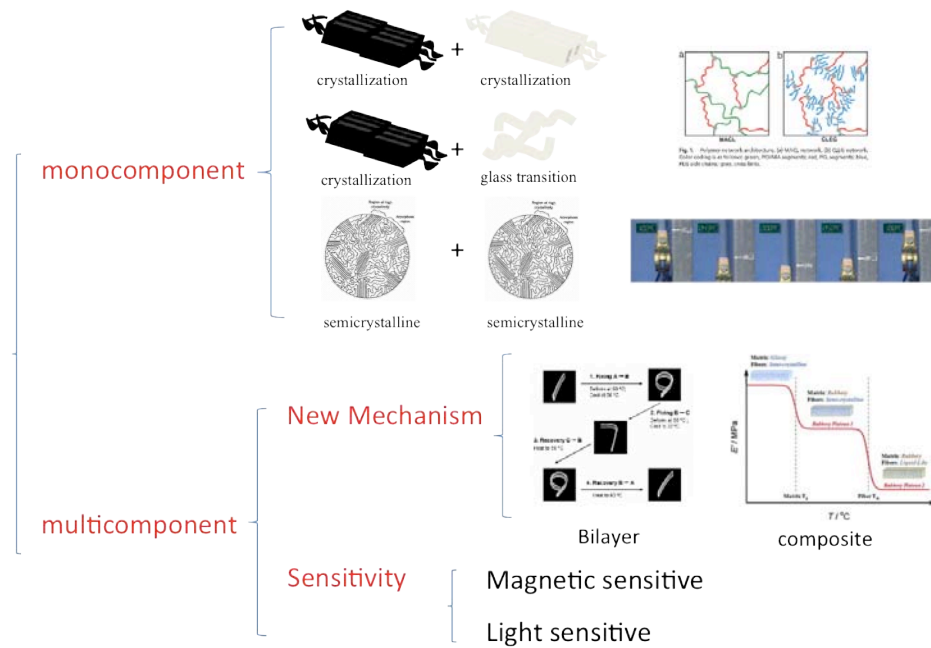


Figure 2.6. Illumination of different category of currently reported triple-shape memory polymers [57-61]

2.2.3.1. Triple-Shape Memory Effect fabricated by Monocomponent Systems

It is generally reported that a triple SME in a monocomponent system is ascribed to a multiphase polymer network that contains at least two separated domains, which are associated with individual transition temperatures. The transition temperature could be a glass transition, melting or LC temperature. Behl et al developed three types of triple SMP by different polymeric networks[62]. The first is a CLEG network realized by the incorporation of PEG segments as side chains with one end dangling into a PCL network; and the second is called MACL network which consists of poly(cyclocyclohexyl methacrylate) chains, which are crosslinked by PCL; and the most recent is a network of cross-linked star-shaped hydroxy-telechelic poly(pentadecalactone) (PPD) and PCL precursors with a low-molecular-weight diisocyanate, herein named the PDCL network, as illustrated in **Figure 2.7** [57, 61, 63]. The TSME

of these three polymeric structure can be realized by a general two-step programming procedure. Most importantly, only a single-step procedure similar to a traditional dual-shape process for application can also generate TSMEs for the latter two types of structure, because of the fact that their reversible segments covalently link to the network [64]. After that, they developed reversible triple SMEs based on the PDCL network by utilizing crystallization-induced elongation and melting-induced shrinkage capabilities of PPD and PCL segments [59]. Similarly, Kolesov and Radusch also studied triple-shape memory behavior of chemically cross-linked blends from ethylene-1-octene copolymers that had different degrees of branching of 30 (EOC30) and 60 (EOC60) CH₃/1000C and/or linear polyethylene (HDPE). It was found that only the cross-linked polymeric system with 50% HDPE and 50% EOC30 demonstrated a pronounced triple-SME, this may be caused by its distinctly segregated phase [3, 65].

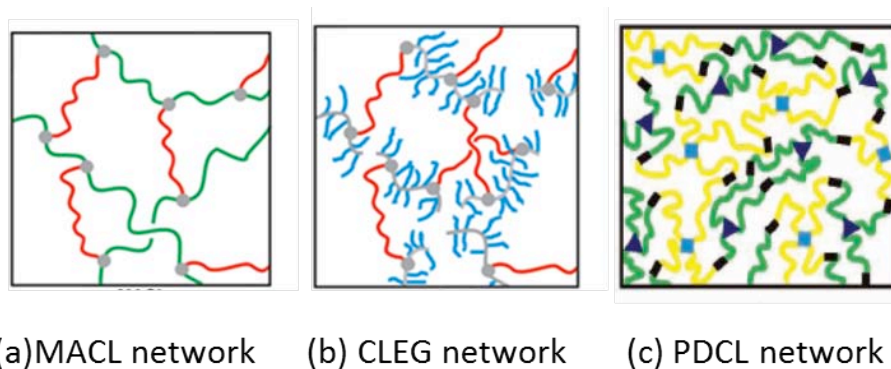


Figure 2.7. Polymeric network architecture of (a) MACL, (b) CLEG, and (c) PDCL network (Color codings in MACL and CLEG networks are as follows: green, PCHMA segments; red, PCL segments; blue, PEG side chains; gray,

cross-links. In PDCL network: green, PPD segments; yellow, PCL segments)[3, 61]

The above mentioned four types of polymeric systems are based on chemically crosslinked polymeric networks in which net-points determine the permanent shape of TSMEs. Similarly, Chenet al. achieved triple shape memory behavior based on physically cross-linked SMPUs with multiple crystalline phases as soft segments. In this system, the TSMPUs consist of two kinds of soft segments with different melting temperatures, e.g., PCL and PTMG segments. A two-step programming procedure for SME can also be achieved when the mass ratio of PCL to PTMG reaches to a balanced value [66]. In addition, Pretsch studied the TSME of a common segmented PEU with crystalline poly(1,4-butylene adipate) PBA as the soft segment [67, 68]. However, the fixing temperature for the second temporary shape was very low at -60°C , since the T_g (-49°C) of the PBA was also utilized as the transition temperature of the triple SME, aside from the T_m of the PBA. So, triple shape memory behavior may be not that attractive.[3]

On a similar basis, but achieved in a homopolymer (rather than copolymer) system, Patheret al. recently reported a side-chain liquid crystalline network which is capable of fixing two temporary shapes through the first isotropic-nematic transition ($\sim 150^{\circ}\text{C}$) and then glass transition ($\sim 80^{\circ}\text{C}$). Increasing the temperature of the fixed sample led to complete and sequential shape recovery, demonstrating a TME [69]. In this system, one-way shape memory cycles were programmed by using (1) T_g , (2) T_i , and (3) combined T_g and T_i as the shape memory transition temperatures (T_{trans}). The T_g type SMPs exhibit excellent shape fixing ($> 97\%$) and R_r ($> 96\%$) with large strains ($> 150\%$). In the T_i type

SMPs, a cooling induced elongation of strain was observed due to the development of an interdigitated SmA mesophase. Shape fixing by the interdigitated SmA was achieved during T_i , unlike conventional shape fixing methods such as vitrification or crystallization. If both T_g and T_i serve as T_{trans} for SMPs, the permanent shape is restored by two stages of shape recovery around T_g and T_i . The dual T_{trans} (T_g and T_i) inherent in this SCLCN allows for the creating of different types of SMCs and the memorization of shape at two different temperature windows, thereby, programmed shapes by different mechanisms would be recovered in a more precise manner.

2.2.3.2. Triple-Shape Memory Polymer Fabricated by Multi-component systems

Unlike the monocomponent triple SMPs, the combination of other components will provide a polymer network with a new mechanism of triple SME or properties like sensitivity and other functions. Xie et al. fabricated a triple SMPs with a bilayer polymeric structure, which consisted of two layers of epoxy resin, which exhibited dual-SMPs of well-separated T_g s [60]. The mechanism of this triple SMEs composed of bilayer epoxy resins could be explained by a stress-balancing mechanism. The final product of Xie's work displayed a strong interface force due to the reaction among the residual epoxy or amine groups on the unreacted surface of the two epoxy layers, which is the key factor for the TSME. [3]

Another more broadly applied method for fabricating TSMP composites was reported by Luo and Mather in 2010 [58]. They simply incorporated non-woven PCL fibers (average diameter almost 760 nm) with a low T_m into a T_g type SMP matrix to form composites with excellent triple SMEs. The intrinsic versatility

of this composite approach enables a large degree of design flexibility for functional triple SMPs and systems. Recently, the incorporation of nanofillers into triple SMPs has also been investigated for specific functions. Kumar et al. proved the non-contact actuation of TSMEs in the above mentioned MACL network nanocomposites with modified silica coated iron (III) oxide nanoparticles [70]. TSMEs were achieved for nanocomposites that contained 40 wt% of PCL, which exhibited a two-step recovery for shapes B and C when stimulated step-wise by increasing the magnetic field strength.

Despite the above mentioned thermal induced triple shape memory effect, the concept of triple shape memory was further expanded by employing different types of stimuli, including heat[71], water[71, 72], light[73] et al. Generally speaking, this dual-responsive triple SMPs were realized by introducing additional sensitive part into SMPs. For example, Luo et al introduced cellulose nanowhiskers(CNWs) into a 1WDSMP, the introduction of CNWs formed additional percolation network as a water sensitive switch in the original 1WSMP and thus realized a water/heat dual sensitive TSMP. Wang et al [74] fabricated a Light/Heat dual sensitive MSMP by hyperbranched polycoumarates.

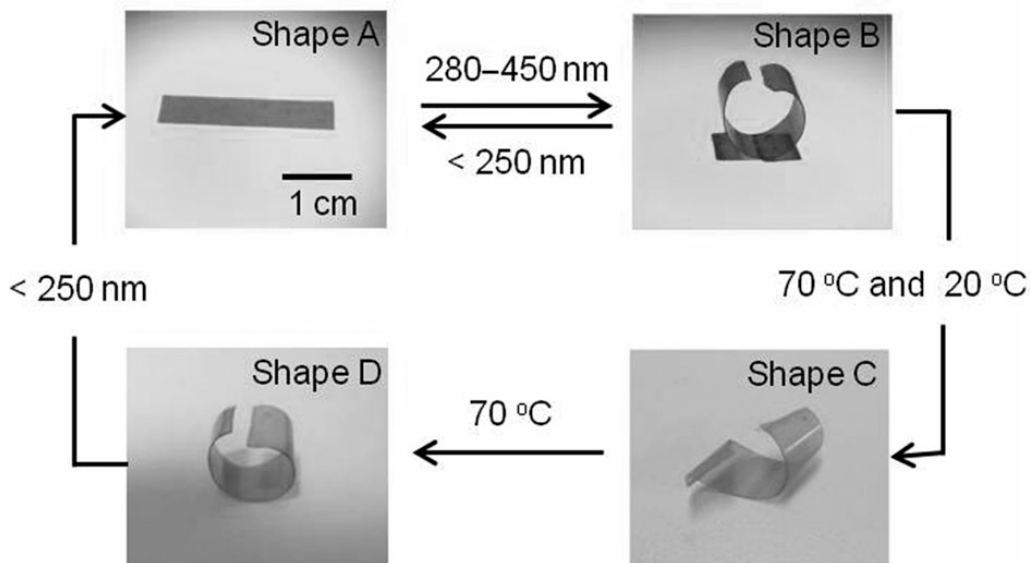


Figure 2.8. Series of photographs of the polymer sample showing a photoinduced multifunctional shape memory. The permanent shape A was irradiated by UV light at $\lambda=280\text{--}450\text{ nm}$ for 20 s to form shape B. Upon being deformed by an external load to the screw shape at $70\text{ }^{\circ}\text{C}$ and cooled/fixated at room temperature, shape C was fixed. Shape D, which is the same as shape B, was recovered by heating again to $70\text{ }^{\circ}\text{C}$. Shape A was recovered by irradiation with a low-pressure Hg lamp at $\lambda=250\text{ nm}$ for 180 minutes. [74]

Another simple approach to realize TSMP or even MSMP is by segmental method, unlike previous reported ones, where the switches are mixed together in macro level, the segment method is more like to divide a SMP into different regions (in macro level) and each region has a different trigger condition. The advantage of this method is simple and localized trigger, we just need to attach two or more SMPs together by glue, but the limitation of this method may be restricted shape change compared with conventional ones. Zeng et al[75] fabricated a MSMP by poly(2,5-furandimethylene succinate) and 1,8-bis-maleimidotriethyleneglycol in four sections with distinct glass transition

temperatures. Xie et al introduced a remoted controllable multi-responsive MSMP by mixing carbon nanotubes and Fe₃O₄ into different region of epoxy resin. Razzaq et al[76] reported a TSMP created by an active component encapsulated in a highly flexible segmented polymer network. Segments with the same composition but different interface areas can be recovered independently either at specific field strengths during inductive heating, at a specific time during environmentally heating, or at different airflow during inductive heating at constant H . Herein the type of heating method regulates the sequence order. Wu et al[73] introduced Zn(Mebip)₂(NTf₂)₂ into part of 1WDSMP, realized a UV/Heat dual segmental sensitive TSMP.

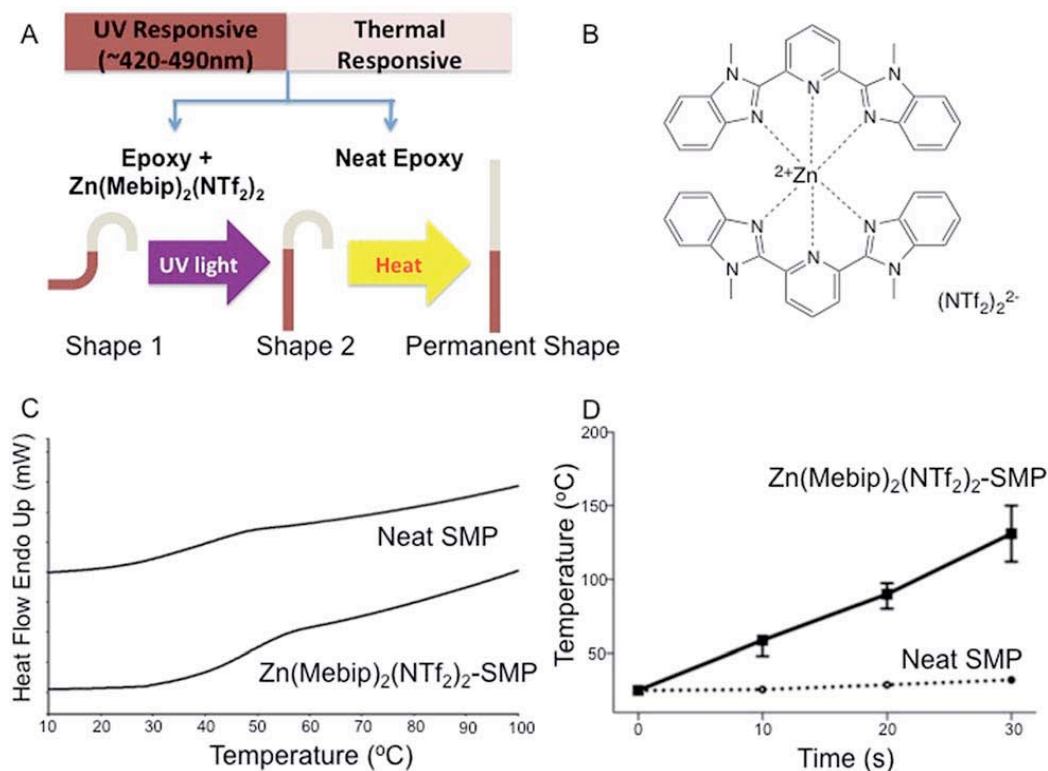


Figure 2.9. (A) Illustration of composition of SMPs and shape recovery routes (from shape #1 to the permanent shape). (B) Molecular structure of Zn(Mebip)₂(NTf₂)₂. (C) Differential scanning calorimetry results of the second

heating curve of each part of the SMP. (D) Temperature–time relationship of each region under UV irradiation. [73]

2.2.4 Multiple Shape Memory Effects

Despite segmented method, another important approach to fabricate MSMP is to employ SMPs with a broad phase transition temperature, which can be understood as the combination of a series of narrow phase transitions. The advantage of this method is that MSMP can be repeatedly programmed. Xie T [77] first reported a tunable MSMP by perfluorosulphonic acid ionomer (PFSA), which has only one broad reversible phase transition and proved its dual-, triple-, and at least quadruple-shape memory effects. Later different TSMPs or MSMPs with same mechanism but different switch system were reported like PCL[78], PMMA[79, 80], PLLA[80], poly[ethylene-co(vinyl acetate)][81], polyethylene[82] and norbornene derivatives[83]. For example, Yang et al[78] fabricated a TSMP by varying the arm numbers of PCL and realized a broad crystalline region. Wang et al[79] and Samuel et al[80] also studied the TSMP or MSMP in PMMA blend system with broad glass transition temperatures.

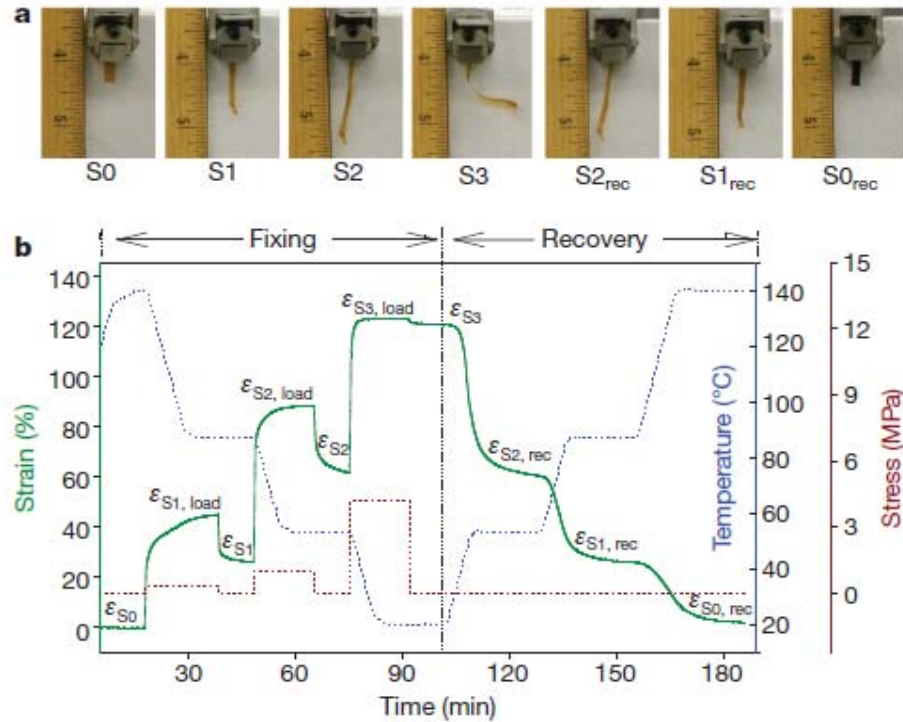


Figure 2.10. Quadruple-shape memory properties of PFSA (a. Visual demonstration. S0: permanent shape; S1: first temporary shape (T_{d1} :140°C); S2: second temporary shape (T_{d1} :107°C); S3: third temporary shape (T_{d3} : 68°C). b. Quantitative thermal mechanical cycle)[77]

2.3. Functional Shape Memory Polymers

The high technological significance of SMP becomes apparent in many established products (e.g., packaging materials, assembling devices, textiles, and membranes) and the broad SMP development activities in the field of biomedical as well as aerospace applications (e.g., medical devices or morphing structures for aerospace vehicles). Inspired by the complex and diverse requirements of these applications fundamental research is aiming at multi-functional SMP, in which SME is combined with additional functions and is proceeding rapidly. Typically, some properties are adhered to shape memory effect like permeability, transparency, and enthalpy. Other properties like color

change, IR sensitivity, magnetic sensitivity, radio frequency sensitivity, electrical conductivity and drug release properties are realized by incorporated with related small molecular with specific functions.

2.3.1. Stress-Free/Free Stand Type 2WSMP

Although the lamination type 2WSMP could realize stress-free 2WSMP at ambient temperature, there are still some limitations, such as the durability of interfacial glue after many cycles and unable to trigger reversible stretching. Aiming to solve this problem, recently a series of free-stand and reversibly stretchable 2WSMP with ambient transition temperature were developed. In general, the recently developed stress-free 2WSMP were based on the combination of semi-crystalline SMPs functional units which could result in oriented crystallization of switches.

One method is to introduce elongation part into the one-way SMP with crystalline switches, the crystalline switches are the reversible shrink part which will expand during cooling and collapse during heating in the direction determined by the elongation part. This concept can be easily understand by a spring-switch model. (see Figure below)

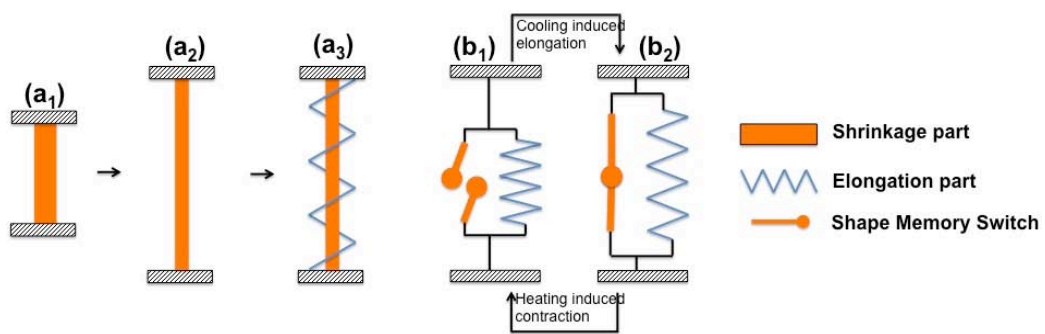


Figure 2.11 Schematic illustration of mechanism of free stand 2WSME.

Recently, we have delighted to see that Lendlein et al[16] reported a polymer which demonstrated a two-way shape memory effect in length change without external force. Lendlein's work has made a progress in removing the external tension for the 2WSME using two kinds of crystalline soft segments in one polymeric network. They convert a normal tripe-shape memory polymer to a 2WSMP through a programming process before the application. The key concept of their work is the separation of the shifting geometry determining function (one crystalline phase) from the actuator function (another crystalline phase) on the level of phase morphology, the actuator domains expand during cooling and collapse during heating in the direction influenced by the shifting-geometry determining domain.[16] They synthesized multiphase copolyester urethane networks with two different crystallizable chain segments (poly(ϵ -caprolactone) and poly(ω -pentadecalactone)) forming the ADs and shape SGDs. A model was derived for this rbSMP system correlating the macroscopic reversible shape shift during heating and cooling with a reversible strain of 21% to the experimentally determined changes of the nanoscaled crystal structure elements, in particular the long period, which is the average distance between two crystalline lamellae consisting of a crystalline and an amorphous part. Later, Gong et al[84] fabricated another stress-free 2WSMP particles by employing poly(ethylene glycol) and poly(ϵ -caprolactone) as ADs and SGDs, and further explored their application as drug carriers.

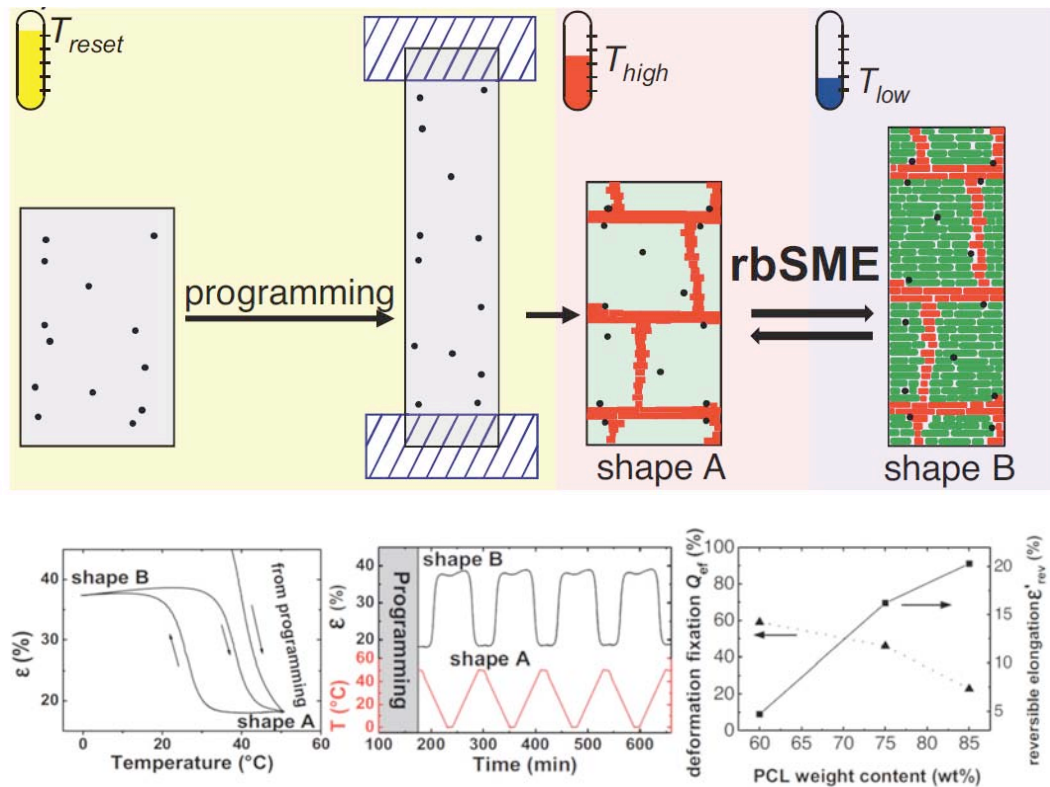


Figure 2.12. Schematic illustration of free-stand 2WSME by Lendlein. [16]

Zhou et al[85] further simplified the molecular approach by simply employ same crystalline switches as both ADs and SGDs. The stress-free 2WSME was realized by partially melt of crystalline switches, where the melt part are ADs and the unmelt part are SGDs. Thus the sample could possess temperature-dependent 1WDSME and stress-free 2WSME. As shown in **Figure 2.13**, a film sample of a POA elastomer was programmed by extension from the original length (L_0) to a temporary length (L_t) and quenching to a low temperature $T_0 \ll T_m$. (a) Partial melting of the extended sample at an intermediate temperature T_i causes partial contraction of the sample to an intermediate length L_i (state 1), which is used as a starting state for three different shape-memory processes. (i) Subsequent heating to $T = T_f$ results in complete melting and irreversible recovery of the original length $L = L_0$ (state 2). (ii) Cooling and recrystallization

causes reverse shape transformation (state 3), which can be repeated multiple times upon sequential cooling–heating cycles (two-way reversibility). (iii) From state 1, the sample can be reprogrammed by forced contraction and subsequent quenching at a low temperature (state 4). This process leads to one-way pseudoreversibility from state 4 to state 2 through the intermediate state 1. The cartoon underneath outlines a phenomenological mechanism of two-way reversible shape memory: In state 3, the extended shape is secured by a crystalline scaffold of oriented lamellae, which percolates through the entire sample and holds extended conformation of the polymer strands in the amorphous phase. Upon partial melting at $T = T_i$, the scaffold loses percolation triggering shape transformation (state 1). At state 1, the shape is controlled by clusters of remaining crystallites that may remain internally percolated and aligned. Upon cooling from state 1, the remaining crystallites serve as seeds and template for recrystallization of the previously molten crystallites at the original position, shape, and orientation. Replicating the original scaffold is the fastest pathway for recrystallization outlined by topological constraints imposed by chemical cross-links and crystallites. (2) Heating the sample significantly above the melting temperature T_m destroys the self-templating ability of the crystalline scaffold and makes shape recovery irreversible (state 2). (b) We have measured contraction of uniaxially stretched samples during heating and subtracted the length increase due to thermal expansion. Relative contributions of the SM processes depend on the temperature of partial melting T_i . With increasing T_i , the contribution of the one-way-RSM (ϵ_{1w}) decreases, while the contributions of the two-way RSM (ϵ_{2w}) and irreversible SM (ϵ_i) increases. When approaching the state of complete melting (state 2), shape recovery is largely irreversible and

the total strain is dominated by ϵ_i . The other contributions into total strain $\epsilon_t = \epsilon_r + \epsilon_s$ are explained in the main text. (c) Graphic representation of the relative contributions of the three different shape memory processes depending on the temperature of partial melting, i.e., intermediate temperature T_i . The maximum contributions of the one-way and two-way reversibilities are achieved at different temperatures $T_i = T_{m1}$ and $T_i = T_{m2}$, respectively. The SM transformation becomes irreversible upon complete melting at higher temperatures $T_i > T_f$.

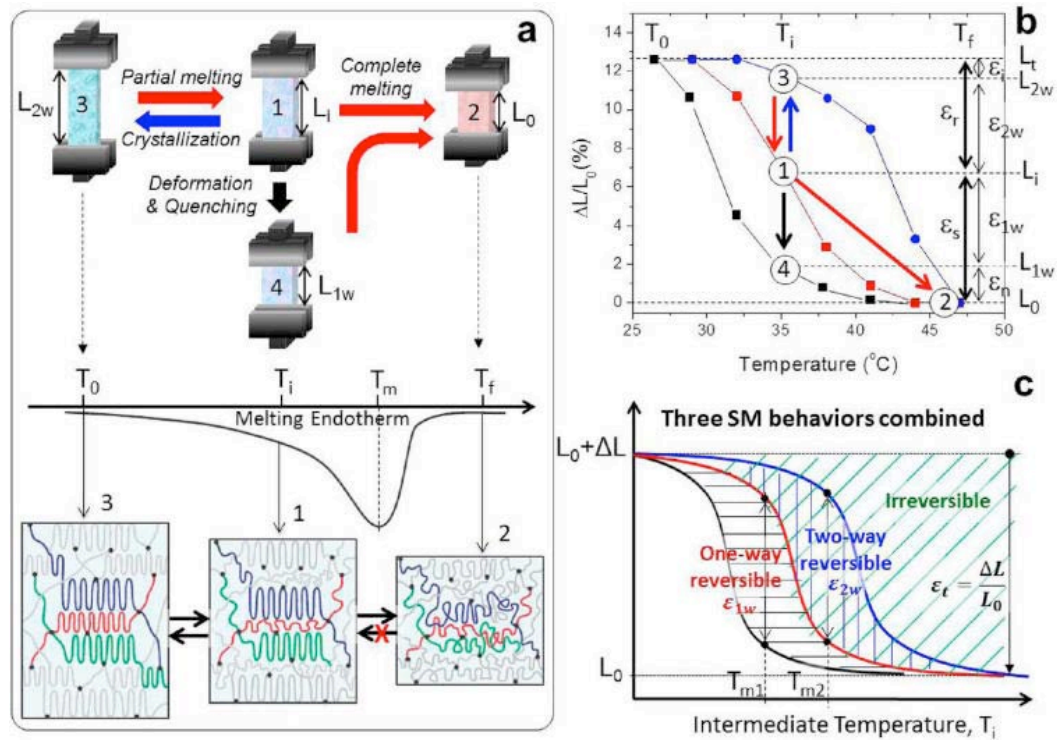


Figure 2.13. Interplay of reversible and irreversible shape-memory processes.

[85]

Our research group [86] also reported another type of stress-free 2WSME by new molecular strategy, which is an interpenetrating network (IPN) with

elastomeric and crystalline components leading to a "switch-spring" composition. In this 2WSMP the switch, a PCL crystalline network, is responsible for the reversible shape shrinkage. While the spring, the compressed PTMEG elastomeric network, provides the push force for shape expansion. This IPN polymer has the desired two-way shape effect (2WSME) as proved by DMA and 2D-XRD.

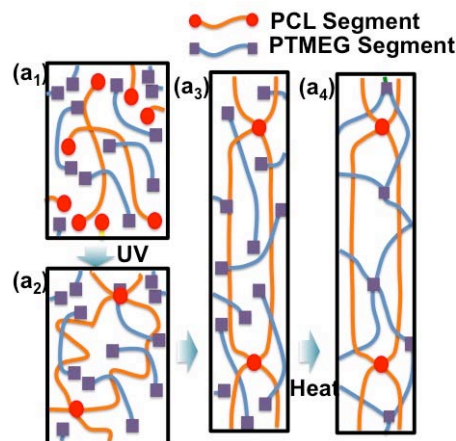


Figure 2.14. Molecular illustration of stress-free 2WSME by new molecular strategy, which is an interpenetrating network (IPN) with elastomeric and crystalline components leading to a "switch-spring" composition [86]

Bothe, M. and T. Pretsch [87] reported another simple approach to realize stress-free 2WSME from a simple T_m-type SMP. They over-stretched the outcome polymer to around 1000% at right above its T_m (60°C), which realized a little part of new and oriented crystal nuclei with higher transition temperature. Once unloaded, thermoreversible specimen expansion and contraction could be detected. Following the microstructural evolution of such a trained specimen by in situ wide-angle X-ray scattering gave evidence for progressive growth of oriented crystallites during cooling. Upon heating, crystallite melting resulted in structural disorder. Beyond this, modification of the training method was used to

introduce a geometrically more complex crystalline order. Here, actuation in the form of a decrease and an increase in sample thickness and specimen twisting and untwisting were witnessed. The novel semi-crystalline polymer actuator highlights an enormous potential for realizing versatile reversible shape changes in elastomers.

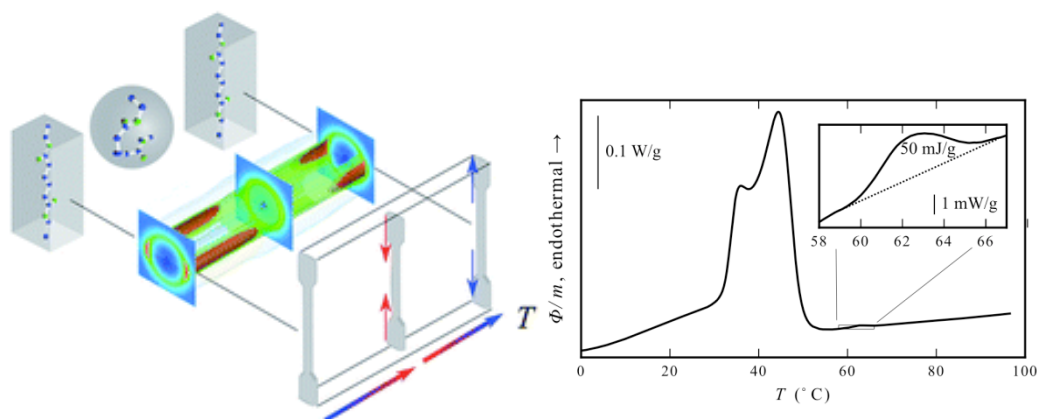


Figure 2.15. Illustration of in situ wide-angle X-ray scattering gave evidence for progressive growth of oriented crystallites during cooling and second heating curve of sample in DSC. [87]

2.3.2. Tunable Transparency

Usually the transparency of SMPs are also tunable when crystalline switches were employed in molecular network. When temperature is below T_m , crystallization will occur for switches, leading to (partially) opaque appearance because of anisotropic nature of crystalline. When SMPs was heated above T_m , the crystalline will be melt and leading to a transparency appearance because of isotropic nature of melt crystalline (amorphous). However, the melt region of a single polymeric crystalline is usually around 10°C due to different degree of perfection of crystalline, thus the transparency can be tunable among different degree of opacities by tuning temperature and crystalline contents. Recently,

Yao et al[88] prepared a series of omniphobic fluorogel elastomers by photocuring perfluorinated acrylates and a perfluoropolyether crosslinker. By tuning either the chemical composition or the temperature that control the crystallinity of the resulting polymer chains, a broad range of optical and mechanical properties of the fluorogel can be achieved.

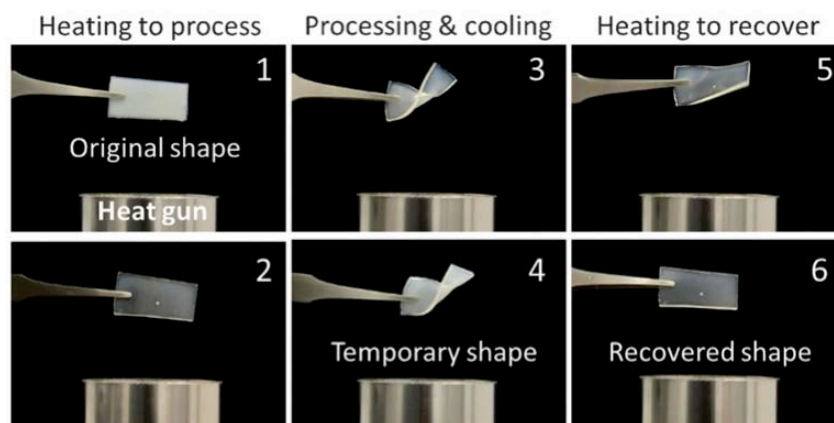
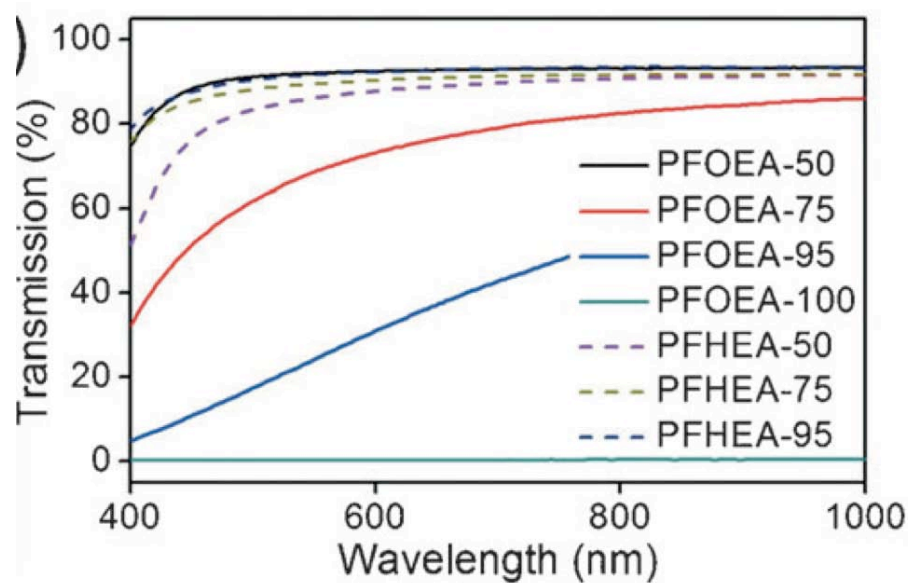


Figure 2.16. optical tests for the fluorogels of different compositions. Samples of 1 mm thickness were prepared for all the optical measurements. c) Demonstration of the shape-memory behavior of PFOEA-95: 1 and 2) converting a rigid film (white) to a soft and flexible (transparent) film upon

heating with a heat gun; 3 and 4) twisting a soft film and keeping the shape when cooling down; 5 and 6) recovering the original shape upon heating. (copy write permission from [88])

2.3.3. Tunable Water Vapor Permeability

Water vapor permeability (WVP) is a property measuring the ability of a material to allow water vapor to penetrate; this property is influenced by the testing standard/condition, thickness, hydrophilicity and mobility of polymer. The mechanism of water vapor transfer through dense film is caused by the brown movement of hydrophilic group which lead water vapor from high pressure surface to low pressure surface. Thanks to the tunable mobility of polymer chain/segments of SMPs across the phase transition region, usually a sharp increase of WVP will be observed once the SMP was heated above the T_{trans} .

Mondal et al[89] has investigated the water vapor permeability of shape memory polyurethane (SMPU) coated cotton fabrics. The SMPUs were tailor made in order to obtain the phase transition temperature (soft segment crystal melting temperature) in the room temperature range. SEM studies were carried out in order to investigate the surface structure of coated and uncoated fabrics. The temperature sensitive water vapor permeability at soft segment crystal melting point was observed for SMPU coated fabrics. When the experimental temperature reached the soft segment crystal temperature of SMPU, an abrupt change of water vapor permeability of SMPU coated fabrics were observed. The significant change of water vapor permeability of SMPU coated fabrics is due to the phase change of SMPU which causes density changes inside the membranes due to micro-Brownian motion of soft segment, therefore, enhanced the water

vapor permeability through the coated fabrics. The water vapor permeability of coated fabrics was also dependent on the primary structure of SMPU. When polycaprolactone glycol (PCL, M_n 3000 g mol^{-1}) was introduced in the polytetramethylene glycol (PTMG, M_n 2900 g mol^{-1}) based SMPU, the water vapor permeability decreases due to the increased interaction between the polymer chains due to presence of ester groups. In contrast increase of polyethylene glycol (M_n 3400 g mol^{-1}) in the SMPU backbone, the WVP increases due to the increasing hydrophilicity of the SMPU.

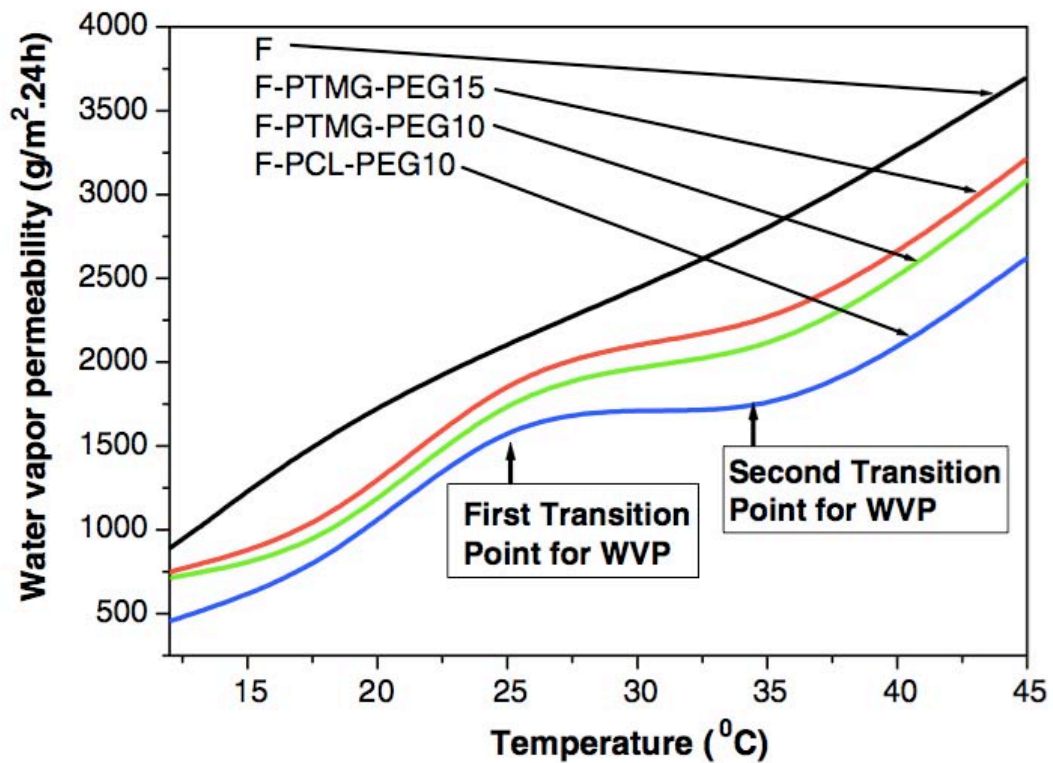


Figure 2.17. Water vapor permeability of SMPU coated fabrics. (copyright permission from [89])

2.3.4. Tunable Stiffness

Change of phase usually accompany with change of stiffness. Shape-memory polymer (SMP) can be deformed by applying a small load above its glass

transition temperature (T_g). Shape-memory polymer maintains its shape after it has cooled below T_g and returns to a predefined shape when subsequently heated above T_g . The reversible change in the elastic modulus between the glassy and rubbery states of an SMP can be on the order of several hundred times. Such change of stiffness/elasticity make SMP a promising material for smart orthotic devices. Hu et al recently developed a smart ankle-foot orthotics device based on SMP, the stiff SMP act as supporting material at room temperature, while became soft and tunable above this transition temperature. Takashima et al [90] evaluated the application of the SMP to soft actuators of a robot based on the change in stiffness. The initial shape and bending displacement of the pneumatic artificial rubber muscle can be changed by controlling the temperature of the SMP sheet.

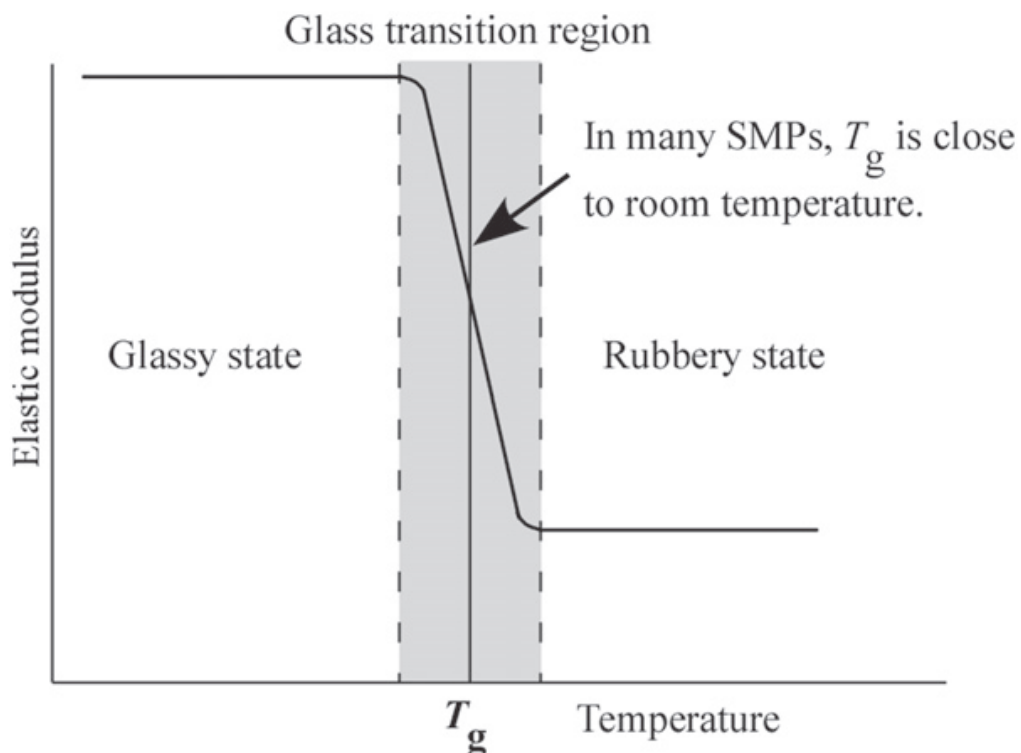


Figure 2.18. Relationship between the elastic modulus and the temperature of the SMP. [90]

Rossiter et al [91] showed a smart material auxetics using a thermally responsive shape memory polymer composites and SMP based auxetic hexachiral structure can be tailored to provide a tunable stiffness response in its fully deployed state by varying the angle of inter-hub connections, and yet is still able to undergo thermally stimulated deployment.

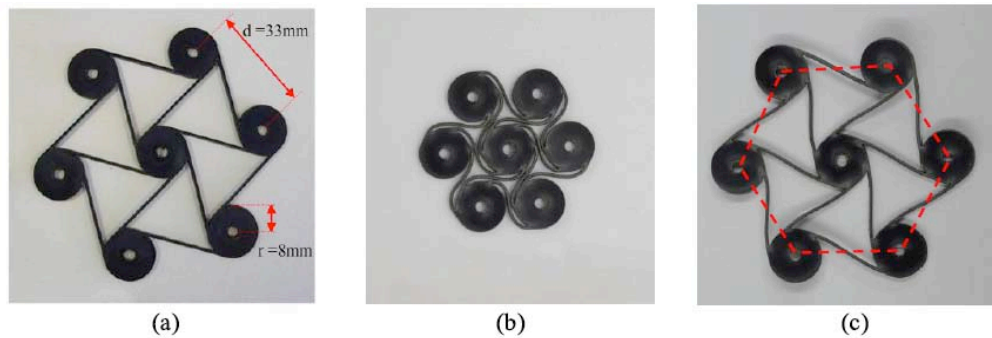


Figure (a) Asfabricated deployed state of laser cut SMP hexachiral auxetic, (b) compressed storage state, (c) deployed structure after shape recovery. [91]

2.3.5. Wettability

It is known that surface wettability is dependent on both surface chemistry and surface topography.[92] Surface chemistry determines the intrinsic wettability of the surface. Surface topography, on the other hand, can significantly enhance the (non)wettability, creating superhydrophilic, superhydrophobic or superoleophobic surfaces, which are of interests for a wide range of applications, including highly sensitive plasmonic devices, oil-water separation membranes and self-cleaning surfaces.[92] Surface topography is determined by geometrical parameters, including feature size spacing, shape, and lattice symmetry. In this regard, controlled deformation of pattern geometry offers an attractive method to tune the surface wettability, especially when this function was introduced or merged with SMPs.

Yao et al [88] fabricated a series of multifunctional SMP with tunable transparency, elasticity, shape memory, and antifouling properties by photocuring hydrophobic perfluorinated acrylates monomer and crosslinker. After infusing with fluorinated lubricants, the fluorogels showed excellent resistance to wetting by various liquids and anti-biofouling behavior, while maintaining cytocompatibility.

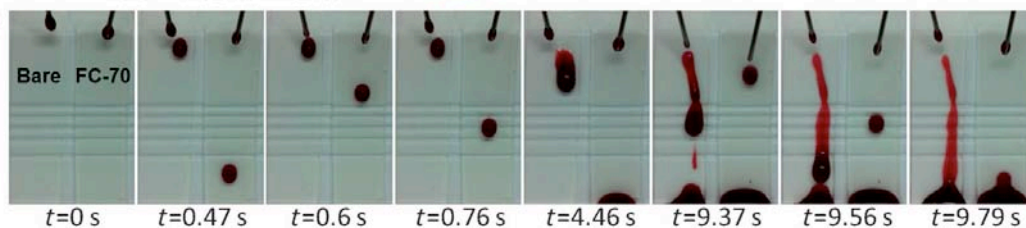


Figure 2.19. Application of blood to bare and FC-70-swollen PFOEA-50 fluorogels: time lapse images show blood sliding on swollen fluorogels and pinning and streaking on bare fluorogels. [88]

Despite the intrinsic hydrophobic nature of raw materials, the secondary surface structure of SMPs can be tuned by various method, thus leading to a superhydrophobicity and tunable adhesion. Sarwate, et al [93] fabricated a series of shape memory polystyrene blocks with superhydrophobic structure using oxygen reactive ion etch (ORIE) and controllable strain recovery. Microhills are first generated on the surface of a PS block by ORIE. The PS block is then heated up, which triggers the strain recovery. During this process of recovering its original shape, the PS block gradually reduces its lateral dimensions, while increasing its thickness. Using different recovery temperatures, the surface morphologies can be controlled, which provides an approach to adjust surface wetting properties, including adhesion.

At a temperature of 148 °C, microhills deformed to high-aspect-ratio nanowires.

The corresponding PS surface has wetting properties similar to those of a lotus surface. The wetting is in Cassie-Baxter state, and a water drop is easy to get off from this surface. When the recovery temperature is increased to 162 °C, microwrinkles appear on the PS surface due to the different stiffnesses between the oxygen-treated top layer and the underlying PS substrate. These microwrinkles, together with nanowires located on their tops, form hybrid micro/nanostructures on the PS surface. The corresponding surface has wetting properties similar to those of a rose petal. The wetting is in a mixed state of Wenzel and Cassie-Baxter.

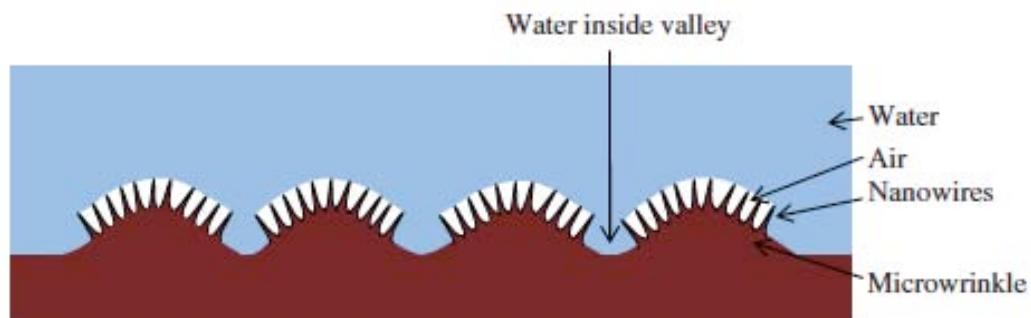


Figure 2.20. Schematic of a mixed state of Wenzel and Cassie–Baxter. [93]

SMP structures with controlled deformation and recovery in different regions could potentially be applied to water collection, nanoparticle assembly, microfluidics, and optical devices. Chen et al [92] created uniformly deformed patterns by shearing SMP pillar arrays. The deformed and original/recovered SMP pillar array has distinct wettability. For deformed surfaces, droplets atop exhibited an anisotropic shape at large spacing ($s = 20$ and $30 \mu\text{m}$). In either case, the water droplet was fully pinned on the inclined surface. On the contrary, the water droplets on the original or recovered pillars have been better described by Cassie-Baxter model with a finite sliding angle. Utilizing these properties

Chen et al designed a surface for water shedding, where the liquid slid to the deformed region. Such surface can be reconfigured and recovered.

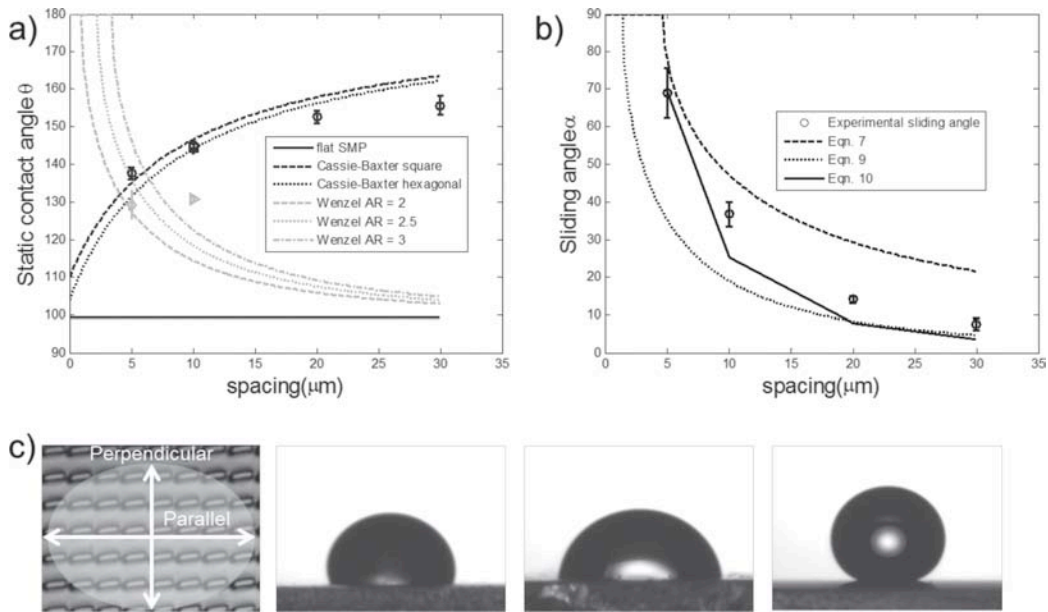


Figure 2.21. Wettability of SMP pillar arrays. (a) Static water contact angles of straight pillars (circles for square array and squares for hexagonal array) and deformed pillars (diamonds for AR = 2 and triangles for AR = 3) and theoretical prediction (lines) by the Cassie-Baxter and Wenzel models. (b) Experimental sliding angles (circles) vs. the theoretical ones according to Equation 7 (- - -) Equation 9 (...) and Equation 10 (—), respectively. (c) Anisotropic wetting on the deformed sample 5, from left to right: top-view optical image of the deformed pillar array with illustration of the direction the droplet being viewed on the deformed pillars; droplet viewed perpendicularly to the deformed pillars; water viewed in parallel to the deformed pillars; the droplet on the original SMP pillars. [92]

2.3.6. Optical Functions

The optical signal play vital role in the modern high-tech applications because of their advantages like facile approach, in-situ monitoring and remote detection. Despite light-sensitive SMPs, embedding SMPs with optical function make them as promising candidates for sensors and actuators. In the following part, the optical function of SMPs were mainly introduced in terms of whether the optical function was realized by introducing additional dyes or by micropatterns.

3.2.1. SMPs with Additional Dyes

Introducing SMPs with additional dyes enable the SMPs with additional optical functions. Usually such function is in consistency with the dyes themselves like thermal chromic, mechanochromic and solvatochromic behavior. The deformation and trigger source (like temperature, water, chemical, stress) to shape memory effect also enabled the dye to exhibit chromic behavior, leading to a change of emission intensity at different conditions.

Kunzelman et al [94] introduced oligo(p-phenylene vinylene) dye into a T_m-type SMP as temperature sensors. The dye concentration was chosen to allow for self-assembly of the dye upon drying, resulting in the formation of excimers. Exposure of these phase-separated blends to temperatures above the melting point (T_m) of the PCO leads to dissolution of the dye molecules, and therefore causes a pronounced change of their absorption and fluorescence color. The optical changes are reversible. Later Ecker et al [95] also reported a SMP with microencapsulated thermochromic pigments (T-PIGs) as temperature sensor. They proved that the color switching temperature of the T-PIGs roughly coincided with the melting temperature of the ester-based switching segment and thus with the activation temperature of the shape memory effect. Torbati et al

[96] found that the emission intensity could be amplified by electrospun. (compared with dense film)

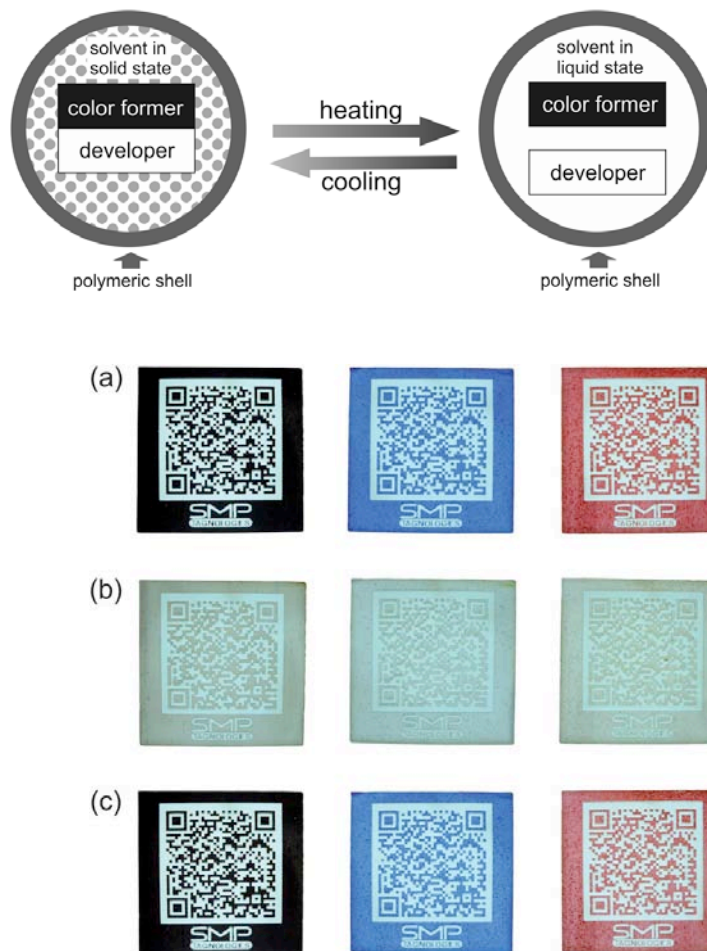


Figure 2.22. Simplified working principle of thermo-reversible color changes in microencapsulated T-PIGs: the polymeric microcapsules remain in a colored state as long as the solvent does not inhibit electronic interaction between color former and developer. Multifunctional QR code carriers at 23 °C (a), 60 °C (b) and 23 °C (c). The QR codes were consistently machine-readable below CST (a and c) and unreadable above CST (b). [95]

Wu et al [97] reported a multi functional SMP based on shape memory polyurethane with covalently connected tetraphenylethylene. The material

displays biocompatibility, reversible mechanochromic, solvatochromic, and thermochromic shape memory effect. The memory chromism represented by the reversible change of emission intensity shows negative correlation with shape fixity, temperature, and existence of solvent. It may be explained that when the soft segments are molten or dissolved in solvent, the shape recovery switch is open, the AIE units are free from crystal binding and can migrate easily to larger areas, thus the AIE units/particles are far apart from each other and the barrier for rotation of phenyl groups is reduced, which lead to the reduction of emission intensity, appeared by no colors or pale colors, and vice versa.

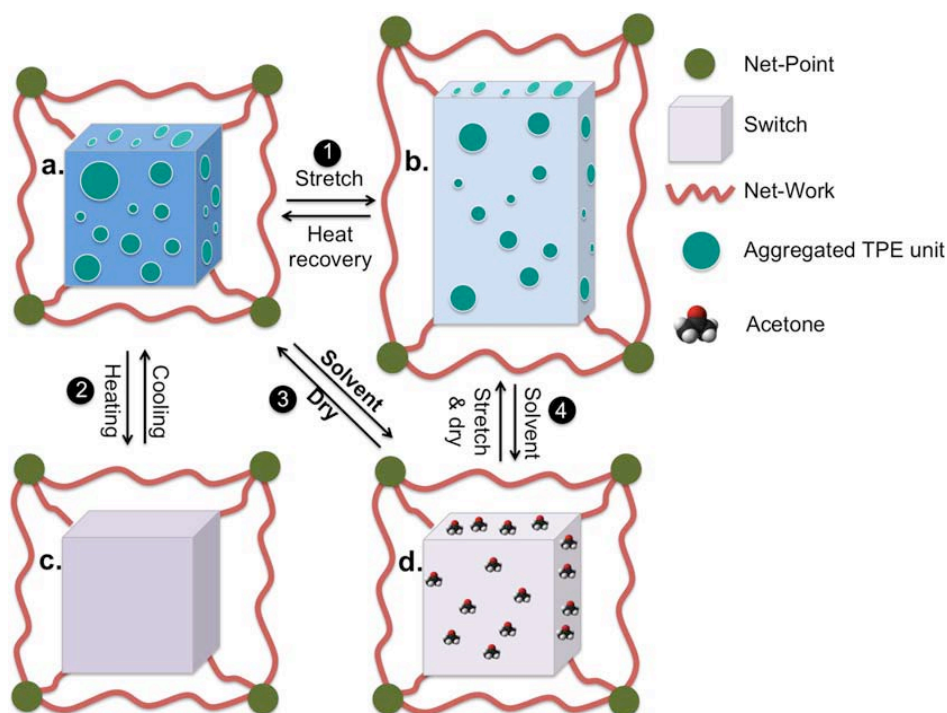


Figure 2.23. A model to illustrate the molecular mechanism during, stretch-recovery process (1), heating-cooling process (2), solvent-dry process (3), and solvent induced shape recovery process (4).

3.3.2. SMPs with Micropatterns

The research on micropatterns has drawn increasing attention because of their

physical properties (e.g. photonic, photonic gaps and mechanical behaviors) could be significantly altered due to change of lattice symmetry, pore size, shape and volume filling fraction.[98] A series of new functional materials with tunable optical properties could be realized when combining micropatterns with SMPs. For example, Yang's group [98] fabricated a shape memory polymer (SMP) membranes consisting of a hexagonal array of micron-sized circular holes and demonstrated dramatic color switching as a result of pattern transformation. The deformed pattern and the resulting color change can be fixed at room temperature, both of which could be recovered upon reheating. Using continuum mechanical analyses, we modeled the pattern transformation and recovery processes, including the deformation, the cooling step, and the complete recovery of the microstructure, which corroborated well with experimental observations. Later, they also introduced gold nanoparticles into the SMP micropillar arrays to realize light-induced tunable transmittance material.[99]

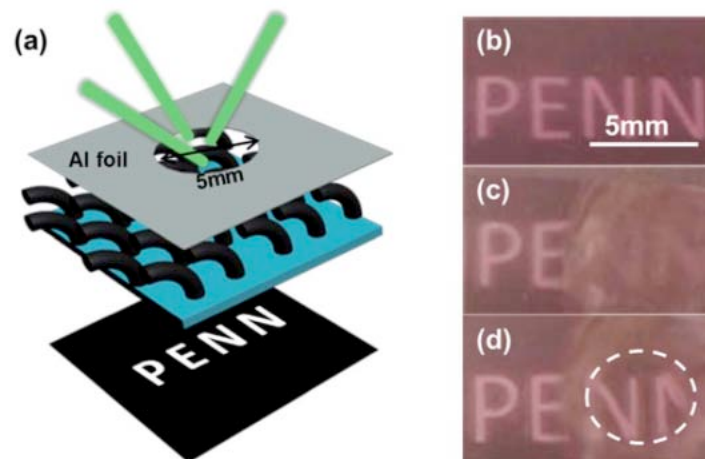


Figure 2.24. (a) Schematic illustration of the setup for localized light exposure. Diameter of the hole in the mask is 5 mm. (b–d) Optical images of SMP-AuNR (SMP-4) micropillars at different stages. (b) Pristine pillars. (c) The right

half of the sample was deformed and became opaque. (d) SMP sample in (c) after laser exposure. The white circle indicates the exposed region. [98]

Despite the tuning of transmittance, the color of SMPs could also be tuned by the micropatterns. Photonic systems with the capability to respond to different stimuli are more and more desirable for achieving multifunctionality and higher levels of performance.[100] Xu et al [101] fabricated a tunable micro-optic (microlens and microprism arrays to diffraction gratings and holograms) by a crosslinked poly(ethylene-co-vinylacetate) based SMP. The precise replication of surface features at the micro- and nanoscale and the formation of crosslinked shape memory polymer networks were achieved in a single step via compression molding. Further deformation via hot pressing or stretching of micro-optics formed in this manner allows manipulation of the microscopic surface features, and thus the corresponding optical properties. Due to the shape memory effect, the original surface structures and the optical properties can be recovered and the devices be reprogrammed, with excellent reversibility in the optical properties. Furthermore, arrays of transparent resistive microheaters can be integrated with deformed micro-optical devices to selectively trigger the recovery of surface features in a spatially programmable manner, thereby providing additional capabilities in user-definable optics.

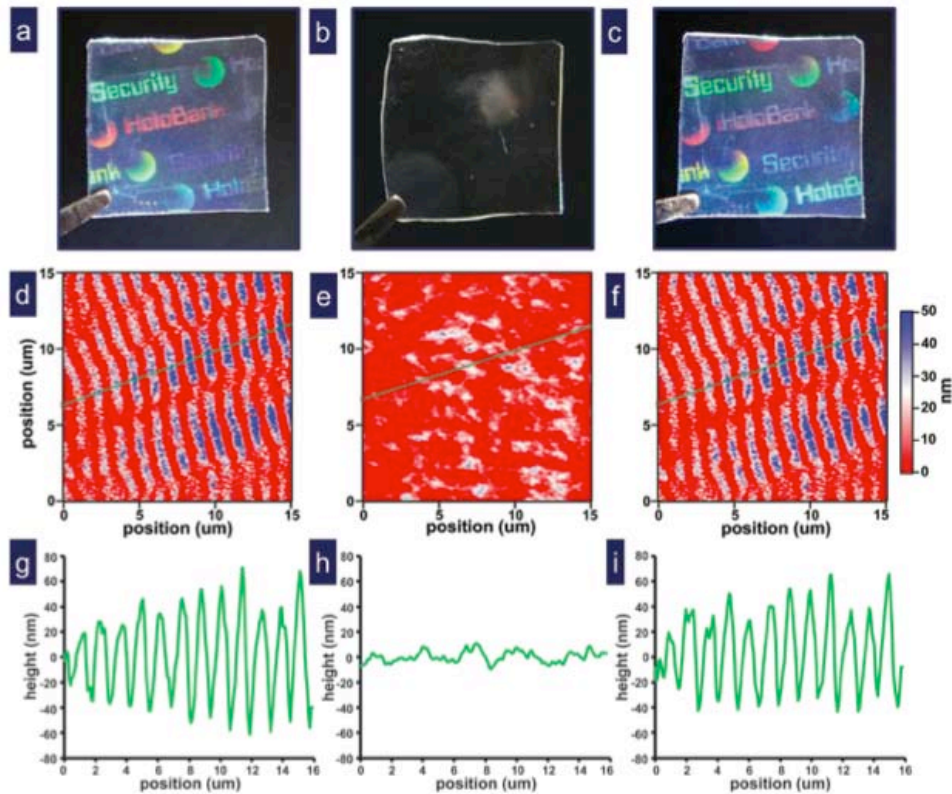


Figure 2.25. Shape deformation and recovery of an SMP hologram. Optical images of the a) original, b) deformed, and c) recovered hologram under white light illumination. Topographic AFM images of the d) original, e) deformed, and f) recovered holographic structure. The corresponding height profiles are shown below (g–i). [101]

SMPs with micropatterns can be further utilized as optical sensors. It was shown that, by using a simple procedure based in replica molding, it was possible to engrave a nanostructured pattern (say, hexagonal) from a colloidal crystal template in the surface of the SMPs. By doing so, Espinha et al[102] showed that the lattice parameter of the 2D grating was programmable and dependent of the strain imposed to the polymer. Secondly, it was feasible to temporarily erase the surface nanopattern from the optical point of view.

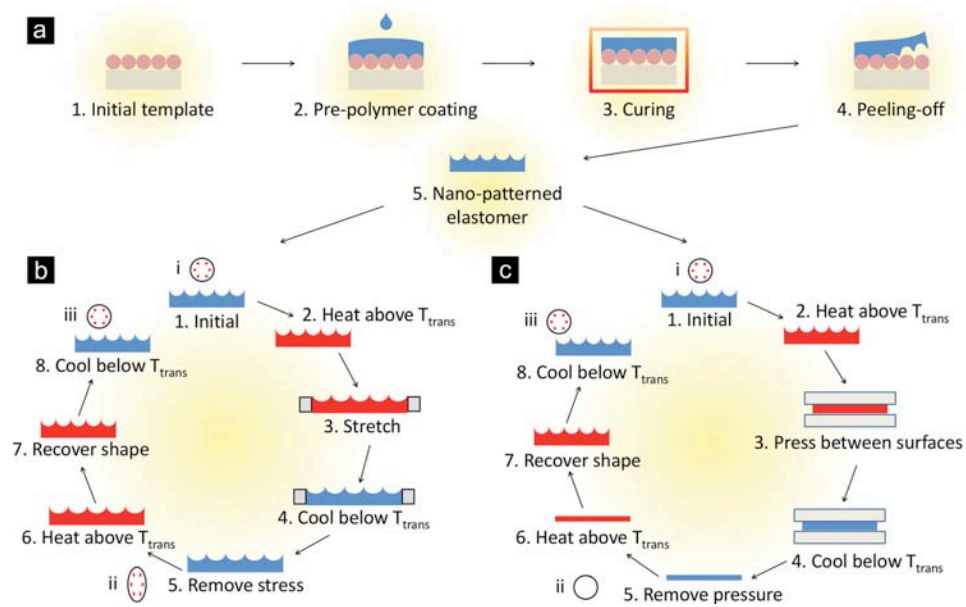


Figure 2.26. Scheme of the protocol followed for the grating imprint on the PDDC-HD elastomer surface (a) and study of its programmable shape-memory properties either varying the lattice parameter (b) or erasing the surface nanotopography (c). [102]

2.3.7. Biomedical Functions

The stimuli induced shape changing was also embedded into biomedical applications, several prototypes including self-tide suture, vascular stent, clot removal and artificial tissues were also developed. However, the complexity and high hindrance of biomedical device also requires SMPs with biological functions, such as bio-compatibility, bio-degradability, drug release and anti-bacterial. Biocompatibility is the very basic requirement of biomedical applications, which refers to the ability of a material to perform with an appropriate host response. Usually researchers will employ cytotoxicity study of a sample/specimen to evaluate the biocompatibility, then move to animal test and finally clinical trails. Biodegradable biomedical device is also fueled with

technical importance because it may resolve the problem of second surgery to remove previously implanted devices such as stent and strews.

Over the last decade, different biocompatible and biodegradable SMPs have been developed composed of biocompatible polyester-type diols (e.g., PCL, polylactide (PLA), polyglycolide and their copolymers), and polyether-type diols to cover wide range of biomedical applications like the controlled drug release, stents, sutures, cellular signaling etc. They provide enhanced capabilities like the achievement of adjustable hydrolytic degradation rate, the switching temperature around body temperature, excellent shape memory property etc. However, the content of urethane units as junction points is extremely small in such SMPs, and they are not considered to constitute hard segments as above-mentioned classical SMPs. For biocompatible segmented SMPUs, the polymeric blocks (e.g, PPDO, PLLA) with high T_{trans} are used as hard segments, to offer physically cross-links. The chemically cross-linked SMPs have also been fabricated by using special polyesters with tri- or tetra-functional reactive groups coupled by urethane units [103].

From 2006, after Lendlein et al first published a work regarding the self-tighten sutures, the attention on biomedical applications of SMPs is increasing. The basic requirement of material for biomedical application should be biocompatible, non-toxic and biodegradable (except artificial bones). Biodegradability is an important function which could solve the problem of second time operation for removing implanted devices. So far different prototypes have been fabricated including biodegradable sutures, bone repair

materials, scaffold for tissue engineering and vascular stent. Typical soft-segments for constructing biodegradable SMPs includes PCL, PLA, PGA and their copolymer with suitable transition conditions. Recently, biodegradability is usually introduced into SMPs together with other functions like self-healing[100], magnetic responsiveness[104, 105], light responsiveness[106], drug release[107], temperature memory[108] and two-way shape memory effect[84], enabling a multi-functional material.

The potential of PU as both SME and bio-functions would not have been noticed until Lendlein et al. [24] published their work on biodegradable SMPU for mini invasive applications. Several basic criteria like biocompatibility, biodegradability, intoxicity, non-antigenic etc. are crucial for the application of SMPU as biomaterials. To satisfy such requirements, the proper choice of both soft segment and hard segment is very important. Typical choices of soft segment are polylactic acid (PLA), polycaprolactone (PCL), polyglycolide (PGA) and their copolymers (both random- and block-). Most of the SMPUs are biocompatible and the degradation products of soft segment remain biocompatible, but the bio-degradability of hard segment may display in different way. Aromatic isocyanates (say MDI and TDI) based SMPUs do not offer biodegradable products and produces residual benzene moiety after degradation. These products are highly carcinogenic and harmful to living organism. On the contrary, aliphatic diisocyanates cause less side effects, especially the lysine-derived diisocyanate (LDI), whose degradation product is lysine and won't significantly affects the pH value around. Therefore, hard segment made of aliphatic isocyanates should be preferred to derive

biodegradable products.

Despite the biodegradability, another attractive bio-function is the antibacterial property. The mechanism of antibacterial property obtained here is similar to other polymeric system including addition of inorganic nano-particles, quaternary ammonium salt, natural products with antibacterial properties or apply plasma treatment. Zhu et al [109] reported a series of SMPU ionomers which exhibit both SME and antibacterial property. The polymer was synthesized by employing PCL, N,N-bis(2-hydroxyethyl)-isonicotinamide as soft segment and MDI, BDO as hard segment (with HSC=25%). They found good antibacterial activity for the above SMPU system, and the rate of reduction of bacteria (*Staphylococcus aureus*) was 100%. Hu et al. [110] also reported a novel SMPU system with core-shell structure performing both good SME and excellent anti-bacterial property. They fabricated the SMPU nanofibers with using coaxial electrospinning and used the core solution of PCL based SMPU and shell solution of pyridine containing SMPU. The introduction of pyridine into the soft segment of the shell solution resulted in excellent antibacterial property against both gram-negative and gram-positive bacteria.

2.4. Supra-molecular Shape Memory Polymers

Generally, polymers exhibit shape memory functionality if the material can be stabilized in the deformed state within the particular application temperature range. This can be reached by using polymer network chains equipped with one kind of molecular switch.

The flexibility of chains should be a function of the temperature in the thermal-induced SMPs. One possibility for a switch function is a thermal-transition of the network chains. At the temperature above $T_{BtransB}$, the chains are flexible; whereas the flexibility of the chains is partly limited at below this $T_{BtransB}$. These functions can be achieved due to the glass transition between the rubber-elastic or viscous state to the glassy state in the T_{BgB} -type-SMPs, or the strain-induced crystallization by cooling the material in the T_{BmB} -type-SMPs. Whereas the permanent shape of SMP networks is stabilized by covalent or non-covalent netpoints with the higher transition temperature (T_{BpermB}).

In fact, the glass transition and the strain-induced crystallization are related to the inter-molecular force. The inter-molecular force plays a key role in the phase transition of reversible phase and the formation of hard domains. Particularly, the inter-molecular hydrogen bonding influences greatly the thermo-mechanical properties of SMPs. For example, in the SMPU composed of hard segments and soft segments, hydrogen bonding between C=O group and N-H influences the phase separation and the formation of hard domains.

Furthermore, the formation of hydrogen bonding is highly sensitive to a change of temperature, concentration of ion and other parameters. One example is that the poly(carboxylic acid)s form inter-molecular complexes with poly(ethylene glycol)(PEG) due to the hydrogen bonding formed between the carboxyl groups of poly(carboxylic acid)s and ether oxygen atoms of PEG. This hydrogen-bonded complex is highly sensitive to a change in the concentration or molecular weight of PEG, temperature and other parameters. In this way, shape memory properties with a shape recovery of 99% are observed in the

poly(acrylic acid-co-methyl methacrylate)/PEG complexes due to their large difference in storage modulus below and above T_{tran} .

Additionally, it was proposed that the thermo-reversible, non-covalent interactions could be utilized in SMPs as many kinds of supramolecular polymers were developed from small molecules or oligomers. Recently; this proposal was confirmed in the cross-linked polymer networks containing only a small fraction of reversibly associating side-groups like ureidopyrimidinone (UPy). In this system, hydrogen-bonding interactions can stabilize mechanically the strained states in polymer elastomers.

Anthamatten et. reported their work by introducing UPy unit into polymer network by radical polymerization. [111] As shown in **Figure 2.10**, a novel type of shape-memory polymer that contains site-specific, thermo-reversible interactions was fabricated. The shape-memory effects can be observed in a lightly crosslinked polymer network containing only a small fraction (ca. 2 mol %) of UPy pendent side-groups. According to their findings, the mechanically strained states in polymer elastomers can be stabilized by H-bonding interactions alone, resulting in strain fixity of about 90 % and strain recovery of about 100 %. They contribute the lack of complete strain fixity to the elasticity of the material itself. They also pointed out that the unique feature of the new shape-memory polymer is the dynamics of its shape-memory response.

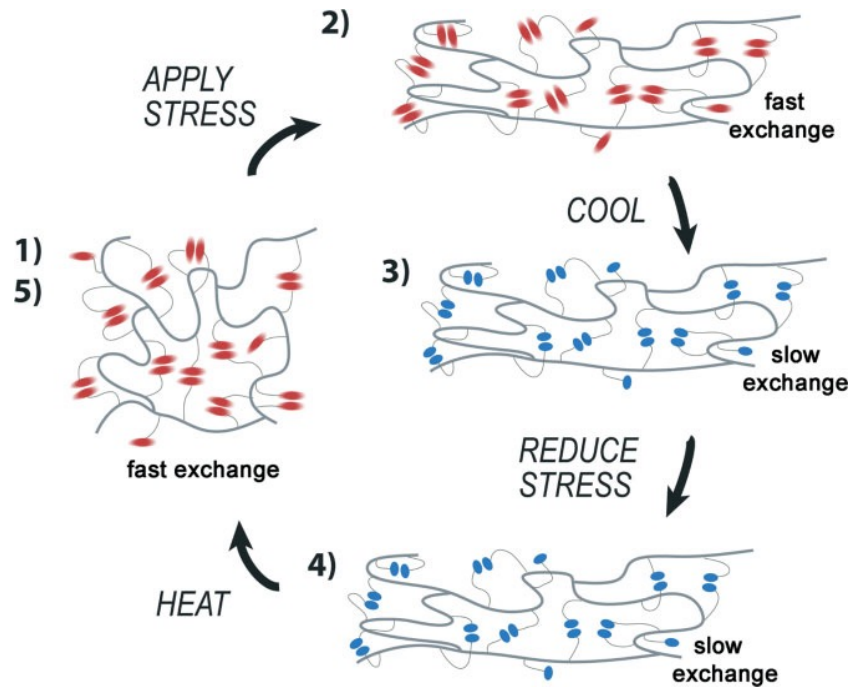


Figure 2.27 Synthesis routine of SMP containing UPy side-groups. [111]

By introducing self-complementary quadruple hydrogen bonding units (UPy) in soft segments, Hu etc later [112] fabricated a kind of thermoplastic shape memory polyurethane that can present a significant shape memory effect under the usually used thermodynamic programming condition. (as shown in **Figure 2.11**) Compared with the control sample, it was observed that the introduction of UPy into soft segments increases the glass transition temperature from 28.3 °C to 73.3 °C. The temporary deformation can be thus fixed well after cooling at room temperature; later thermal induced shape memory recovery can be triggered by raising the temperature to 86°C. The immediate shape recovery ratio and shape fixity ratio can be 95.8% and 95.9%. Even after 24 hours relaxation for the stretched films, the corresponding R_r and R_f can be 94% and 60%. In contrast, the sample without quadruple hydrogen bonding shows that the elasticity and the deformation cannot be fixed after 24 hours relaxation.

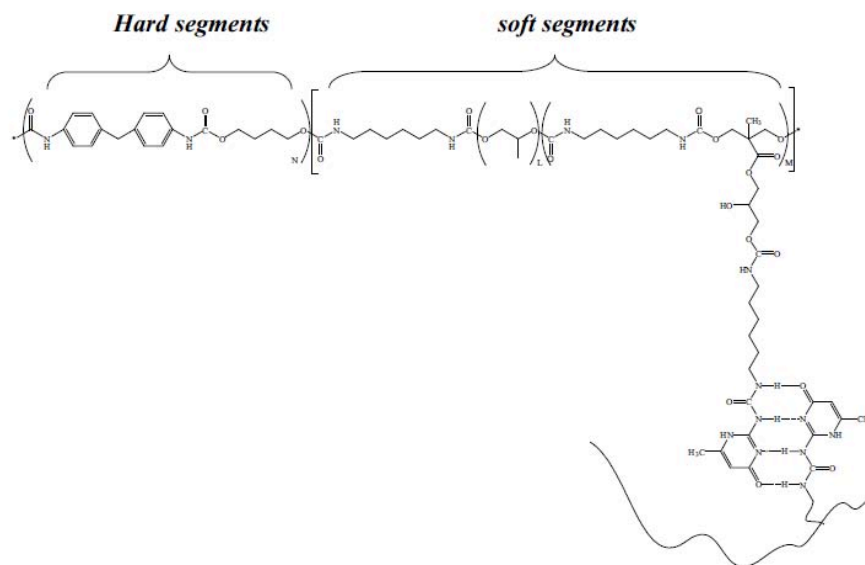


Figure 2.28. Molecular model of SMPU with UPy switch[112]

Later in 2012, Matiland etc.[113] introduced UPy unit to Tg-SMPU, and thus realized triple-shape memory polymer. (As shown in **Figure.2.12**) Triple shape properties arise from the combination of the glass transition of (meth)acrylate copolymers and the dissociation of self-complementary hydrogen bonding moieties, enabling broad and independent control of both glass transition temperature (Tg) and cross-link density. Specifically, ureidopyrimidone methacrylate and a novel monomer, ureidopyrimidone acrylate, were copolymerized with various alkyl acrylates and bisphenol A ethoxylate diacrylate. Control of Tg from 0 to 60 °C is demonstrated: concentration of hydrogen bonding moieties is varied from 0 to 40 wt %; concentration of the diacrylate is varied from 0 to 30 wt %. Toughness ranges from 0.06 to 0.14 MPa and is found to peak near 20 wt % of the supramolecular cross-linker. A widely tunable class of amorphous triple-shape memory polymers has been developed and characterized through dynamic and quasi-static thermomechanical testing to

gain insights into the dynamics of supramolecular networks.

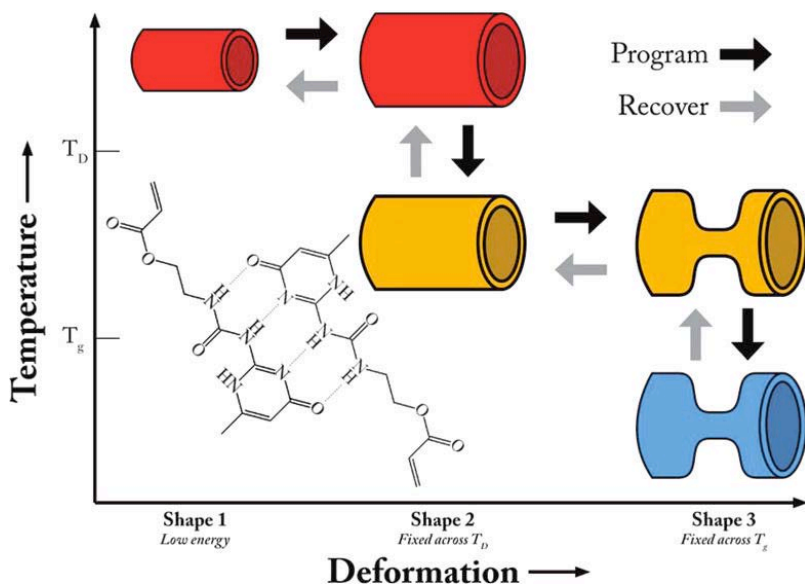


Figure 2.29 Triple-shape memory polymer containing UPy unit. [113]

In addition, supramolecular physical netpoints were also achieved through the inclusion between α -CD or γ -CD and PCL or PEG by Zhang et al. [114-117]. In their system, the α -CD or γ -CD inclusion crystallites with PEG or PCL served as a fixing phase while the naked PEG crystallites and PCL crystallites served as a reversible phase. (shown in Figure.2.13)

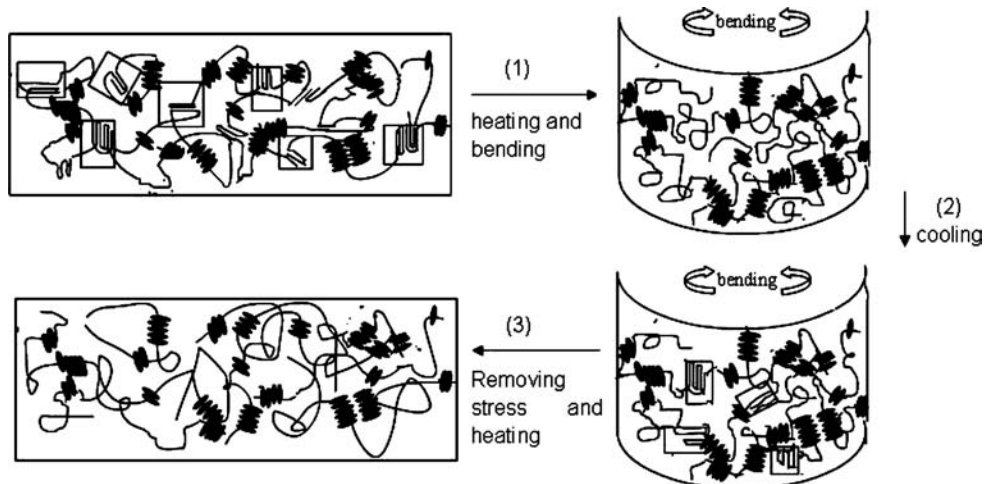


Figure 2.30. Schematic representation of the proposed chain structures.

Therefore, these various investigations imply that there are close relationship between shape memory functionality and supramolecular chemistry. The molecular design of SMPs should consider carefully the non-covalent interactions in particular the hydrogen bonding. In this condition, the introduction of large fraction of hydrogen-acceptors and hydrogen-donors in polymer chain would influence greatly the properties of SMP networks including the shape memory properties.

CHAPTER 3 EXPERIMENTAL

This chapter includes synthesis of SMPUs with different forms and the characterization techniques to prove their molecular structure, shape memory behavior, and other functionalities.

3.1 Material and equipment

The main raw materials used in this project are tabulated in **Table 3.1** with the suppliers' information. The main equipments used in the study are shown in **Table 3.2**.

Table 3.1 Raw materials used in the synthesis of SMPUs

Chemical	Abbreviation	Supplier	
Poly(ϵ -caprolactone)	PCL	Daicel Industrial	Chemical
poly(tetramethylene ether) glycol	PTMEG, Mn=1000	Aldrich Company	Chemical
PPG-diamine	PPG230, Mn=230	Aldrich Company	Chemical
benzil dimethyl ketal,	DMPA	Aldrich Company	Chemical
hydroxyethyl methacrylate		Aldrich Company	Chemical
Oxiranylmethanol		Aldrich Company	Chemical
1,6-diisocyanatohexane	HDI	Acros	
4,4-diphenylmethane diisocyanate	MDI	Aldrich Company	Chemical
1,4-butanediol	BDO	Aldrich	Chemical

		Company	
N,N-dimethylformamide	DMF	Aldrich Company	Chemical
1,2-bis(4-hydroxyethoxy phenyl) 1,2-biphenyl ethylene	TPE	Prof. Tang group	Benzhong's
Zinc di[bis(trifluoromethylsulfonyl)imide]		Aldrich Company	Chemical
N-methyl-1,2-phenylenediamine		Aldrich Company	Chemical
pyridine-2,6-dicarboxylic acid		Aldrich Company	Chemical
acetonitrile (HPLC degree)		Aldrich Company	Chemical
sodium carbonate		Aldrich Company	Chemical
chloroform (HPLC degree)		Aldrich Company	Chemical
Methanol (HPLC degree)		Aldrich Company	Chemical
dichloromethane (HPLC degree)	(HPLC degree)	Aldrich Company	Chemical
Poly(phosphoric acid)		Aladdin Reagents Co., LTD	
Neopentyl glycol diglycidyl ether	NGDE	Daicel Industrial	Chemical
diglycidyl ether of bisphenol A	E51	Daicel Industrial	Chemical
Gold nanoparticles (d=10nm)	AuNPs	Aldrich Company	Chemical
acetone (HPLC degree)		Aldrich Company	Chemical
2,6-dihydroxymethyl pyridine	HMP	Acros	
poly(4-vinyl phenol)	PVP	Sigma Aldrich	

Hexaphenylsilole	HPS	Prof. Tang Benzhong's group
Multiwalled carbon nanotube	MWCNT	Chengdu Organic Chemicals Co., Ltd of Chinese Academy of Sciences

Table 3.2 The main equipment used in the project

Equipment	Supplier
Cryo-ultramicrotome-Frigocut 2800E	Leica Inc.
Diamond Differential Scanning Calorimeter	Perkin-Elmer Inc.
Diamond Dynamic Mechanical Analyzer	Perkin-Elmer Inc.
Digital camera	Pixera Corporation, Japan
Fourier Transform Infrared Spectroscope-2000	Perkin-Elmer Inc.
Instron 5566	Instron Corporation, USA
JM-500ZGX Vacuum Drying oven	Jinma Electronic Light Technological Research Institute, China
Scanning Electron Microscopy-Leica Stereoscan 440	Leica Camera AG Corporation
Muffle Furnace	Carbolite Corporation
Scanning Probe Microscope	Seiko Instruments Inc.
Small Angle X-ray Scatter	Bruker Corporation
Ultrasonicator	Shanghai Sheng PU Ultrasonic Equipment Factory
Vacuum Oven	Sheldon Manufacturing, Inc.
Waters Gel Permeation Chromatography	Water Corporation
Photoluminescent	SLM 8000C spectrofluorometer
Ultra-fast time-resolved fluorescent spectrometry	Designed in Prof. KS Wong's Group in HKUST

UV source	SunSpot SM 2 from Shenzhen Wisbay M&E Co., LTD
Laser source	Optlaser model G2000 532nm laser module
Transmission electronic microscope	JEOL JEM-2011 TEM
2-D X-ray Diffraction	Oxford Diffraction
Wide Angle X-ray Diffraction	Philips Corporation

3.2 Preparation of Functional SMPs

3.2.1 Synthesis of Memory Chromic SMPUs Films

The 1,2-bis(4-hydroxyethoxy phenyl) 1,2-biphenyl ethylene (TPE units) were synthesized according to the literature.[118]

Bulk polymerization of shape memory polyurethane 6.91g PCL powder were added to the flask with mechanical stirring, then dehydrate at 353K for at least 2 hours. Then the system was cooled down to 343K and filled with nitrogen. Then 0.55g HDI and 0.02% wt catalyst (Dibutyltindilaurate, dissolved in 0.1mL MDF) were added via syringes. After heating and stirring for 0.5 hour, related amount of dye (solved in 0.1 mL DMF) was injected and kept stirring for another 0.5 hour. Then 1.51g HDI and 0.94g BDO were added dropwise, and the temperature was raised to 353K for another 15mins. Then the reaction system was sealed and removed to oven under 373K over night. Then the sample was taken out and solved in proper amount of DMF, then precipitated in methanol, then put into vacuum oven until stable weight. $M_n=1.58 \times 10^4$ Da, $PDI=2.10$, $T_{trans}=37.0^\circ\text{C}$.

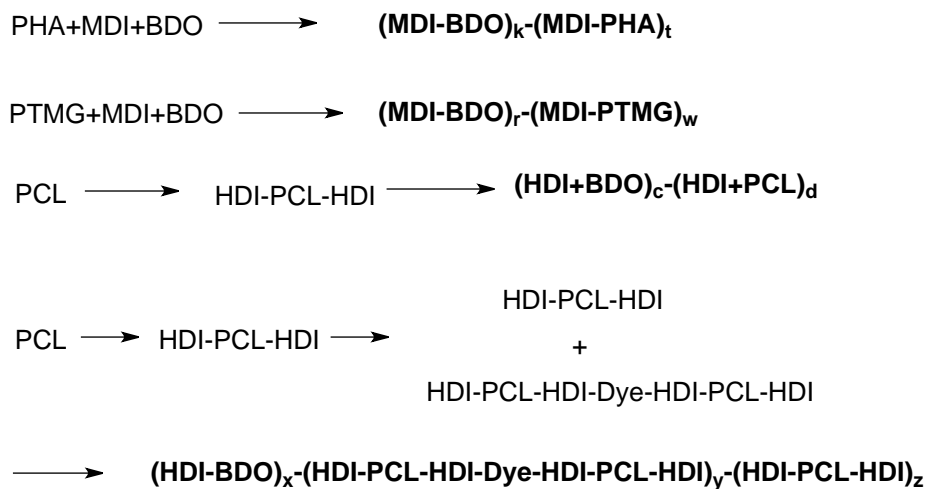


Figure 3.1. Illustration of general synthesis procedure of SMPUs

Preparation of the memory chromic SMPU film All the film in this paper are prepared by solving 1.0g polymer and related amount of dye in DMF of 100°C, then casting into preheated Teflon mold(10cm×10cm) and put into oven at 70°C for 12 hours. The obtained film was measured by micrometer and the part with thickness around 0.1 mm was cut with 1 cm in width and 7cm in length for further photo-luminescent measurement.

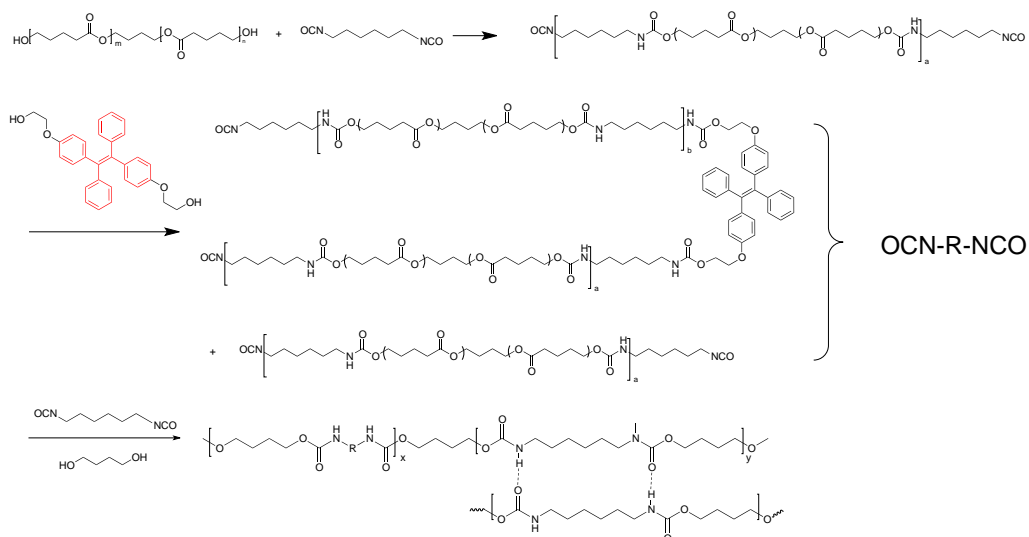


Figure 3.2. Illustration for the polymerization of SMPUs with covalently connected TPE units.

3.2.2 Preparation of stand-free two-way shape memory polymers by interpenetration network

Synthesis of epoxy terminated PTMEG macromonomer: dry PTMEG (9.00g, 9mmol) and HDI (3.16g, 18.8mmol) was added into a flask with mechanical stirring and filled with nitrogen, then the system was heated to 80°C, then dibutyltin dilaurate (0.02% wt) was added, the reaction was traced by IR every 30mins, until the ratio of peak strength at 2926 cm^{-1} to 2272 cm^{-1} became constant. Then the system was cooled to room temperature, then oxiranemethanol (1.42g, 19.2mmol) was added dropwise with mechanical stirring. Then the system was heated to 40°C with constant stirring for one hour, and subsequently heated to 70°C, the reaction is also traced by IR detection till the peak at 2272 cm^{-1} disappear. The reaction mix was poured out and sealed at room temperature.

Synthesis of 2-Hydroxyethyl acrylate terminated PCL macromonomer: dry PCL (5.09g, 1.27mmol) and HDI (0.45g, 2.67mmol) was added into a flask with mechanical stirring and filled with nitrogen, then the system was heated to 80 °C, then dibutyltin dilaurate (0.02% wt) was added, the reaction was traced by IR every 30mins, until the ratio of peak strength at 2926cm^{-1} to 2272cm^{-1} became constant. Then 2-hydroxyethyl acrylate (0.35g, 3.01mmol) was added dropwise with mechanical stirring, the reaction is also traced by IR detection till the peak at 2272cm^{-1} totally disappear. Then the reaction mix was poured out and sealed at room temperature.

Synthesis of interpenetration polymer network: The IPNs were synthesized with different ratio of PCL/PTMEG content. (as see table 1). For example, epoxy terminated PTMEG macromonomer(1g), 2-Hydroxyethyl acrylate terminated PCL(1g), benzil dimethyl ketal (0.04g) and PPG-diamine(0.05g) were firstly solved in DMF(4ml) at room temperature. The solution was then poured into a mold (2 cm in width and 6 cm in length), UV lamp (80W) was subsequently applied at 12cm top of the mold for 2 hours. Then the pre-IPN became gel-like and was stretched to 100% and fixed on a PTFE mold, then transfer to 80°C oven for overnight.

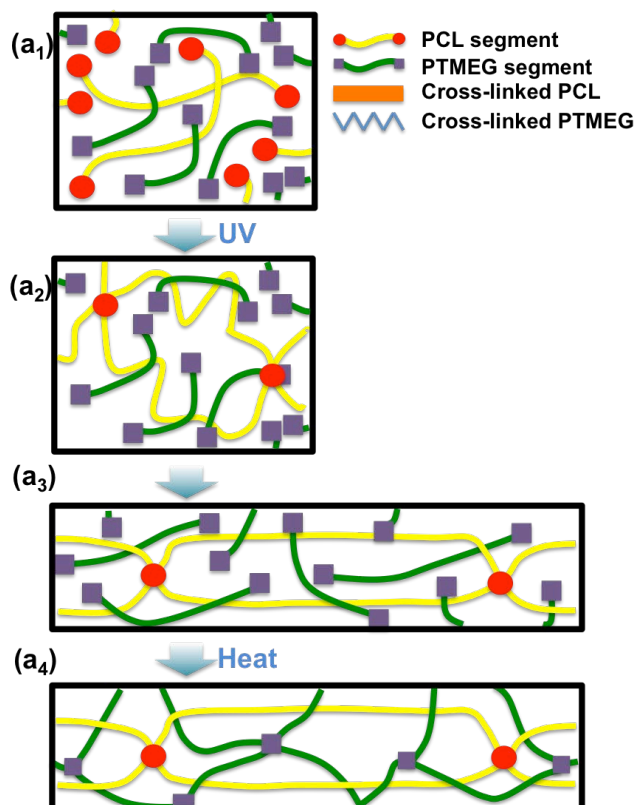


Figure 3.3. Illustration of synthesis procedure of stand-free two-way shape memory polymers

3.2.3 Preparation of Light/Heat dual sensitive SMP nanocomposites

3.2.3.1 Synthesis of UV/Heat dual sensitive SMP nanocomposites

Synthesis of 2,6-Bis(1-methylbenzimidazol-2-yl)pyridine (Mebip) and related Zinc complex were synthesized according to literature with slight modification.[119-121]

Synthesis of SMP nanocomposite: The molar ratio of the liquid epoxy precursor for all the SMP samples was E-51/NGDE/Jefamine = 2:1:3. Weighted nanoparticles (Bulk $\text{Zn}(\text{Mebip})_2(\text{NTf}_2)_2$ in $\text{CH}_2\text{Cl}_2/\text{MeCN}$) were dispersed into the mixture of E51 and NGDE first, then the solvent was removed under vacuum. The nanoparticles was further dispersed by ultrasonication for 10 mins. Next, Jeffamine was added into the dispersion. The obtained mixture was

further mixed mechanically for 30s before cured. The multicomposite SMP was synthesized in two steps. First, the neat SMP monomer solution was partially cured for 60 mins at 80°C in a 7.5cm×2.5cm Teflon mold. Then, the neat SMP was evenly cut into 2 pieces in the long axis and leave the right part in the mold. (the left side were left blank) Finally, the Zn(Mebip)₂-SMP monomer solution were casted into the related blank part of the mold and fully cured. The overall measurement of the demonstration sample is 75mm×2mm×1mm. Two composite region are both 25mm in length. The mass ratio of Zn(Mebip)₂ in the region are 10%.

3.2.3.2 Synthesis of Visible Light/Heat dual sensitive SMP nanocomposites

The molar ratio of the liquid epoxy precursor for all the SMP samples was E-51/NGDE/Jefamine = 2:1:3. Weighted nanoparticles (PVP protected AuNPs in CH₃Cl[122]) were dispersed into the mixture of E51 and NGDE first, then the solvent was removed under vacuum. The nanoparticles was further dispersed by ultrasonication for 10 mins. Next, Jeffamine was added into the dispersion. The obtained mixture was further mixed mechanically for 30s before cured. The multicomposite SMP was synthesized in two steps. First, the neat SMP monomer solution was partially cured for 60 mins at 80°C in a 7.5cm×2.5cm Teflon mold. Then, the neat SMP was evenly cut into 2 pieces in the long axis and leave the left part in the mold. (the right side were left blank) Finally, the AuNPs-SMP monomer solution were casted into the related blank part of the mold and fully cured. The overall measurement of the demonstration sample is 75mm×2mm×1mm. Two region are both 32.5mm in length. The mass ratio of

AuNPs/PVP in left region is 10%, while the sole mass ratio of AuNPs is 0.003%.

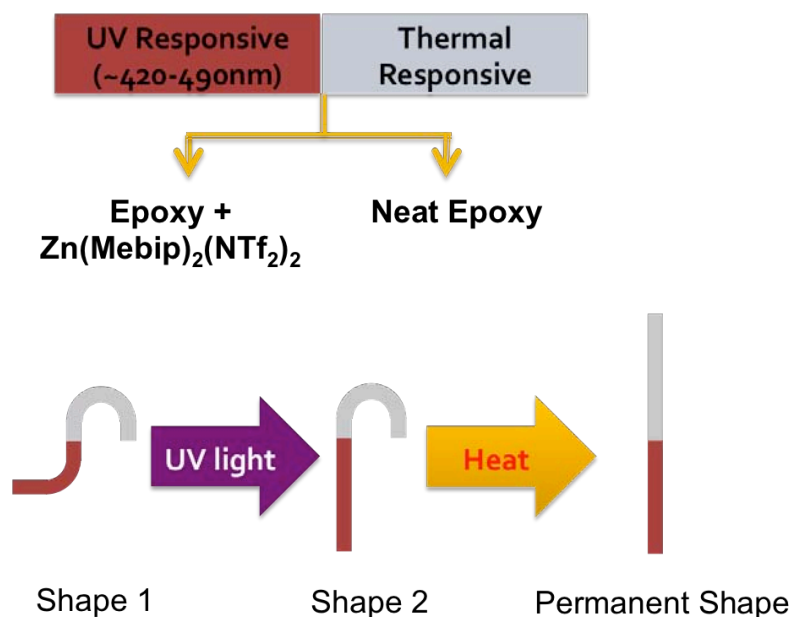


Figure 3.4. Fabrication method of light/heat dual sensitive triple shape memory polymer.

3.2.4 Preparation of SMPUs with supra-molecular switches for moisture management

Synthesis of supra-molecular shape memory polymer (Supra SMP 1&2)

The Supra-SMPs were synthesized with different hard segment content as shown in table below. For example, DHMP (2.90g, 20.8mmol) were first solved in DMF (10mL) at 45°C for 5 mins to get a transparent solution. Then HDI (3.34g, 19.8mmol) was added into the mixture dropwise with stirring. The solution was maintained at 45°C for another 60mins with mechanical stirring. Then a solution with HDI (1.40, 8.3mmol) and BDO (0.68, 7.5mmol) in DMF (10mL) were poured into the reaction system. Then the reaction system was stirred at 45°C for another 5 hours. Then the solution was casted into a pre-

heated Teflon mold (10cm×10cm) and put into 60°C oven for 24 hours, then transfer to vacuum oven at 50°C for another 24 hours.

Table 3.3. Receptie of Supra-SMPs

	DHMP (g)	HDI (g)	MDI (g)	BDO (g)	HSC (%)
Supra-SMP1-25	2.9	3.34	1.59	0.48	25
Supra-SMP1-35	2.9	3.34	2.53	0.82	35
Supra-SMP1-45	2.9	3.34	3.81	1.29	45

	DHMP (g)	HDI (g)	HDI (g)	BDO (g)	HSC (%)
Supra-SMP2-25	2.9	3.34	1.395	0.684	25
Supra-SMP2-35	2.9	3.34	2.226	1.134	35

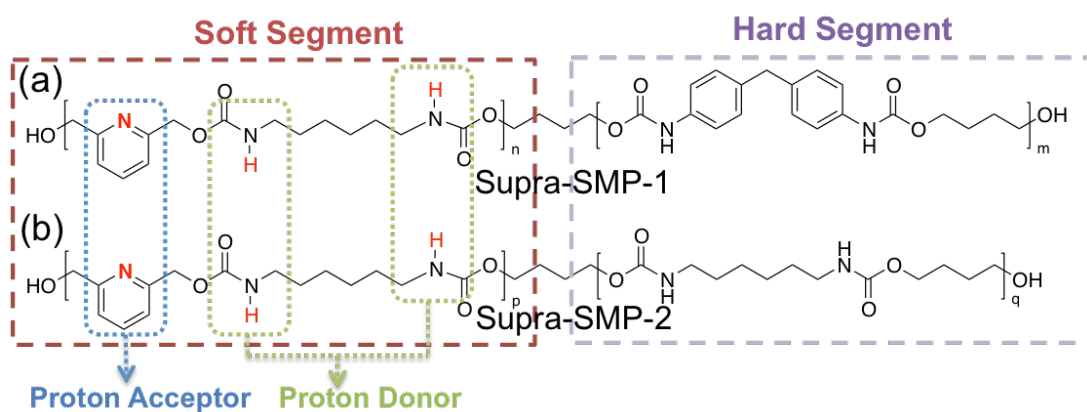


Figure 3.5. Polymer structure of Supra-SMPs.

3.3 Characterization techniques

3.3.1 Molecular weight test

The molecular weight of the SMPU samples was assessed using a Waters gel permeation chromatography (GPC) system equipped with a refractive index detector (Waters 2414 refractive index detector) and a UV detector (Water 2489 Uv/Visible Detector) equipped with a Waters Styragel HR4 (for DMF) column. A Waters 1515 Isocratic HPLC pump was used. The refractive index obtained by the Waters 2414 refractive index detector was employed for data analysis. The solvent used was high performance liquid chromatography DMF. It was ultrasonicated before use to get rid of trifle bubbles which may affect the refractive index. The temperature of the column and refractive index detector was 30°C. The standard calibration curve was obtained by using narrow distributed polystyrene-medium molecular weight calibration kit provided by Polymer Laboratories. The flow rate was 1.0 mL/min. The concentration of the standard samples and polyurethane samples were prepared in DMF at a concentration of about 0.25-0.1% following the column specification. The number-average (M_n) and weight-average (M_w) were determined and the polydispersity index was calculated for each polymer using a Breeze GPC soft ware.

3.3.2 FTIR spectrometry

The FTIR transmission and reflection spectra were determined by using a Perkin-Elmer spectrometer in the region of 700–4000 cm^{-1} at the ambient temperature. The SMFs were cut into small sects and each sample was scanned

16 times at a resolution of 2 cm^{-1} and the scan signals were averaged. The FTIR spectra of shape memory bulks were obtained by using a Perkin-Elmer universal accessory. To make a comparison, all IR spectra were normalized by using the height of the 1412 cm^{-1} peak, assigned to the C—C stretching mode of the aromatic ring [123-125].

3.3.3 Melt flow index

The melt flow index (MFI) was tested with a Davenport melt flow indexer MFI-10. Samples were pre-heated in a barrel held at 210°C for 6 minutes. The test was conducted five times and averaged on each polymer melt.

3.3.4 Mechanical property test

The fiber tenacity was tested with the tensile tester Instron 4411 following the standard ASTM D2256. The sample gauge length between clamps was 20 mm and the stretching speed was 300 mm/min. Fiber cross-section areas were measured from the cross-sectional photos taken by using an optical microscope (X 400 times). Film samples of $60 \times 5 \times 0.5\text{ mm}^3$ in dimension were cut out from the cast films. The sample gauge length was 20 mm. To make a comparison with the shape memory fiber, the film tensile strength was also measured following the specification of ASTM D-2256, where the stress unit was cN/dtex while not MPa. For fibers, the tensile speed was 10 mm/min and load cell 5 N. For films, the tensile speed was 10 mm/min and load cell 2.5 kN. Measurements on each sample were repeated 10 times to obtain average values.

3.3.5 Shape memory effect test of SMPs

For memory chromic SMPU The shape memory properties were measured with Perkin-Elmer Diamond Dynamic Mechanic Analysis in the SS control mode. Due to the limit of the stress that could be applied by this machine, the polymer film was cut into about 2.0mm width. Initial length of the testing was set to 10.00mm. In each testing cycle, the test was set to begin from 0°C (20°C for the first cycle) to 55°C at heating rate of 2°C/min with constant force of 5mN. Then 1205mN (for the 1st and 2nd cycle, while 1505mN was applied for the 3rd and 4th cycle) force was applied to the film and hold for 5 mins. Then the temperature was cooled down to 0°C at a cooling rate of 2°C/min while maintaining the force to fix the temporary shape. Then the applied force was recovered to 5mN and the polymer was heated to 55°C again at same heating rate.

For stand-free 2WSMP The shape memory properties were measured with Perkin-Elmer Diamond Dynamic Mechanic Analysis in the SS control mode with constant tensile of 2mN to avoid bending. The polymer film was cut into about 3.0mm width. Initial length of the testing was set to 15.00 mm. To mimic real application, the tests were set as following,

Step (1): The sample was heated from lab temperature (around 22°C) to 60 °C at the heating rate of 5°C/min.

Step (2): The sample was hold at 60 °C for about 10 mins till fully contracted.

Step (3): Then the chamber was removed to let the sample cool to room temperature for about 25 mins till fully elongated.

For light/heat dual sensitive SMPs Shape fixity (R_f) and shape recovery (R_r) were evaluated by comparing the bending angle, fixed angle, and recovered angle. Samples were heated at 80°C and bend to 180°C (bending angle) and then quenched in ice water for 5 mins. The fixed angle was measured before the samples were reheated to 80°C. The final angle was measured as the recovered angle.[126] For electromagnetic heating at two wavelengths, the SMP composites were cut into rectangular (25mm×2mm×1mm). The UV source was generated from SunSpot SM 2 from Shenzhen Wisbay M&E Co., LTD. The sample surface temperature during heating was recorded with IR camera and IR thermometer.

3.3.6 Photo-luminescent and time-resolved photo-luminescent

PL spectra were recorded on a SLM 8000C spectrofluorometer. Laser pulses of 343 nm were employed as the excitation light source for the PL measurements. The time-resolved PL measurements was carried out according to the literature[127].

3.3.7 Shape recovery stress test

The shape recovery stress tests were also carried out using the same equipment Instron 4466. First, the sample was stretched to 50% strain at a speed of 10 mm/min at ambient temperature and the strain was maintained for 10 minutes to fix the internal stress. Then the upper clamp was retreated to the position where exactly no force was applied to the sample. After 5 minutes, the temperature was increased to 70°C and the stress change versus time was recorded for analysis. The cN/dtex was also used as the unit of recovery stress because most of the test samples were in fiber forms. The linear density of the rectangular

film is obtained similarly as that of the fibers by dividing the film quality by the film length.

3.3.8 Differential scanning calorimetry

The thermal properties of samples were studied using a DSC (Perkin-Elmer, Diamond) with nitrogen as the purged gas. The sample was first scanned from 0°C to 250°C (initial temperature and end temperature may be different for different samples) at a scanning rate of 10°C/min, then cooling down to 0°C at the same scanning rate to remove the thermal history. The sample was subsequently heating to 250°C at the same scanning rate.

3.3.9 X-ray diffraction

The wide angle X-ray diffraction (XRD) data were recorded at a voltage of 40V, 30mA current with a radiation wavelength of 1.542 Å. Spectra were obtained in a range of Bragg's angle $2\theta = 10^\circ \sim 45^\circ$ with scanning step size 0.02° and time per step 1 second. The 2DXRD was conducted on Oxford Diffraction with Cu as X-ray Source at room temperature.

3.3.10 Dynamic mechanical analysis

The DMA test was operated in a tensile mode. The heating rate was 2°C/min, the frequency 1 Hz, and the oscillation amplitude 5.0µm. The test was conducted over the temperature range from -120 to 200°C. The gauge length between the clamps was 15 mm. Modulus was usually calculated by the determined force, the cross-section area and the caused strain employed in testing specimens. If the cross-section area was used in the calculation of stress

and modulus, then the units will be GPa or MPa. Melt spun fibers cross-sectional areas could be measured from the cross-sectional photos taken by using an optical microscope (X 400 times). However, for the wet spun fiber, the cross-section area which was not strictly regular was difficult to measure. Then the resulting data about the storage modulus was obtained by using linear density instead of cross-section areas similar to the calculation of fiber initial modulus in ASTM D2256. The unit of the storage modulus was N/dtex.

3.3.11 Atomic force microscopy

The phase separation morphology of the samples was observed using an atomic force microscope in the tapping-mode under an ambient environment ($22\pm 2^\circ\text{C}$, $45\pm 5\%$ RH). To prepare a section of a fiber, a small piece of fiber was first embedded in epoxy resin one day before the test. After the epoxy was completely solidified, the sample was trimmed to the shape of a pyramid, and its tip was cryo-ultramicrotomed with a diamond blade to form an observation section. NANOSENSORS™ PPP-SEIHR AFM probes (Seiko Instruments / high force constant) was used. The silicon cantilever spring constant was 15 N/m, length 225 μm and resonance frequency 130 kHz. Height and phase images were recorded simultaneously.

3.3.12 Polarizing optical microscopy

A Leitz wetzlar polarizing optical microscope equipped with a Mettler FP 80 hot stage and a controller were used to observe the crystalline morphology. A digital camera was used to capture images in converging white light with analyzer and polarizer crossed. The fiber cross-section was obtained by using

microtome. First, a monofilament was embedded in epoxy resin one day before test. After the epoxy was completely hardened, it was microtomed in the fiber transverse direction with a diamond knife (Micro Star Co.) and a Reichert–Jung Ultracut microtome (at the ambient temperature).

3.3.13 Scanning electron microscopy

The polymer surface and fracture surface images were taken using a Leica Stereoscan 440 (SEM) Scanning Electron Microscopy operating at 20 kV and a JEOL JSM-6335F field-emission scanning electron microscope operating at 5kV. Composite film surface was etched by using DMF.

3.3.14 Small angle x-ray scattering

SAXS (small angle x-ray scattering) tests of SMFs, Elasthan fibers and shape memory films were conducted on the SAXS equipment Nanostar. The x-ray source was Cu K α and the wavelength was about 0.154 nm. Every sample was scanned in the range of 0.14° ~ 2.8° (2 θ) at a scanning rate of 0.05° min⁻¹.

3.3.15 Cytotoxicity test

The cytotoxicity test was conducted by Intertek Testing Service Hong Kong Ltd following ISO 10993-5:1999, biological evaluation of medical devices: tests for cytotoxicity: in vitro methods. The test article was the shape memory fabrics; the negative control was saline; the positive control was natural latex rubber sheeting. Three milliliters of L-929 mouse fibroblast cell suspension were placed into wells of six well, multiwell tissue culture plates, to prepare monolayers of cells. Following incubation, the culture medium was aspirated

from the monolayers. The medium was replaced with serum-supplemented culture medium containing not more than 2% of agar. The agar layer was thin enough to permit diffusion of any leached chemicals. The test article and the negative and positive controls were placed, in triplicate cultures, so that they were in contact with the solidified agar surface. The test article was applied so that the shape memory fabric surface was in contact with the agar. All cultures were then incubated for not less than 24 hours in a humidified incubator at $37(\pm 1)^{\circ}\text{C}$ and $5(\pm 1)\%$ carbon dioxide. After incubation, an inverted microscope was used to examine each culture.

3.3.16 Water vapor permeability

WVP was conducted according to ASTM E96C, desiccant method with slight modification. The polymer films were covered to a glass cup filled with preheated calcium chloride and sealed. The gained weights were recorded every fixed period at different RH.

CHAPTER 4 MEMORY CHROMIC POLY-URETHANE WITH TETRAPHENYLETHYLENE

4.1. Introduction

Shape memory polymers (SMPs) are one group of the most promising smart materials and have drawn increasing interests because of their great potential in different applications such as sensors, actuators, biomedical devices and textiles.[8-10, 30, 128-131] Typical SMPs have networks realized by the formation of well separated hard and soft phases. The hard phase acts as net-points which determine the permanent shape while the soft phase as the switch and can immobilize the temporary shape with different transition stimuli. Take the thermal sensitive SMPs as an example: when they are deformed above the transition temperature (T_{trans}) of soft segments and then cool down, the network will be fixed and the internal stress will be stored (such process is called programming). Upon heating to T_{trans} or above, the internal stress will be released which enables the recovery of the polymer to the origin shape. With the rapid development of SMPs, recent research interest moves to the integration of SMPs with additional functions such as biodegradability, drug release and thermochromism.[128, 132]

Chromic materials, which show emission color or intensity change induced by external stimulus including: temperature, solvent, light, electro-bean, pressure and humidity, have aroused interest in recent years due to their potential applications in both low and high technology areas.[133-135] Taking the advantage of high Φ_F value in the solid state, aggregation induced emission

could select different kinds of stimuli like heat, chemical, magnetic and electronic fields, infrared light and laser to realize the transformation of both shapes and colors of the polymer.

4.2. Polymer Design

For achieving the above objectives, we selected a linear, phase-separated polyurethane as the structural matrix for our polymer system, because the switching of such polymers can be easily adjusted to different temperatures while keeping sharp transitions in narrow temperature ranges by tailoring the molecular weight of the soft-segment and the hard segment contents.[148] The soft-segment we chose to fabricate shape memory polyurethane is oligo-(ϵ -caprolactone)diol ($M_n=4000$) which has biocompatibility, biodegradability, and transition temperature which is close to the body temperature. The hard segment content (HSC) is also essential to realize the outstanding shape memory effect and recovery force. Previous studies indicated that HSC ranging from 20% to 30% could provide relatively high recovery stress and benefit to phase separation.[149] Besides, as aromatic di-isocyanates processes relatively high toxicity in the degradation process, while the low toxicity was observed in aliphatic diisocyanates.[150] So we chose 1,6-hexamethylene diisocyanate (HDI) and 1,4-butanediol (BDO) as diisocyanate and chain extender to form hard segment (HSC=25%). The TPE-diol was directly connected to the polymer backbone (other than by physically mix) to increase the dye/matrix compatibility and the reliability of the performance in case the solvent extraction of the TPE unit is out of polymer film.

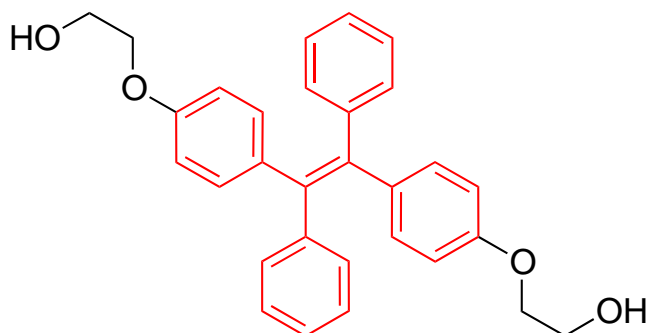


Figure 4.1. Chemical structure of tetraphenylethylene (The red part) unit used in Memory chromic Polyurethane

Implanting the colorants to the soft segment in the SMPs is a key for achieving chromism because the aggregation and de-aggregation of dyes can easily take place due to the flexibility of soft segments at switch conditions. At the same time, by choosing proper components of the polymer matrix and the dye, the polymer can have biocompatibility and biodegradability. In the work being reported here, the tetraphenylethylene (TPE) unit (see Figure 4.1) is covalently connected to the biodegradable soft-segments of the SMP backbone. We studied the shape and color response of the polymer to force, strain, heat and solvent. It is anticipated that this material will have a variety of applications such as biomedical devices, textiles and different sensors responsive to temperature, chemical, magnetic, electronic, infrared and laser media.

4.3. Results and discussion.

We measured the shape-memory properties and recorded the change in elongation during programming and recovery by the cyclic thermomechanical experiment. The melt temperature was first tested by differential scanning

calorimetry. As shown in figure 4.2, the second heating curve indicated the melt temperatures of soft-segments (37°C) and hard-segments (130°C). Two different external stresses were employed to test the SME at different degree of strains. There are four steps in each cycle, (as shown in Figure 4.3), 1st step is the deformation of the permanent shape and corresponds to a standard stress-strain test. After having maintained this strain for 5 minutes to allow relaxation for chains, the stress was then held constant while the sample was cooled (2nd step), whereby the temporary shape was fixed. Then stress is completely removed after 10 minutes (3rd Step), and the sample is now in its temporary shape. Heating in 4th step (2 K min⁻¹) actuates the shape-memory effect. The strain fixity (R_f) and the strain recovery (R_r) are the two important parameters employed to describe the SM effect.[24] The R_f is defined as the reciprocal of deformed degree under external force applied during the programming process and deformed degree after removing such force, which describes the ability of the soft segment to fix the mechanical deformation. While the R_r is defined as the ratio of angle or length of original shape and that of recovered shape, which quantifies the ability of the material to recover its permanent shape. For our polymer, R_f ranges between 88% and 93%. R_r gradually approaches 100% at 2nd cycle because of reorientation of the polymer chains in the non-oriented films during the early cycles. [24] In the first and third cycles, R_r has values between 76 and 80% for our multi-block copolymers and reaches to almost 100% in the second and fourth cycle. The fastest recovery of the sample is recorded at $T_{trans}=37^\circ\text{C}$.

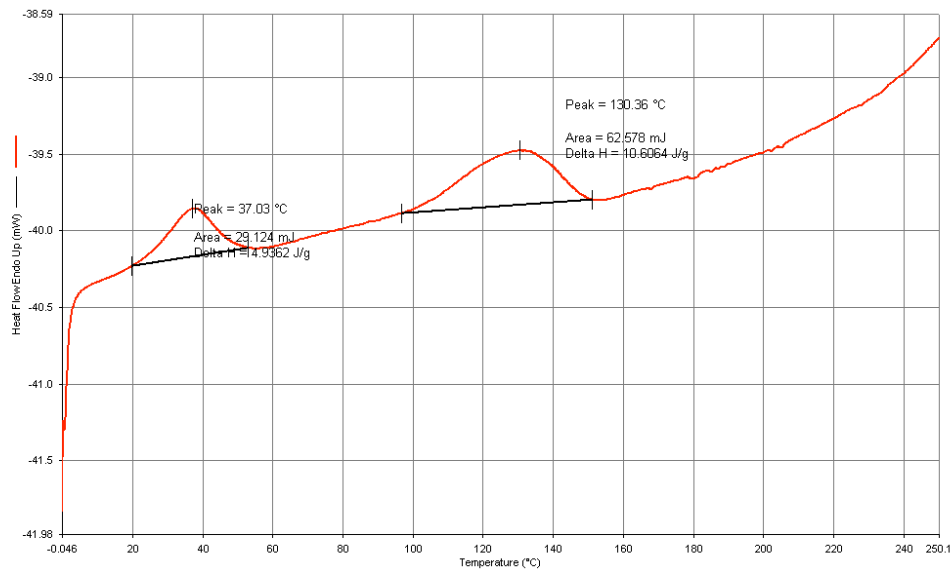


Figure 4.2. Second heating curve of differential scanning calorimetry (DSC) of the outcome polymer

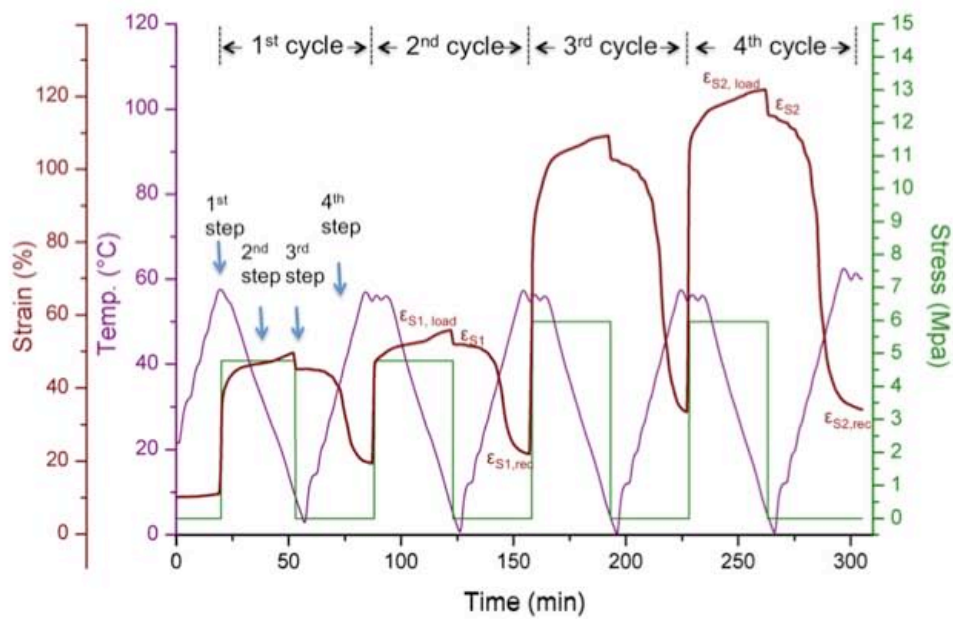


Figure 4.3. Dynamic mechanical analysis of SMPU

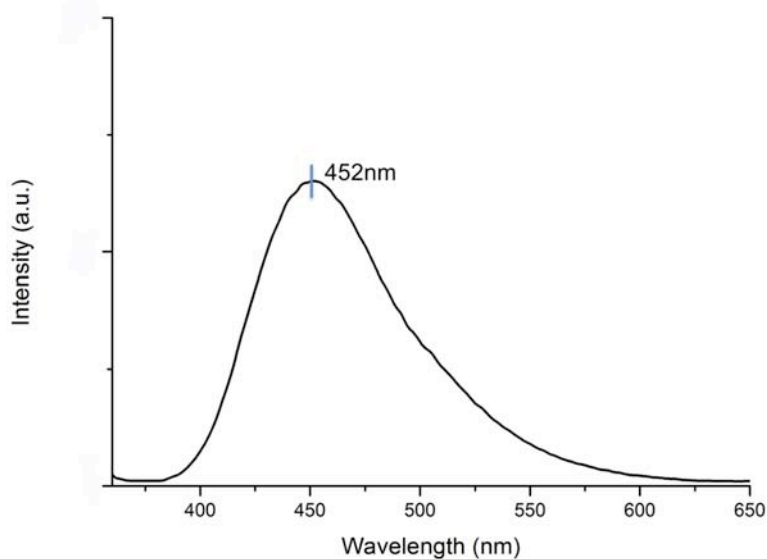


Figure 4.4. Photoluminescent of TPE-diol crystalline

Photoluminescent (PL) measurement was then applied to investigate the correlation between shape memory effect and chromic property. The PL property of neat TPE crystals was shown in Figure 4.4. Figure 4.5 shows the PL of SMPU film (0.1mm in thickness) with 0.1%wt TPE. Such films develop a broad green band around 479nm. Although similar phenomena were also observed with a lower concentration of TPE unit (0.05%wt and 0.02%wt), the emission intensity decreases proportionally to the concentration and almost no shift of wavelength at maximum emission intensity were observed. The film was first stretched to 100% strain at room temperature to mimic the situation in practical utilization. The emission intensity in the center position of the deformation area decreased to about 30% compared to the original state. After annealing in the oven at 50 °C for 1min, the film was tested again 3 minutes after it had been removed from the oven for cooling down, almost 100% recovery of both strain and fluorescent intensity was observed. This

phenomenon was partially attributed to the change of thickness accompanied with the deformation-recovery process. At the same time, the time-resolved PL (see Figure 4.6) indicated the decrease of lifetime after the polymer film was stretched. As shown in Figure 4.6, the decay dynamics of the emission of polymer film (original state and stretched state) at 460 nm. At the original state, the PL is due to aggregated TPE with a relatively long lifetime. Double exponential [i.e., $A_1\exp(-t/\tau_1) + A_2\exp(-t/\tau_2)$] fit indicates PL decay with time constants of $\tau_1=1.67\text{ns}$ and $\tau_2=0.26\text{ns}$ with $A_1/A_2=3.03$. On the other hand, when pumped the polymer of the stretched state, the emission dynamics shows slower decay with time constants of $\tau_1=1.27\text{ns}$ and $\tau_2=0.24\text{ns}$ with $A_1/A_2=1.72$. Weighted mean lifetime determined from $\langle\tau\rangle=(A_1\tau_1+A_2\tau_2)/(A_1+A_2)$. The weight mean lifetime of original state is 1.32ns, while slightly decrease to 0.89ns at stretched state. The decrease of lifetime demonstrated some degree of de-aggregation during stretching process. Besides, the slight blue shift in Figure 4.5 (from 479nm to 468nm) after stretching was attributed to the formation of microcrystalline of TPE units under external force. This band matches that observed for crystalline and is indicative of aggregation induced emission of TPE units (see Figure 4.4). The small peak around 390nm is believed to belong to the stoke shift of the hard segment of polyurethane matrix.

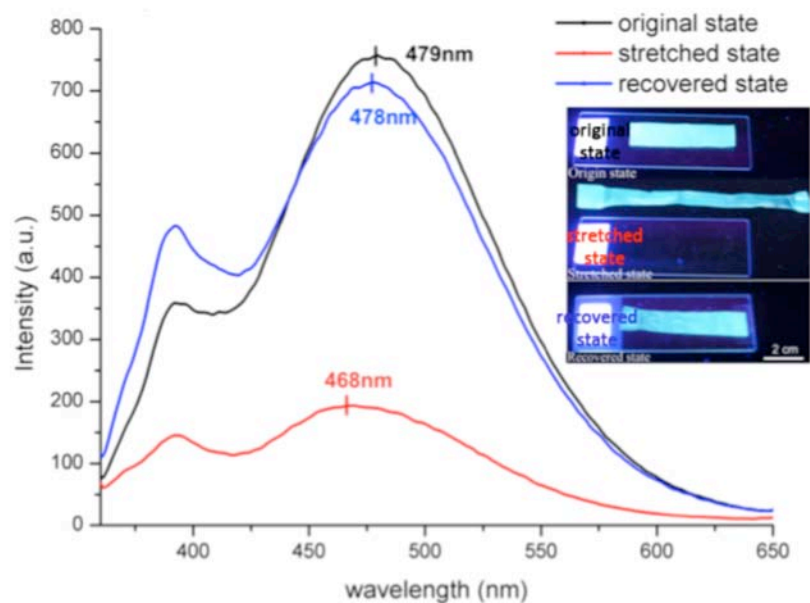


Figure 4.5. PL emission (excited at 343 nm) spectra of SMPU film with 0.1% wt TPE at different state (black line--original state, red line--stretched state and blue line--subsequently recovered state); demo of one film with 0.1% wt TPE under 365 nm UV lamp at different state.

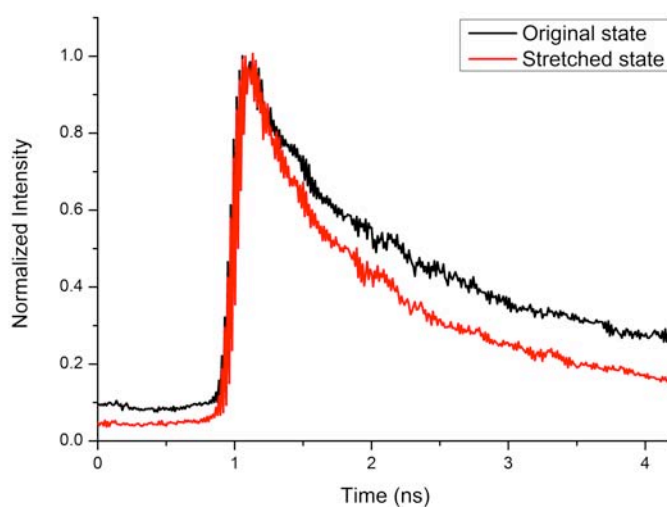


Figure 4.6. Ultra-fast time-resolved fluorescent spectrometry.

Subsequently the strain-intensity relationship, which can be transferred to shape fixity, was studied by testing the center area of the film which was stretched to different degree of shape fixity. As shown in Figures 4.7 and 4.8, when the polymer film was stretched to different degree of shape fixity, the emission intensity was decreased, similar to the inverse proportional function. The emission intensity of polymeric film decreased dramatically before 100% shape fixity, in which region the film displays relatively high sensitivity to the shape fixity and is more suitable to for mechano-sensor. In this region, the volume of the film can be regarded as independent with the deformation (change of volume is less than 10%), and the decrease was attributed to both the change of thickness of the film and de-aggregation of TPE units. However, when the film was stretched longer, the volume of the film will increase accompanied with the stretching, while the thickness changed less and less, and thus decreasing the concentration of the dye in the longitudinal axis direction of the excited area. However the narrower width will supply more dye into the excited region, thus leading to slower decrease in the emission intensity.

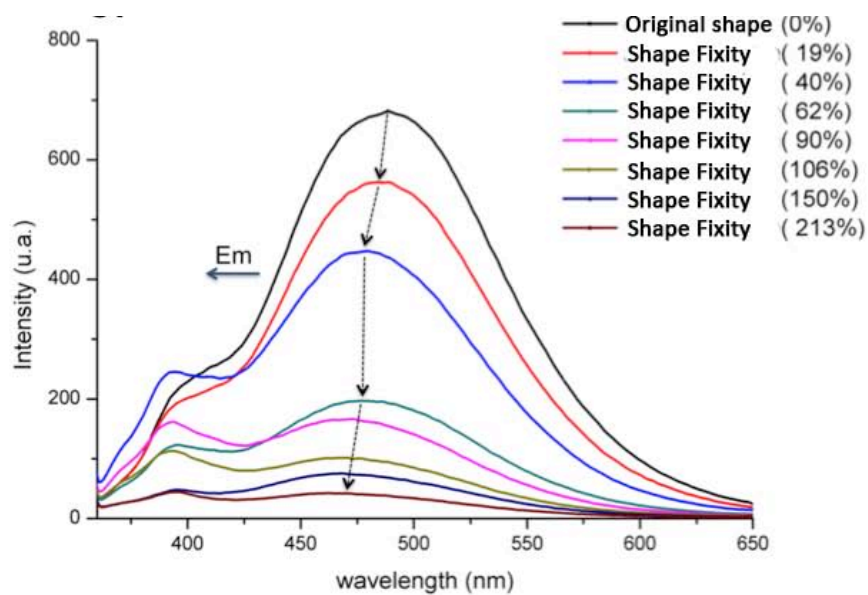


Figure 4.7. PL emission spectra of SMPU films of SMPU and TPE as function of drawing ratio in stretched films.

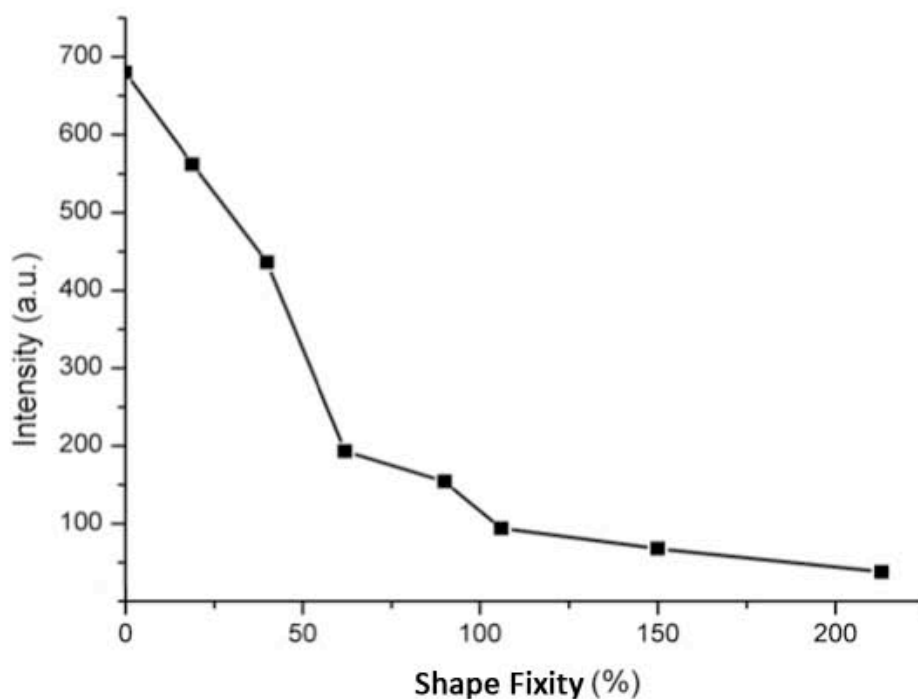


Figure 4.8. Emission intensity of SMPU with 0.1% wt TPE film (excited by 343 nm) at 479 nm at different shape fixity.

As alternative approaches, we investigated the temperature and chemical dependency of the emission intensity (See figure 4.9). The selected polymer film was cut into rectangular shape and fixed in the cell by a clip, by pouring the silica oil with different temperatures into the pre-heated cell, the samples were recorded immediately. The temperature-intensity relationship was recorded. (Figure 4.9.) The intensity-temperature relationship was also similar to an inverse proportional function. (Figure 4.10) The emission intensity decreased fast within the melt region of PCL domain. This phenomenon was attributed to the following three aspects. First, parts of the aggregated dyes were solved in PCL accompanied with the rise of temperature. Secondly, the heat led to the softening of the amorphous region and melting of small crystalline region of soft-segments, and thus facilitating the rotation of phenyl group on dye, leading to dissipation of energy in the form of rotation instead of fluorescent emission. Another reason could be attributed to the increased instability of the aggregated dye after heating, and thus inducing part of de-aggregation. When the temperature was raised to higher than 40 °C, we believe the major aspect responsible for the decrease in emission intensity is increasing the solubility of TPE units into the PCL region. When the temperature was heated to around 130°C, the TPEs in soft phase are almost dissolved, while those acting as chain extenders between HDI are still emissive. As shown in figure 4.11, the polymer film was green in color when immersed into silica oil with room temperature, while became blue (recorded by camera) when immersed into high temperature. (However, it is colorless when seen by naked eyes). When the polymer film was picked out of the hot silica oil, it soon became green again, demonstrating the feasibility of this material as potential reversible temperature sensor.

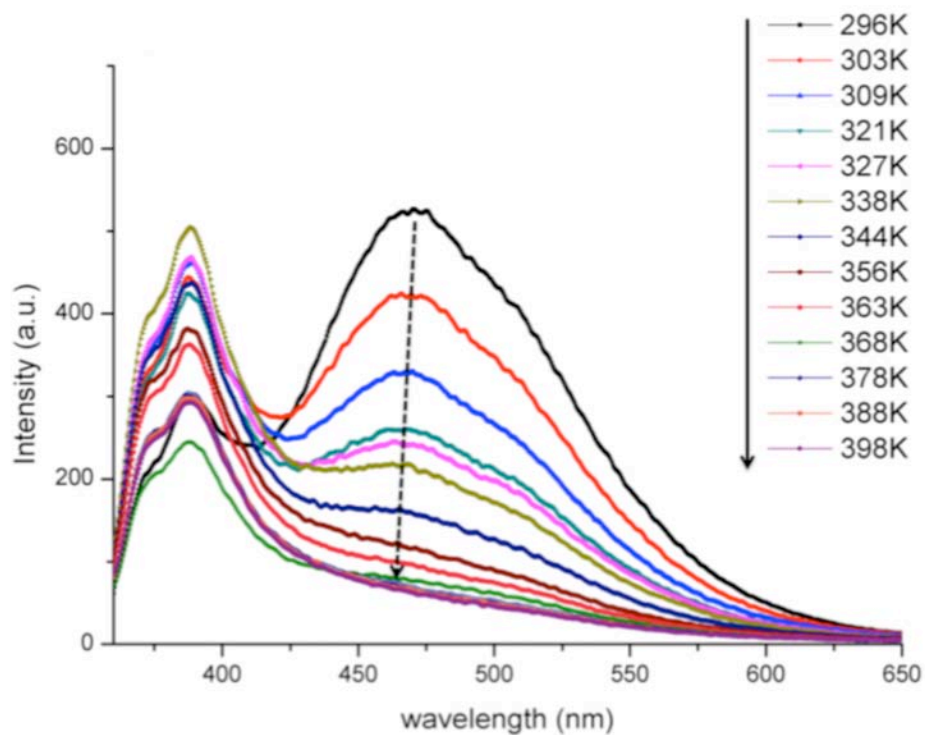


Figure 4.9. Illustration of temperature dependent photoluminescent. All the samples are excited at 343nm UV light and recorded their emission intensity at 479nm for PL test.

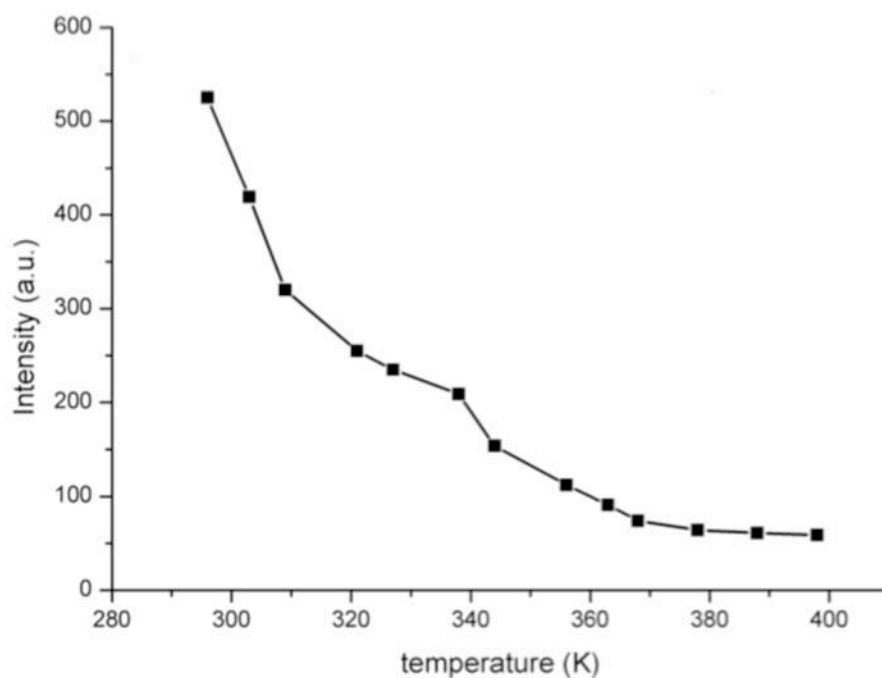


Figure 4.10. Intensity-Temperature relationship of SMPU.

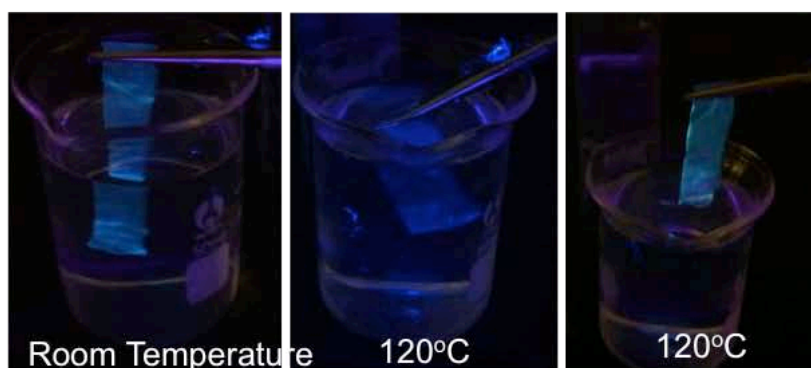


Figure 4.11. Demonstration of temperature dependent photoluminescent. Related demos were recorded by immersing the polymer film into silica oil with different temperature under a UV lamp (excited by 365nm UV lamp).

The chemical sensitivity was also studied by observing the photoluminescent properties of polymer film immersed into a solvent for several cycles. (Figure 4.12) The acetone was selected because of its good solubility to both TPE and PCL. It was found that the acetone can induce both shape recovery and a decrease in emission intensity. The emission intensity decreased about 85% after one minute and seldom changed after 1 min. (Figure 4.15). This phenomenon was caused by the penetration of acetone into the polymeric network. The acetone first acted as a solvent to solve the crystal region of PCL, and thus transferring the polymer film into an elastomer. At the same time, when the solvent encountered TPE during penetration, the TPE units were solved and so decrease the emission intensity. As shown in Figure 4.13, such a process was tested for three cycles (wet-dry) and the fluorescent output remains relatively the same in each cycle. Due to higher thermal condition for drying (compared to the annealing process), the hard segments form a higher degree of aggregation, and thus inducing the higher intensity of peaks around 390nm. As shown in Figure 4.14, we immersed pre-stretched polymer film into the acetone;

it is observed that the decrease of emission intensity accompanies the recovery of geometry.

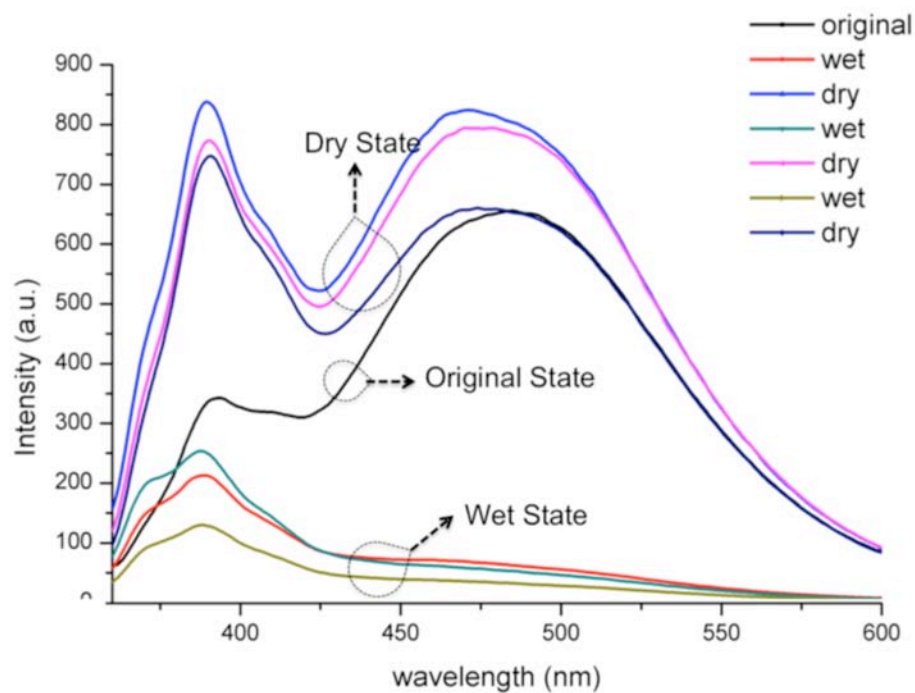


Figure 4.12. Chemical sensitive photoluminescent. All the samples are excited at 343nm UV light and recorded their emission intensity at 479nm for PL test.

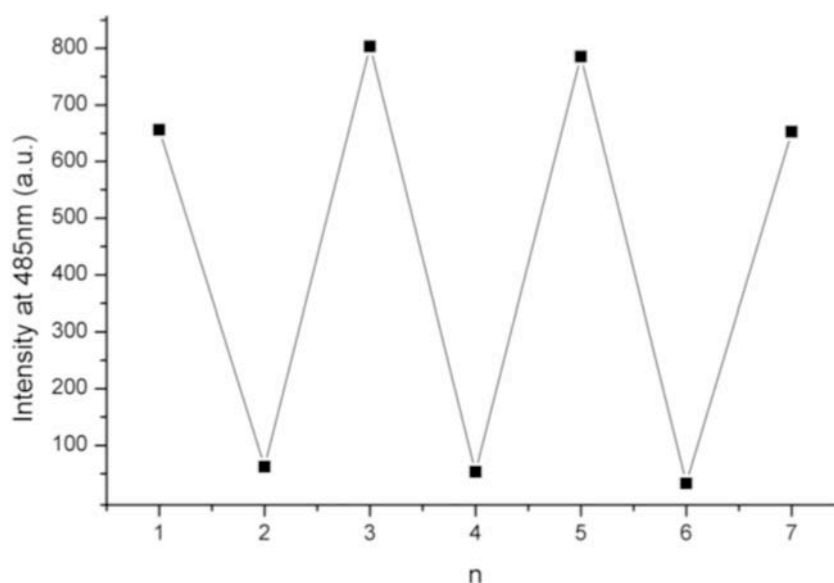


Figure 4.13. Chemical sensitive photoluminescent of different cycles.

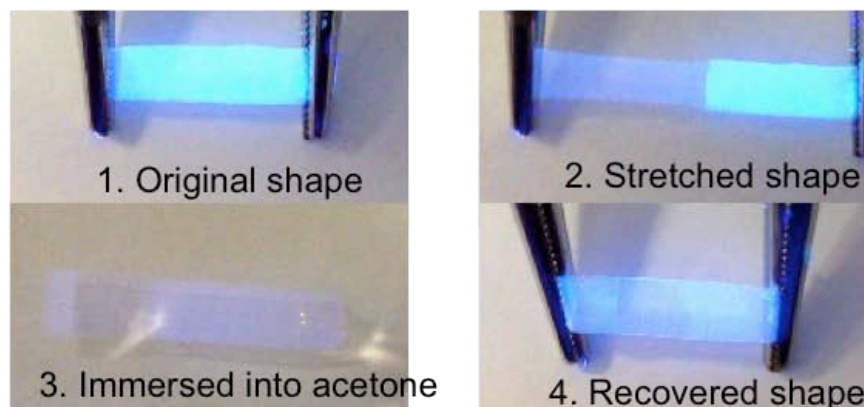


Figure 4.14. Demonstration of solvent induced shape recovery and chromic behavior. The polymer film 1 was first stretched 2 and then immersed into acetone 3 and then took out from solvent and wait till dry 4 at room temperature. The demos were recorded under a UV lamp (excited by 365nm UV lamp).

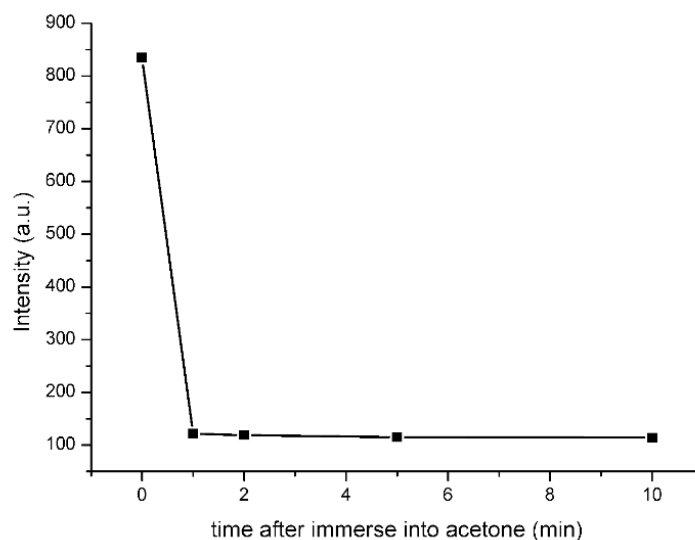


Figure 4.15. PL of SMPU immersed into acetone as a function of time.

Later, to further explore the possibility of out-coming polymer as biomedical device, the cytotoxicity test was carried out. As shown in Figure 4.16, the outcome polymer display low toxicity and thus a feasible candidates for further biomedical application.

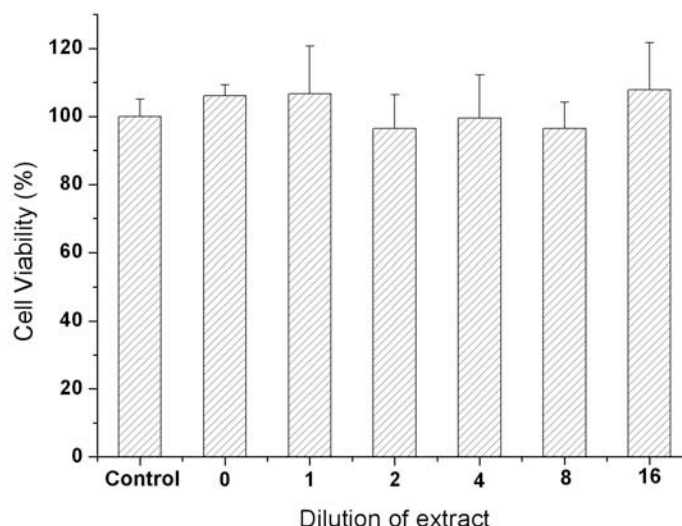


Figure 4.16. Cytotoxicity test of SMPU.

A model was constructed to explain the molecular mechanism of phenomena mentioned above. As shown in figure 4.17, when the polymer film was stretched (process 1), both de-aggregation of TPE units and the decrease of dye concentration in excitation area contributed to the mechano-chromic effect while the shape recovery of the film upon heating enabled this effect with reversibility. Besides, when the material was exposed to heat (process 2) or solvent (process 3), the TPE units will be dissolved in PCL region or the solvent. Thanks to the formation of physical crosslink, the polymer networks are not destroyed by heat (below 150°C) or some organic solvent (low polarity). When such factors were restored, the polymer soon also recovered to the original state. Thus the material displayed potential application as temperature and chemical sensors. At the same time, the solvent also induced the recovery of the stretched together with the further decrease of emission intensity. This athermal shape recovery also enriched the potential application of this material, especially in the heat-labile materials.

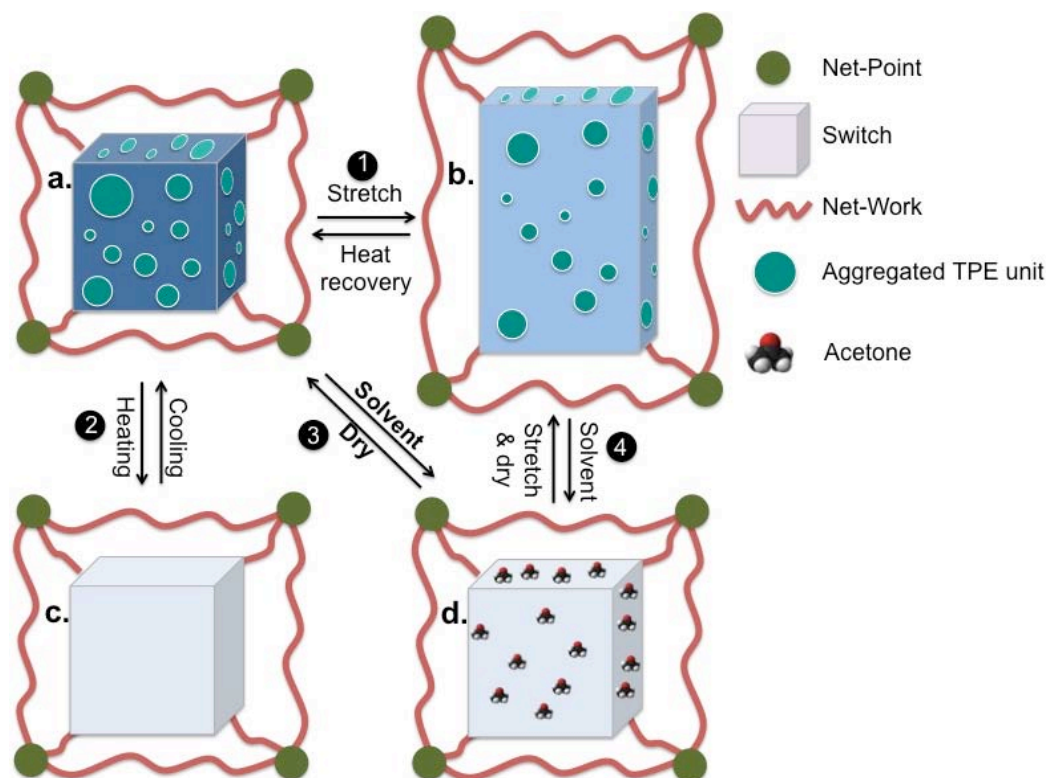


Figure 4.17. A model to illustrate the molecular mechanism during, stretch-recovery process (1), heating-cooling process (2), solvent-dry process (3) and solvent induced shape recovery process (4).

4.4. Summary

We here reported a chromic polymer which is responsive to its shape memory properties and has both the behavior of SMPs and chromic materials. We employed a strategy to fabricate such a smart material which represents a new principle for making chromic materials. This material is made of shape memory polyurethane with tetraphenylethylene units covalently connected to their backbone. The aggregation and de-aggregation of the TPE clusters are governed indirectly by the shape memory properties such as original shape, shape deformation and stimuli. We can imagine that when the soft segments are

molten or dissolved in solvent, the switch is open, the AIE units are free from crystal binding and can migrate easily to larger areas, thus the AIE units/particles are far apart from each other, the emission intensity reduces or disappears, which leads to no color or pale colors. Such simple approach enabled the material with reversible mechano-, solvato- and thermochromic shape memory effect. Since the switch is a fundamental structural character of SMPs, the shape memory properties have led to the chromism and we call this memory chromic.

CHAPTER 5 TWO-WAY SHAPE MEMORY POLYMER BY INTERPENETRATING POLYMER NETWORK

5.1. Introduction

Two-way shape memory polymers (TWSMPs), or reversible shape memory polymers are one of the most promising smart materials because of their potential applications as artificial muscle, actuators, sensors etc.[3] Current approaches for fabricating TWSMPs include combining liquid crystalline into a polymer network, [11] applying constant external stress to SMPs with semi-crystalline switch [12] or by simply laminated structures[13]. None of the above mentioned methods could realise reversible shrinkage without external tensile at ambient temperature. It is hoped that we can solve this issue by a simple method, which is employing an interpenetrating polymeric network (IPN) with elastomeric network and crystalline network. Thus, we constructed a series of polymers with UV-crosslinked crystalline segment and thermal-crosslinked elastomeric segment as IPNs and explore their possibilities for two-way shape memory effect. When heating the outcome IPN, the pre-stretched crystalline segment will shrinkage and press elastomeric segment. When dropping the temperature to room temperature (20°C), the stored energy in elastomeric segments will provide the force for crystalline segment to recrystalline in the reverse direction, which lead to an elongation of the IPN. Dynamic mechanic analysis (DMA) and differential scanning calorimetry (DSC) proved the reversible shrinkage rate as high as 5.47% and ambient transition temperature around 43°C. The mechanism was also proved by 2-dimentional X-ray

diffraction (2DXRD). This work demonstrated a simple way of fabricating stress-free TWSMPs.

Shape memory polymers have drawn increasing attention because of their technological significance in many applications like biomedical materials, textiles, packaging materials, actuators, sensors, and aerospace materials.[15, 97, 151] Traditional thermal induced one-way dual shape memory effect depends on the formation of well separated hard and soft phases with different transition temperature in the elastic network.[1] Generally, the transition temperature of soft-segment (T_{C2}) is lower than hard-segment (T_{C1}). The hard phase acts as net-points which determine the permanent shape while the soft phase acts as the switch to immobilize the temporary shape and provide the inner force for recovery. When the SMPs are deformed above T_{C2} and then cool down, the soft-segment will be fixed and the internal stress is saved. Upon re-heating to T_{C2} or above, the internal stress will be released and enable the recovery of the polymer to its origin shape. [3-10] This shape will stay unchanged when dropping the temperature below transition temperature. However, TWSMPs could switch to previous shape when stimulus is over/reverse stimulus is applied.

5.2. Statement of problem and polymer design

Currently there are three types of TWSMPs, liquid crystalline elastomers (LCEs) type,[11] semi-crystalline switch type [12] and laminated structure type.[13] For the LCEs, the molecular chain of LCEs generally adopt a prolate shape in the nematic state. If the crosslinking process takes place without any external intervention, the alignment of the prolate molecule is random, thus resulting in an overall non-orientation nematic state which is called polydomain

LCEs. When stretching is applied during the crosslinking process, a monodomain LCEs can be obtained, in which the director is aligned along the stretching direction. Thus the directed molecular morphology change below & above T_c contributes to the overall geometry change of the LCEs.[14] For semi-crystalline type, the Two-way shape memory effect (TWSME) is based on the cooling-induced elongation (CIE) and the melt induced contraction (MIC) of the semi-crystalline switch under a tensile load. With constant tensile, the soft-segment (semi-crystalline type) will grow into crystallites oriented along the stretching direction when cooling. While entropy driven contraction will occur when the soft-segment was melt above the transition temperature.[15] For laminated structure type, the TW-SME was achieved by combining pre-stretched SMPU layer and elastomer layer with adhesives. The SMPU layer provides the force for bending upon heating while the elastomer layer provides the force for recovery when cooling.[13] However, Each of these approaches has disadvantages. For LCEs, a high transition temperature is required and the synthesis procedure is relatively complicated. While for SMPs with semi-crystalline switch, the external force is essential. At the same time, the laminated architecture can only realize bending, although applicable for other complicated deformation, it can not realize reversible shrinkage. To our best knowledge, so far none of above mentioned methods could realise reversible shrinkage without external tensile at ambient temperature. Recently, Lendlein et al solved this problem by employing two kind of crystalline soft-segments in one polymeric network with proper programming process, which convert a normal tripe-shape memory polymer to a two-way shape memory polymer. The key concept of their work is the separation of the shifting geometry determining

function from the actuator function on the level of phase morphology, the actuator domains expand during cooling and collapse during heating in the direction determined by the shifting-geometry determining domains.[16]

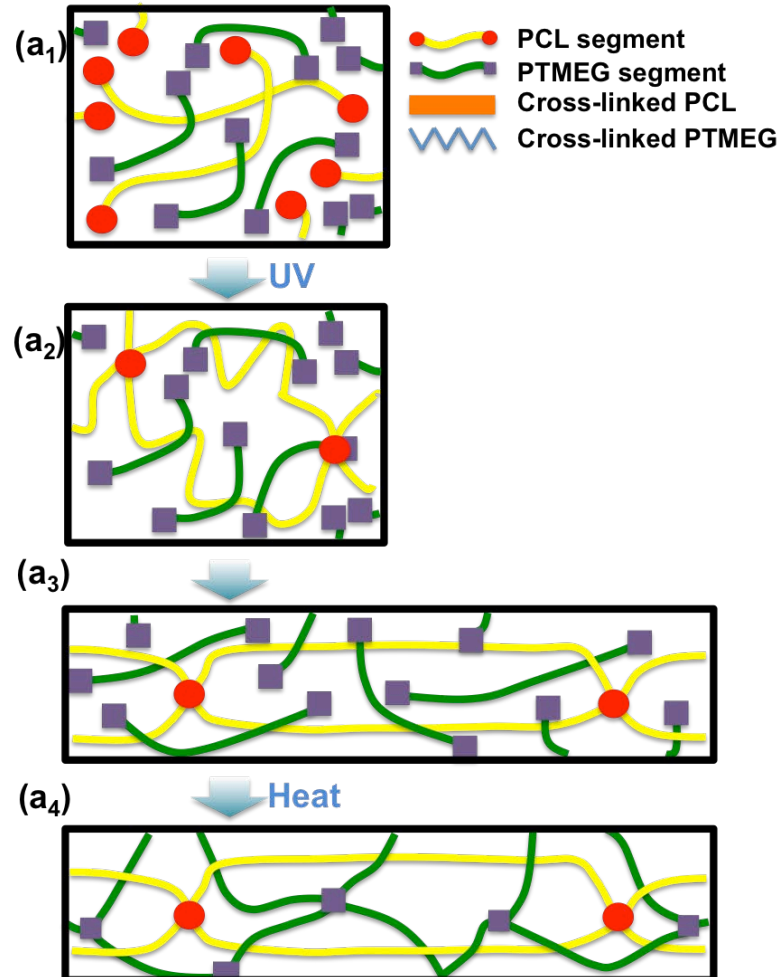


Figure 5.1. Illustration of the synthesis and mechanism of the polymer network and two-way shape memory effect.

We anticipate that the issue can also be solved through employing elastomeric network and crystalline network into IPNs. Besides, although the SMPs with (semi-) IPN structure have already been reported, all of them are one-way dual/triple shape memory polymers, where the other polymer network just act as reinforcement or two polymeric networks with two transition temperature were mixed together.[152-154] It is also first time to report IPN with TWSME. Our

originality is to embed a cross-linked crystalline system and cross-linked elastomeric system together to form IPN, where the crystalline system acted as reversible segment, while the elastomer segment act as spring to provide the force to recrystalline. As shown in **Figure 5.1**, the crystalline segments were first cross-linked under UV, then stretch and fixed at 100% degree of strain, then the amorphous segments were cross-linked to form elastomeric segments under heating and then cooling down and force to fix IPN was released. When heat the out-come IPN, the crystalline segment will shrinkage and press elastomeric segment at the same time. When drop the temperature to room temperature (20°C), the stored force in elastomeric segments will provide the force for crystalline segment to recrystalline in the reverse direction, which lead to elongation of IPN. By such synthesis and programming routine, a series of polymer network were synthesized and explored if they could exhibit reversible shrinkage without external tensile at ambient temperature by DSC and DMA, the mechanism was also proved by 2DXRD.

(a_{1~4}) is to explain the synthesis routine while (b_{1~5}) is to explain the mechanism. At first, (a₁) illustrate the mixing of all raw materials and then apply UV to get (a₂) where PCL segments were cross-linked and the system become gel-like, then the system was stretched and fixed at MEG we as shown in (a₃), then in (a₄) the system was heated to cross-link PTMEG segments and remove solvent. Yellow lines with two red spots represent the terminal modified PCL unit (UV sensitive) while the green lines with two squares at each end represent the terminal modified PTMEG unit. (Thermal sensitive) Cross-linkers (DMPA and PPG230) are hidden in this figure. (b₁) indicated the cross-linked PCL was stretched and fixed (b₂), then PTMEG was cross-linked and serve as spring-like

elastomer (b_3), then the system was released and heated above the transition temperature of PCL (b_4), leading to shrinkage of semi-crystalline PCL segments and contraction of the system, at the same time, the PTMEG segments (elastomer) were also compressed, then the system was cooling down to room temperature (b_5), during this process, the compressed PTMEG segments release the force, where PCL will crystalline in the direction of the force, leading to cooling-induced elongation.

5.3. Results and discussions

The basic principle we employed to fabricate TW-SME with IPN structure is to take advantage of semi-crystalline switch as reversible phase while introducing the elastomer part to replace the external tensile and provide the inner force for recovery. Although TW-SMP with poly(cyclooctene) was reported to obtain high shape changing rate (about 100%), considering their high transition temperature (compared to body temperature),[12] Poly(ϵ -caprolactone)diol (PCL, $M_n=4000$) was chosen as semi-crystalline switch because of its semi-crystalline nature, ambient transition temperature (close to body temperature) and biodegradability.[155] poly(tetramethylene ether glycol)diol (PTMEG, $M_n=1000$) was chosen as elastomer part because of their elasticity after cross-linking.[156] The general synthesis and programming process of IPNs are shown in Figure 5.2. To realize the programming process, the two macromonomers were modified with different end group that could enable the cross-linking to different stimuli. As the oligo-PCL need to be cross-linked first and such cross-linking process should have little interference to the other components of the reaction system, thus oligo-PCL were modified with vinyl group at each end of molecular chains, which make them possible to cross-link

under the existence of the UV light and photo-crosslinker (DMPA). The oligo-PTMEG was modified with epoxy groups, which is cross-linkable with cross-linker (PPG230) and heating (around 80°C). Moreover, the thermal cross-linking of the oligo-PTMEG will also evaporate the solvent. As studied by Chung et al, higher tensile could lead to higher degree of strain increment for semi-crystalline type TW-SMPs.[12] Thus all pre-IPNs were stretched to 100% degree of strain and fixed for the subsequently cross-linking. (all polymers can not be properly fixed at higher degree of strain because of slippery or break) At the same time, to study the influence of the macromonomers ratio to the overall performance of IPNs, a series of IPNs with different PCL/PTMEG ratio were synthesized and studied by differential scanning calorimetry and dynamic mechanical analysis. (see **Table 5.1**) Due to the load PCL content, the sample No.1 is with poor mechanical property and thus unstretchable after first step of crosslinking. For comparison purpose, solely cross-linked PCL and PTMEG were also synthesized, (C-1 and C-2) while the C-1 was fixed to 100% strain before dried in an oven with 80°C. A demo of two-way shape memory effect of outcome sample was shown in **Figure 5.3**.

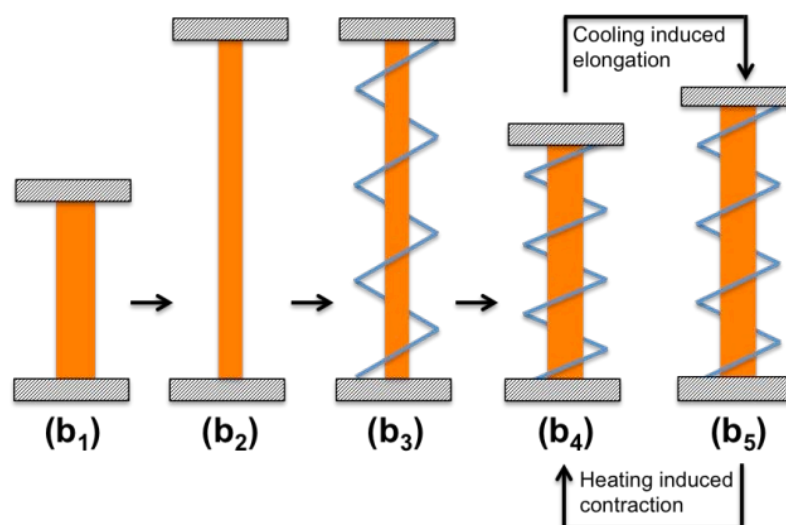


Figure 5.2. The general synthesis and programming process of IPNs.

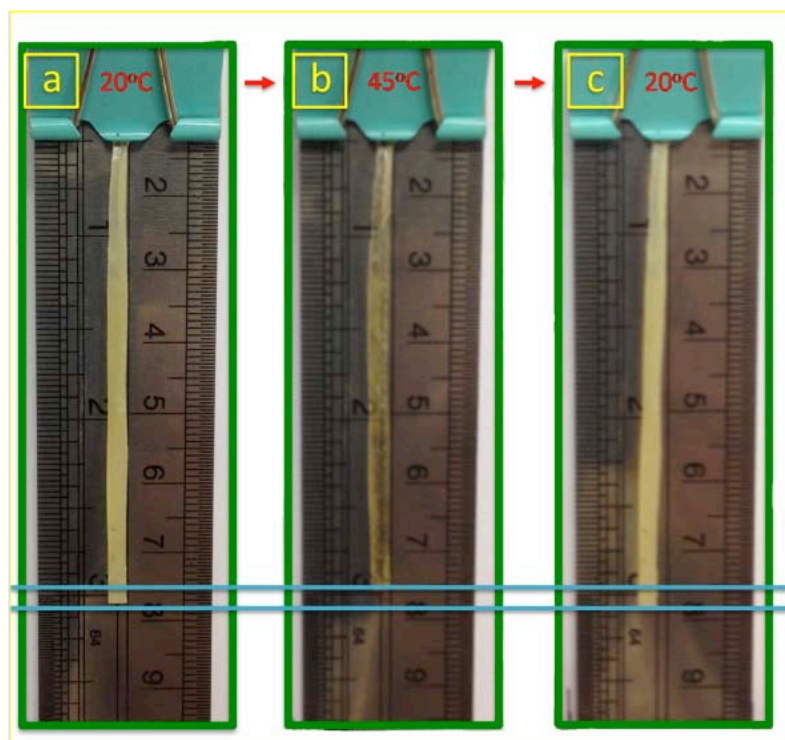


Figure 5.3. The demo of two-way shape memory effect of the polymer at different temperature.

Table 5.1. Recipes of IPNs with different ratio of PCL and PTMEG content.

No.	PCL/PTMEG	PCL [g]	PTMEG [g]	DMPA [g]	PPG230 [g]	DMF [mL]	T_m [°C]	R_{sc}
1 ^{a)}	0.50	0.50	1.00	0.020	0.090	4	-	-
2	0.75	0.64	0.86	0.026	0.077	4	43.40	144%
3	1.00	0.75	0.75	0.030	0.068	4	42.60	931%
4	1.25	0.83	0.67	0.033	0.060	4	42.83	003%
5	1.50	0.9	0.60	0.036	0.054	4	43.55	475%
6	1.75	0.95	0.55	0.038	0.049	4	43.61	205%
7	2.00	1.00	0.50	0.040	0.045	4	44.21	405%
C-1	∞	1.50	0	0.060	0	4	45.8	1.631% ^{b)}
C-20		0	1.50	0	0.135	4	n.d.	0.226% ^{b)}

C-1 & C-2 represent control sample No. 1 & No. 2, n.d. = not detectable. R_{sc} = shape changing rate. ^{a)} (Sample 1 is not stretchable after UV induced crosslinking.); ^{b)} (C-1 & C-2 exhibited thermal expansion and contraction as normal materials do.)

As control sample 1, PCL samples cured with DMPA “melt” to a stable rubbery plateau above T_m that is void of macroscopic flow. The melting temperature (T_m), only slightly modified from the linear polymer, as we shall show, acts as the transition temperature to trigger a shape memory behavior of the networks. For 1W-SME, cooling below T_m leads to crystallization that serves as the fixing mechanism of deformed PCL samples, while heating above T_m leads to chain mobility that allows strain recovery to mechanical equilibrium in accordance with the applied load. Similar to reported polyurethane with PTMEG1000 as soft segment, PTMEG samples cured with PPG230 (control sample 2) display no melting after cross-linking and acted as elastomer part. Further guarantee the existence of two components by DMA is not consulted because the T_g of both PCL and PTMEG may mix together.

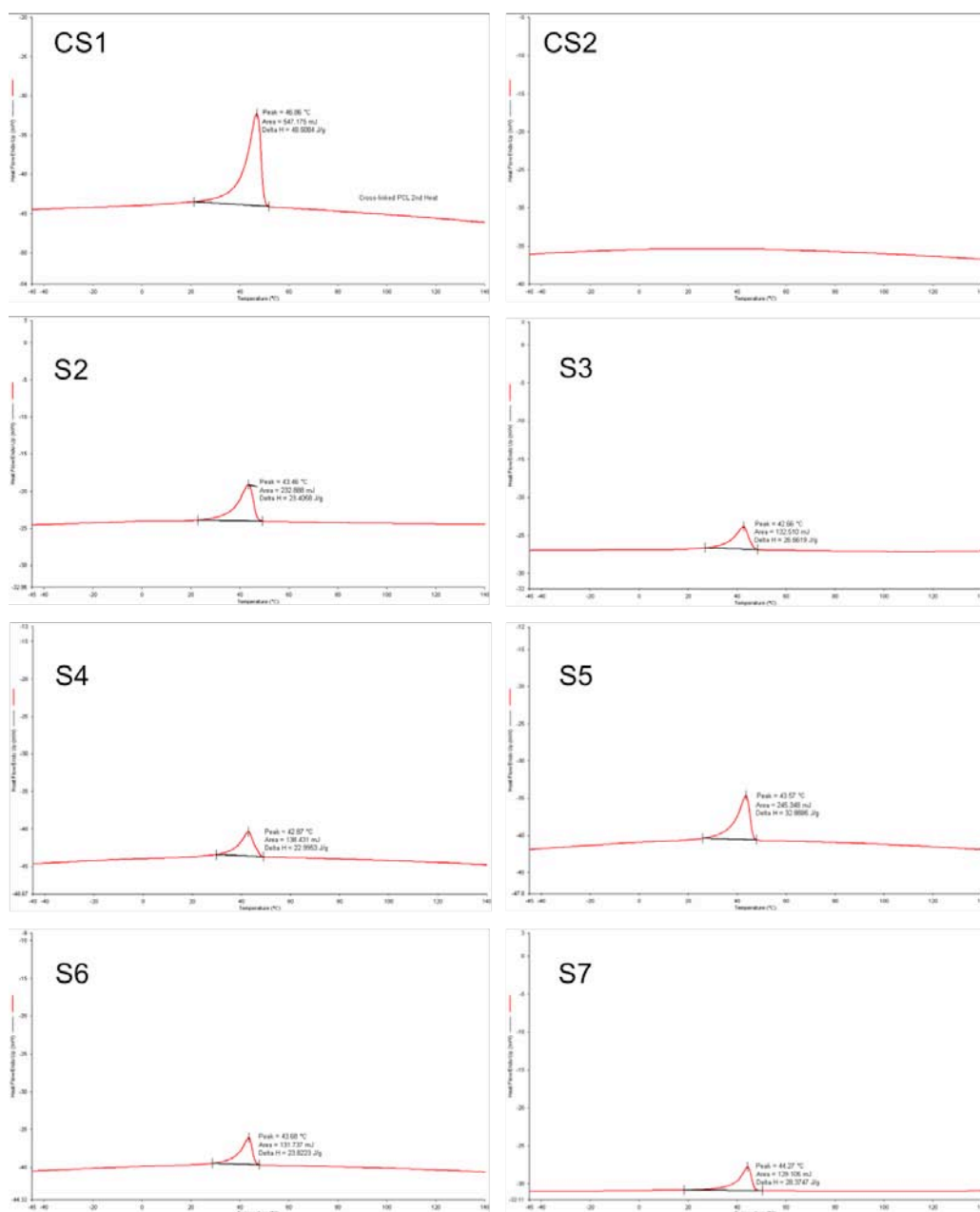


Figure 5.4. Differential scanning calorimetry of out-come samples.

In order to evaluate the possibility of tuning the transition temperatures by macromonomers ratio, melting thermograms obtained using differential scanning calorimetry (DSC) for IPN samples with different ratio of PCL and PTMEG were conducted. (**Figure 5.4**) The results are also summarized in **Table 5.1**. Inspection of **Table 5.1** reveals that the transition temperatures, T_m modestly decrease with increasing PTMEG content, except sample 2. We

attribute this trend to a constraining effect of cross-linked PTMEG on crystal growth, specifically the local chain mobility necessary for chain insertion into a growing crystal is suppressed in the neighborhood of PTMEG. However, the abnormal effect from sample 2 may be caused by the phase separation because of the low PCL content.

In order to study the relationship between TW-SME and macromonomer ratio, dynamic mechanical analysis was carried out. For each sample, the testing was performed for at least three cycles. The purpose of the first cycle is to remove the mechanical history, while the second cycle and the third cycle could efficiently express the reversible shape-changing rate and verify the repeatability. So in each figure from **Figure 5.5**, we selected the beginning temperature from the middle of the first cycle, where the polymers were fully contracted/expanded, to the end of the second cycle, where the polymers were fully expanded/contracted. Typically, for each figure, there are five high-lighted points marked as ①~⑤. ① is the thermomechanical analysis (TMA, which can also be understand as stain) value at the end of the first cycle and the beginning of the second cycle, it illustrated the initial shape when temperature was cooling down. When temperature begin to raise, there's a small sharp peak ③ occur, that's maybe caused by the excessive heating induced over expansion. Soon the peak will comply to another balance ② when the temperature reach to 65°C for about 10 mins, which illuminated the shape above transition temperature. Then the polymer was about to cool to room temperature, a slight jump ⑤ of TMA could be observed, that's probably caused by excessive cooling induced over shrinkage. At last, when the polymer was totally cooled to the room temperature or the shape almost doesn't change, this is the recovered state ④.

Generally speaking, materials will suffer from heating induced expansion and cooling induced shrinkage, such deformation in volume will amplify when the phase transition occur at the same time. Such phenomena are also suitable for control samples 1 & 2, where effective reversible deformation rate of 1.63% and 0.23% was observed (see **Table 5.2**) However, after proper programming process, the outcome polymer display the reverse phenomena, heating induced shrinkage and cooling induced expansion. As summarized in **Table 5.2**, the thermal induced shrinkage (①→②) and cooling induced expansion (②→④) will firstly increase then decrease accompany with the increasing of the PCL/PTMEG ratio. The different between shrinkage and expansion may be caused by imperfect crosslinking, so we chose the lower one as shape changing rate. The maximum reversible shape changing rate is realized for sample 5. This is the synergy result from the PCL and PTMEG. The higher content of PCL will provide higher recovery force while the lower content of PTMEG provide the less recovery force, thus hindered the tensile induced elongation. Compared to TW-SMPU with semi-PCL switch, which display a reversible shrinkage around 24%, [157] the IPN system may not reach such high deformation rate because of the non-constant stress supplied by PTMEG network when shrinkage and the limit of the mechanical properties of the pre-IPNs. It's maybe understand like that the tensile provided by PTMEG, like spring which obeys Hooke's law ($f=kx$), will decrease with the elongation. Only proper x could provide enough force for recovery. Besides, we believe the TW-SME could be further improved by replacing PCL with lower molecular weight one. Worth to mention, this reversible shape-changing rate is still similar to the two-way shape memory alloy (TW-SMA).

Table 5.2. The deformation rates from different temperature points.

Sample name	①→②	②→③	②→⑤	②→④
Control Sample 1	+1.631%	+2.048%	-0.389%	-1.512%
Control Sample 2	+0.226%	+0.833%	-0.305%	-0.203%
Sample 2	-0.144%	+0.492%	+0.131%	+0.154%
Sample 3	-0.931%	+0.500%	-0.046%	+1.051%
Sample 4	-3.033%	+0.790%	-0.087%	+3.403%
Sample 5	-5.475%	+0.740%	~0.000%	+5.858%
Sample 6	-1.205%	+1.580%	-0.262%	+1.356%
Sample 7	-1.405%	+1.258%	-0.296%	+1.393%

The $\text{①} \rightarrow \text{②} = \frac{L_{\text{②}} - L_{\text{①}}}{L_0} \times 100\%$, where L is the length of the polymer at different state, while L_0 is the original length of the polymer.

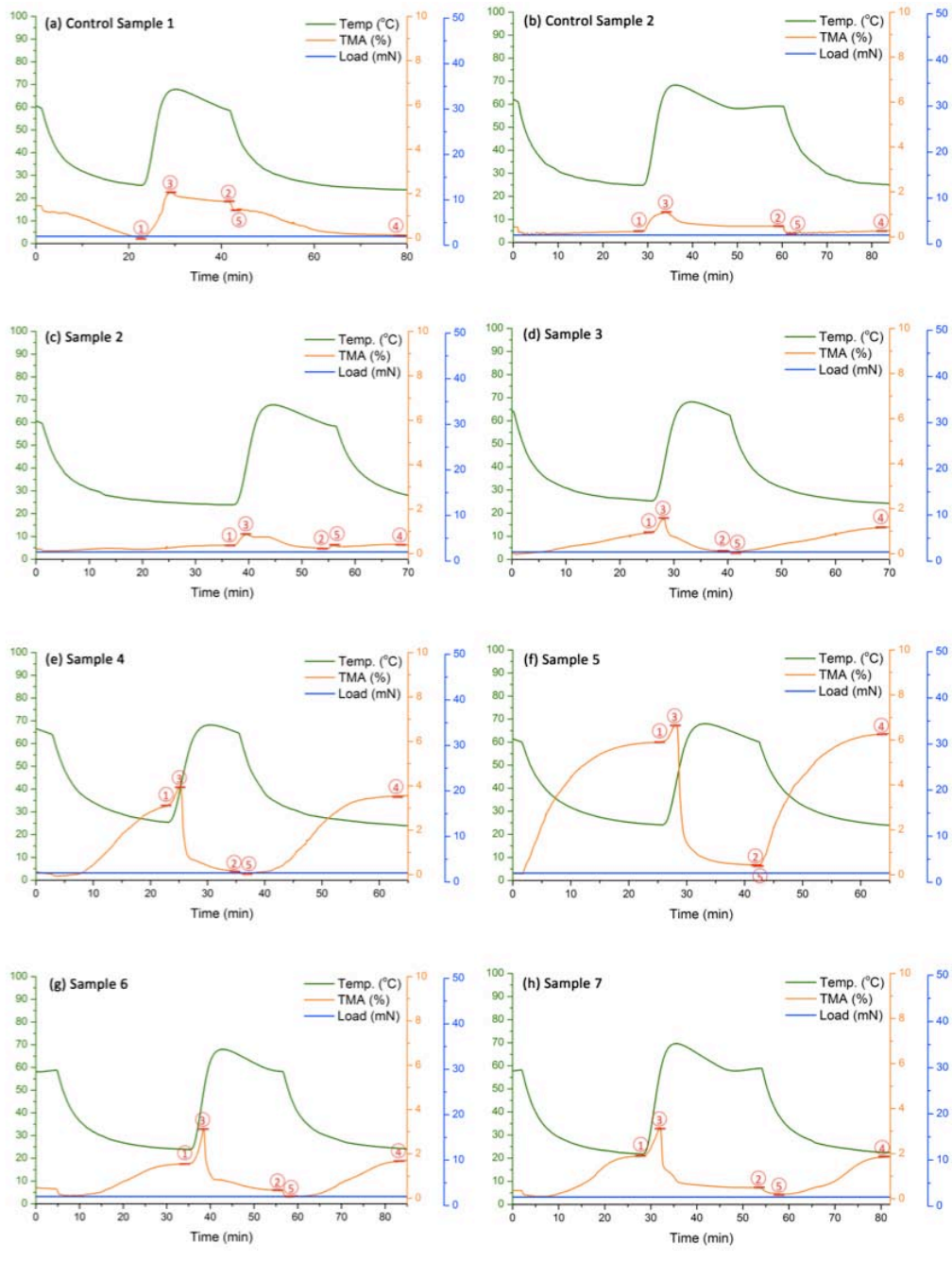


Figure 5.5. The dynamic mechanical analysis (SS control) of different samples. The green lines represent the temperature, the blue lines represent the constant load (2mN) and the orange lines represent the thermomechanical analysis (change of the strain).

The 2DXRD was usually employed to study the alignment of the polymeric crystalline. As reported elsewhere,[157] the undeformed PCL shows two

evident sharp Debye Scherrer reflections with uniform intensity along the azimuthal angle. The rings correspond to two of the characteristic reflections of the PCL orthorhombic crystal form, located at 21.4° and 23.7° and related to the (110) and (200) planes.[158] No change in angular position along 2θ is found, suggesting that the orthorhombic structure of the crystal phase and the plane spacing remain unchanged. (**Figure 5.6**) The specimens undergoing elongation due to cooling under various ratio of PTMEG presented oriented Debye Scherrer rings, denoting the presence of preferred orientation of crystallites.[159] Usually the peak width at half-height (PWHH) was employed to evaluate the degree of orientation, thus the change in the XRD intensity along one single Debye ring was taken into account. In **Figure 5.7** the plot of the XRD intensity of the most intense peak ((110) at 2θ (21.4°) vs. the azimuthal angle, β , is represented for the specimens cooled under fixed stress conditions and for the unstretched specimen. However, due to the low R_{sc} , the Debye Scherrer rings did not display the discontinuity as reported by S. Pandini, so we chose a sample with relatively high R_{sc} (S5) which displayed oriented distribution (compare to pure PCL without tensile, which is uniformly distributed [157]), indicating better crystalline alignment at proper ratio of PCL/PTMEG. As reported elsewhere, [160, 161] the row nucleation process produces linear nuclei parallel to the strain direction, followed by the oriented growth of folded-chain lamellae. The result also suggested that this orientation process regards not just the elongation exerted by cooling under expand force of PTMEG segments.

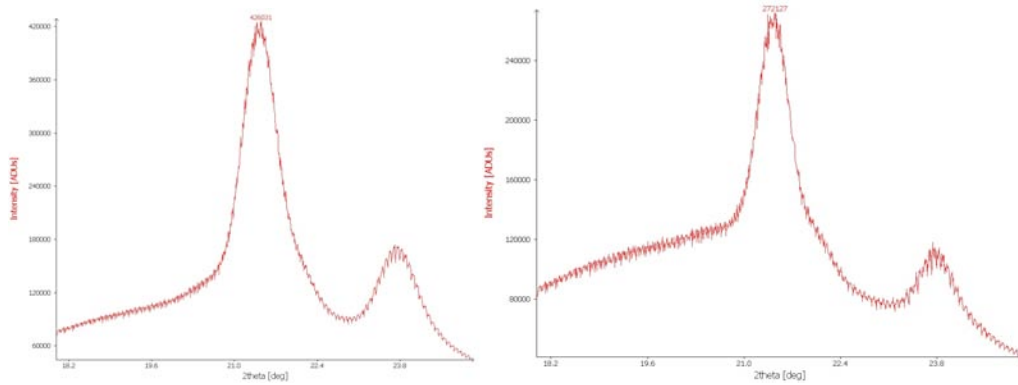


Figure 5.6. The 1D-XRD of Sample C-1(left) and Sample 5(right).

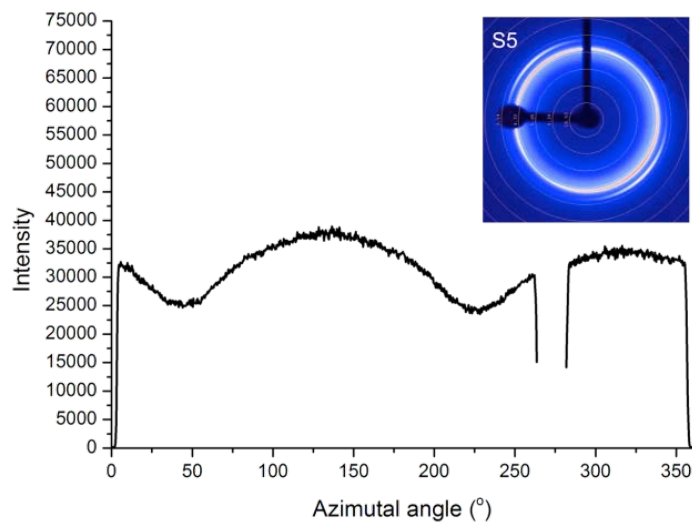


Figure 5.7. Illustration of 2DXRD of the IPNs (S5 for example), the intensity at 21.4° vs. the azimuthal angle with Debye Scherrer reflections.

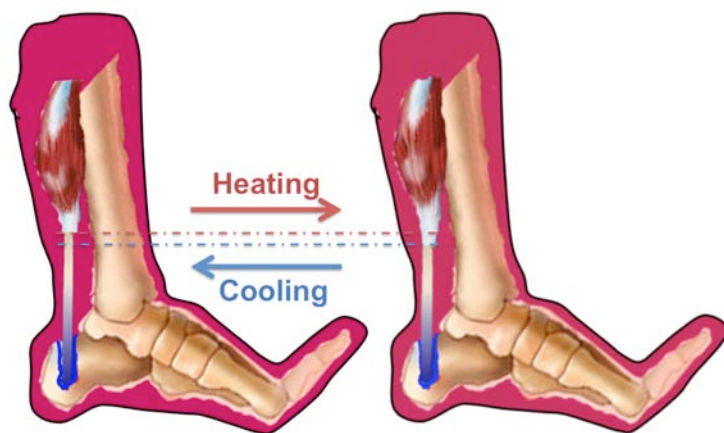


Figure 5.8. Potential application of out-come polymer as artificial tendon.

5.4 Summary

In this work, a novel molecular strategy was employed to fabricate TWSMPs, which is employing an interpenetrating network (IPN) with elastomeric network and crystalline network. The crystalline network is responsible for the reversible shape shrinkage, while the compressed elastomeric network provides the force for shape expansion. From the result obtained, it is feasible to construct a stress-free two-way shape memory polymer which is switchable at ambient temperature around body temperature by IPNs. The differential scanning calorimetry demonstrated that the transition temperature is around 43°C. The dynamic mechanical analysis proved the two-way shape memory effect with a reversible deformation rate as high as 5.47% (similar to shape memory alloy, we believe this value can be further improved by replacing PCL with PCO, which displayed relatively higher R_{sc} and T_m). The 2DXRD indicated that the TWSME was contributed to the switch-spring structure. When heating the outcome IPN, the cross-linked crystalline segment will shrinkage and press elastomeric segment at the same time. (Heating induced shrinkage) Then dropping the temperature to the room one (20°C), the stored energy in cross-linked amorphous segments provided the orientation force to crystalline segment to recrystalline. This material may have potentials for the wide applications like sensors, actuators and artificial muscles. (See **Figure 5.8**)

CHAPTER 6 A FACILE APPROACH TO LIGHT/HEAT DUAL SENSITIVE TRIPLE SHAPE MEMORY POLYMER

6.1 Introduction

In the present work, a facile approach was employed to fabricate Light/heat dual-responsive triple shape memory polymer (SMP) by simply mixing $\text{Zn}(\text{Mebip})_2(\text{NTf}_2)_2$, a metallocsupramolecular unit formed by coordinate 2,6-bis(N-methyl benzimidazolyl)-pyridine (Mebip) ligands to Zinc di[bis(trifluoromethylsulfonyl)-imide] ($\text{Zn}(\text{NTf}_2)_2$), or Gold Nanoparticles (AuNPs) into one part of epoxy resin. Dissimilar to previously reported Light sensitive SMPs with sophisticated molecular structure and relative poor mechanical properties, the advantage of this approach is that the Light-sensitivity was simply achieved by employing $\text{Zn}(\text{Mebip})_2(\text{NTf}_2)_2$, a UV-Heat transfer compound,[119] and AuNPs, into the polymer matrix without significant sacrifice of thermal and mechanical properties. Also thanks to the light-heat transfer nature of $\text{Zn}(\text{Mebip})_2(\text{NTf}_2)_2$ and segmented material structure, the outcome polymer displayed UV sensitivity to composite part, while leaving the shape of neat SMP part unchanged under UV source (solely thermal sensitive). Thus the outcome composite displayed excellent UV and heat selective localized triple shape memory effect.

Shape memory polymers (SMPs) are a class of stimuli-responsive materials which are able to revert to the pre-defined shape upon a stimulus.[3, 151] Traditional SMPs are generally realized by introducing net-points into a

polymer with proper phase transition temperature (T_{trans}), forming thermal induced one-way dual-shape memory polymers (1WDSMPs).[162] The net-points determine the permanent shape, while the rest polymer act as switch to immobilize the temporary shape. A typical programming cycle for 1WDSMPs consists of four steps. First, the SMP was heated above its T_{trans} . Then the SMP was deformed and fixed by external force. Then the fixed SMP was cooling down (below the T_{trans}) and release the external force, the network will reach to a thermodynamic unstable while dynamic stable state. (so called temporary shape) Finally, the SMP was heated above its transition temperature, the switch is on (the mobility of the polymer will increase) and network will reach to a dynamic and thermodynamic stable state (so called permanent shape). [97, 163]

The SMP which could also memorize 2 temporary shapes and realize shape changing among three shapes, were called triple shape memory polymers (3SMPs).[164-166] Typically the 3SMPs were realized by introducing additional switches (either chemically or physically) into a normal 1WDSMP network, which could be a polymeric switch[59, 62, 68]/network[58] with distinct T_{trans} , self-complementary hydrogen bonding moieties,[113] or even utilize the two phase change in crystalline type switch (for example, PCL[58]). These unique abilities of 1WDSMPs and 3SMPs have been utilized for a number of applications in biomedical, packaging, textile and aerospace areas. [1, 151, 167]

Despite commonly utilized direct heating, other alternative triggering mechanisms like light and magnetic fields have also been developed.[126]

These methods enabled remote triggering of shape recovery and make SMPs more feasible in vivo applications. In previous demonstrated light-induced shape memory system,[168] light-sensitive components such as gold nanoparticle (responsive to laser in visible light region), graphene oxide (responsive to infrared light region), organo-metal compound and cinnamic groups (responsive to UV region) were embraced into polymer network either covalently or non-covalently to realize such purpose. Zhao et al. introduced functionalized AuNPs into the biodegradable SMPs to realize the visible light triggered shape recovery.[169, 170] Rowan et al reported a covalently cross-linked metallocupramolecular shape memory polymers with metal salt and poly(butadiene) which was end-capped with Mebip.[119, 171] The key component in fixing and releasing the temporary shape is the UV induced heating effect on metal-ligand units that lead to their dissociation-association. This mechanism was previously proved by Weder et al[119] for fabricating UV-induced self-healing, where new bonding could be reversibly formed among the neighbor fracture surfaces. For SMPs with cinnamic groups, their SME are realized by reversibly photo fixing ($\lambda > 260\text{nm}$) and photo cleaving ($\lambda < 260\text{nm}$) of cinnamic groups.[17] Although polymers with cinnamic groups and -OMebip are UV responsive, they are covalently connected to the polymers to realize light sensitivity. Therefore, compare to other commercial polymers like epoxy resin and polyurethane, the polymers mentioned above are difficult to fabricate and their mechanical properties are relatively poor. Compared to tuning molecular structures, blending light-heat transfer components into original polymer matrix is better because they are easy to process and maintain (even enhance) the original mechanical performance of

the matrix. However, to the best of our knowledge, so far there's few report on the UV-sensitive SMPs with composite approach.

6.2 Polymer design

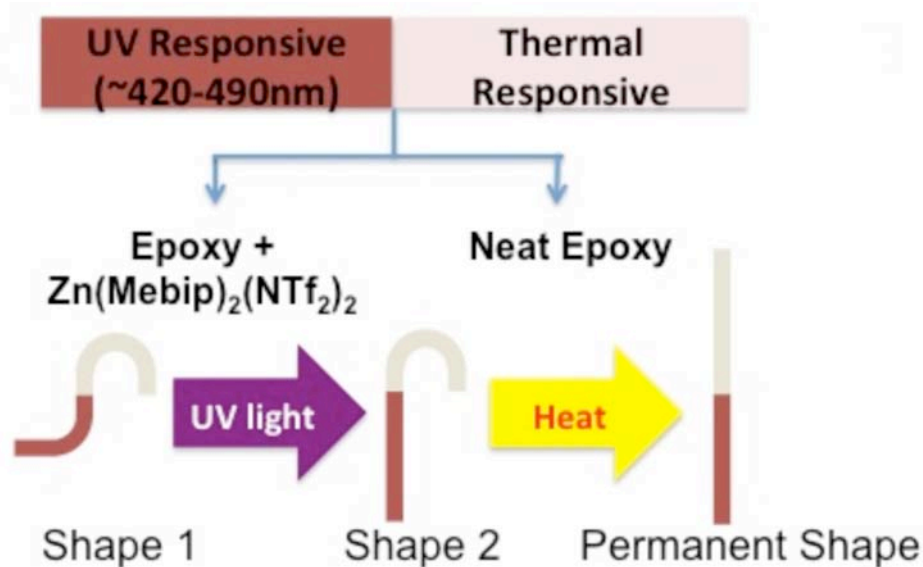


Figure 6.1. Illustration of composition of SMP, shape recovery routes (from shape #1 to the permanent shape).

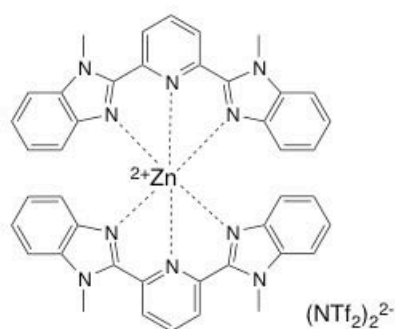


Figure 6.2. Molecular structure of Zn(Mebip)₂(NTf₂)₂.

Driven by increasing sophisticated demand of materials and devices, developing SMPs with additional functions like dual-responsiveness[165] are fueled by technological needs.[28, 172] Here, we report a triple shape memory polymer composite featuring both remote triggering of the shapes recovery with UV source and heat. Our approach for light-sensitive is based on the principle that the $\text{Zn}(\text{Mebip})_2(\text{NTf}_2)_2$, as shown in Figure 1B, can transfer UV source into heat.[119] Mebip and related Zinc complex were synthesized according to literature with slight modification.[119-121] Epoxy resin was chosen as the matrix because of its facile synthesis routine, tunable transition temperature at different region and great mechanical property (for example, high recovery force[173]). The shape memory behavior of epoxy resin has been investigated elsewhere.[174] The bi-responsive shape SMPs in present work was realized by casting the $\text{Zn}(\text{Mebip})_2(\text{NTf}_2)_2$ embedded epoxy prepolymer to the surface of pre-cured neat epoxy resin. Such a conceptual material design was shown in **Figure 6.1**. The target SMP consist of two regions: the $\text{Zn}(\text{Mebip})_2(\text{NTf}_2)_2$ -SMP (right region) and neat SMP. The permanent straight shape was first deformed into the shape 1, in which strains were introduced into each region. For shape 1, the recovery of the $\text{Zn}(\text{Mebip})_2(\text{NTf}_2)_2$ -SMP region can be remotely actuated by the UV source without enacting the recovery of the other region. As such, after UV irradiation, it could recover to the permanent shape by heating. Since the approach relies on selective localized actuations, a broad shape memory transition or two distinct shape memory transitions, which are required for other known triple shape memory polymers, are not needed here.

6.3 Results and discussions

Detailed raw materials for synthesis and characterization method are available in supplemental information. (SI) The molar ratio of the liquid epoxy precursor for the SMP samples was E-51/NGDE/Jeffamine (D230) = 2:1:3 because, according to our previous experience, the T_g of the outcome polymer with this recipe is in body temperature region. Weighted nanoparticles (0.2g bulk $Zn(Mebip)_2(NTf_2)_2$ which was solved in $CH_2Cl_2/MeCN$) were dispersed into the mixture of E51(1.0g) and NGDE(0.3g), then the solvent was removed under vacuum. The nanoparticles was further dispersed by ultrasonication for 10 mins. Next, Jeffamine (0.47g) was added into the dispersion. The obtained mixture was further mixed mechanically for 30s before cured. Inspired by Xie's work,[126] the SMP was synthesized in two steps. First, the neat SMP monomer solution, a mixture with E51 (2.5g), NGDE (0.7g) and Jeffamine (1.1g), was partially cured for 60 mins at 80°C in a 7.5cm×2.5cm Teflon mold. Then, the neat SMP was evenly cut into 2 pieces in the long axis and leave the right part in the mold. (the left side were left blank) Finally, the $Zn(Mebip)_2$ -SMP monomer solution were casted into the related blank part of the mold and fully cured. The overall measurement of the demonstration sample is 75mm×2mm×1mm. Two regions are both around 37mm in length. The mass ratio of $Zn(Mebip)_2(NTf_2)_2$ was 10%.

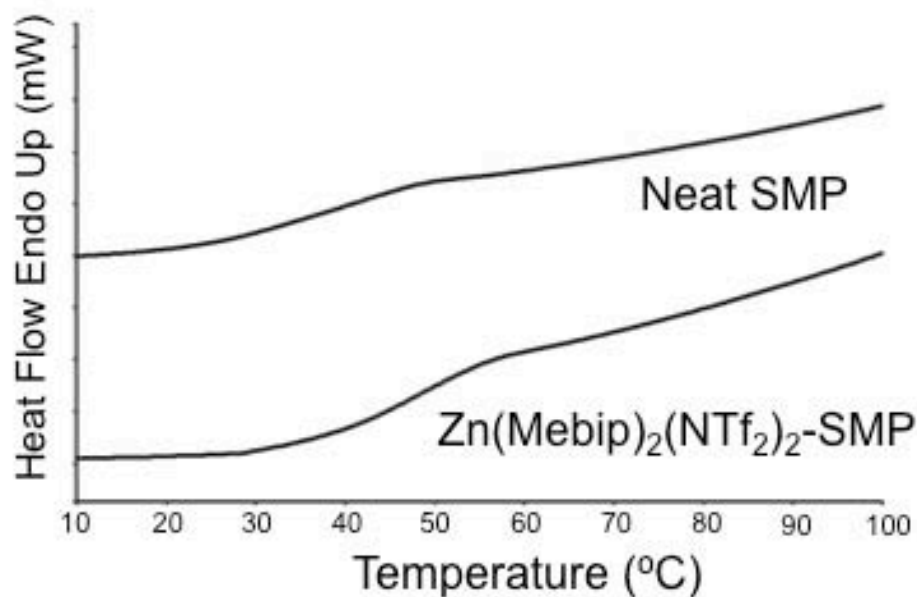


Figure 6.3. Differential scanning calorimetry of the second heating curve of each parts of the SMP.

Generally, the value of T_{trans} is important as it determined the application area of the outcome polymer.[9, 175] For example, a T_{trans} close to (usually slightly below) 37°C is preferred for biomedical applications,[176] while a high T_{trans} (say, 100°C) is required for aerospace applications[167]. Either dynamic mechanical analysis (DMA) or differential scanning calorimetry (DSC) can be employed to study the T_{trans} . In our work, the T_{trans} of the outcome SMPs were evaluated by DSC with a scanning rate of 10°C/min. As the material is with two parts (neat SMP and composite SMP), their T_{trans} were studied separately. As shown in **Figure 6.3** (the 2nd heating curve of the sample, as the first heat curve is to eliminate thermal history), the phase change of two parts are in glass transition nature and their glass transition temperatures (T_g) are close to or slightly higher than body temperature. For neat SMP, a apparent T_g was found at 37°C, while the T_g of Zn(Mebip)₂(NTf₂)₂-SMP is slightly shifted to

48°C. This phenomenon may be caused by the rigid nature of the organo-metal additives which hindered the mobility of the molecular chain. This result suggested that the T_{trans} of both part are close to body temperature. The T_g of $\text{Zn}(\text{Mebip})_2(\text{NTf}_2)_2\text{-SMP}$ could be further tuned to body temperature by slightly increase the ratio of NGDE in matrix.

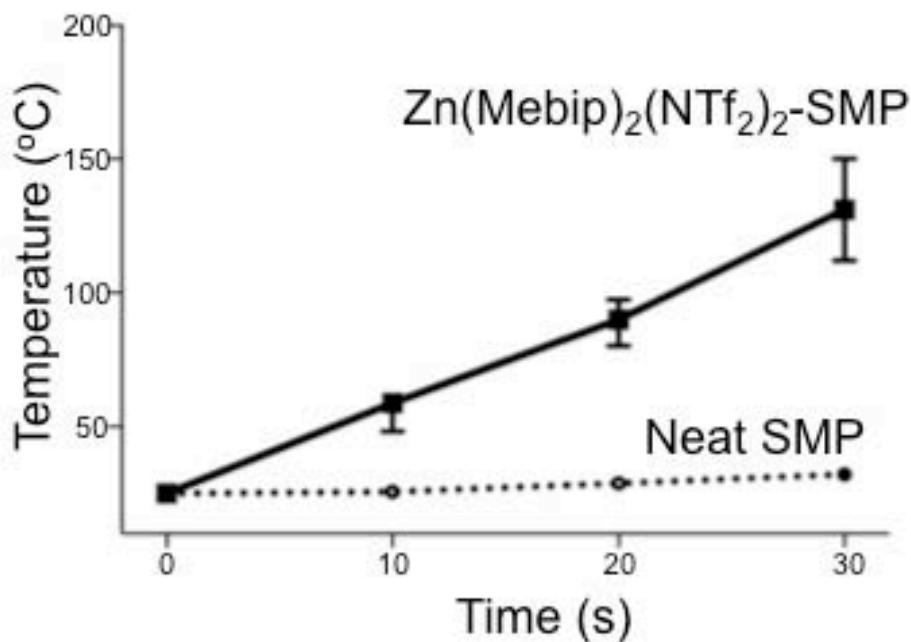


Figure 6.4. Temperature-time relationship of the each region under UV irradiation.

The pre-requirement of triple shape memory effect with two types of stimuli is that, at least one part of the sample is selectively responsive to a stimulus while the other part is less affected under the same stimulus. In our case, we anticipated that the $\text{Zn}(\text{Mebip})_2(\text{NTf}_2)_2\text{-SMP}$ should be sensitive to both UV and heat while the neat SMP part is solely thermally responsive. To prove the selective activation of the sample under UV source, the temperature-time relationship of each region (neat SMP part and composite part) was conducted. The UV source was generated from SunSpot SM 2 from Shenzhen Wisbay

M&E Co., LTD. The sample surface temperature during heating was recorded with IR camera. As shown in Figure 6.4, the temperature of $\text{Zn}(\text{Mebip})_2(\text{NTf}_2)_2\text{-SMP}$ part rapidly increased above their transition temperature after 10 seconds while the temperature of neat SMP part maintained below its transition temperature. This indicate that the $\text{Zn}(\text{Mebip})_2(\text{NTf}_2)_2$ is an efficient light-heat transfer agent. The light-heat transfer mechanism has been reported elsewhere.[119] Besides, the slight of temperature increase from neat SMP may be caused by the heat effect from the UV source, but such heat effect is not high enough to trigger the shape recovery of the neat SMP part.

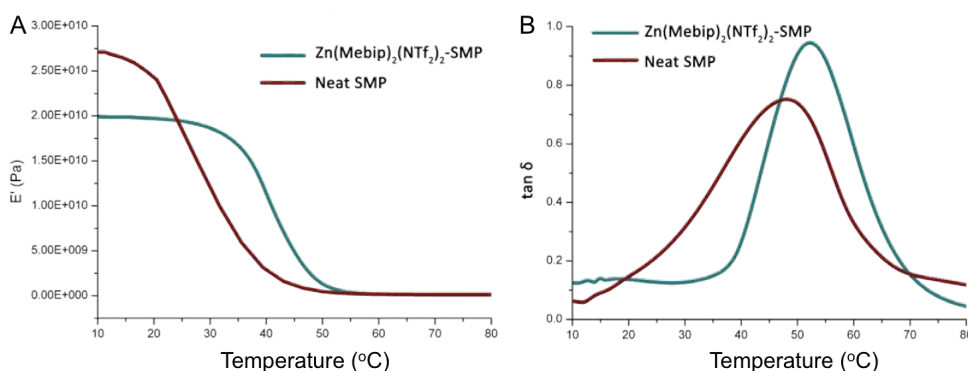


Figure 6.5. Dynamic mechanical analysis and demonstration of triple-shape effect. (A) and (B) illustrated the elastic modulus and $\tan \delta$ of each SMP part.

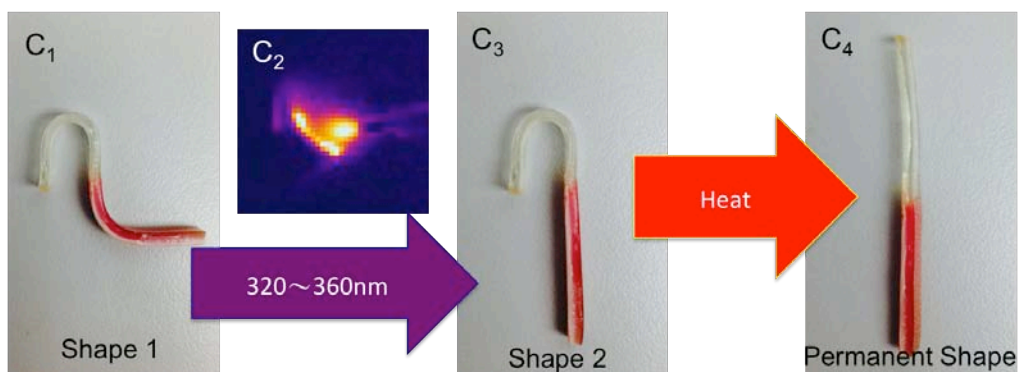


Figure 6.6. The deformed sample (C_1) was exposed to UV source and heat sequentially, leading to temporary shape 2 (C_3) and permanent shape (C_4). C_2 is the IR image taken by a FLIR E55 IR camera from above of the sample when it was exposing to UV source.

The mechanical properties of the SMPs were further studied by dynamic mechanical analysis (DMA) on a PerkinElmer DMA 8000 with bending method and the heating rate is $2^\circ\text{C}/\text{min}$. As shown in **Figure 6.5. A and 6.5.B**, the elastic modulus of neat-SMP and $\text{Zn}(\text{Mebip})_2(\text{NTf}_2)_2$ -SMP below the T_g are around 2.0×10^4 MPa and 2.7×10^4 M, while decreasing to 1.3×10^4 MPa and 1.6×10^2 MPa above T_g separately. The T_{gS} determined by $\tan\delta$ are slightly higher than ones determined by DSC. The shape memory effect of the sample was conducted by bending test with angle as recover factor.[126, 177] Shape fixity (R_f) and shape recovery (R_r) were evaluated by comparing the bending angle, fixed angle, and recovered angle. Samples were heated at 80°C and bend to 180° (bending angle) and then quenched in ice water for 1 min. The fixed angle was measured before the samples afterwards. The each region of the sample was then exposed to UV and subsequently heat. The final angle was measured as the recovered angle. The shape fixity and shape recovery ratio of each part are all close to 100%. Furthermore, a demonstration was

made to illustrate the UV/Heat sensitive triple shape memory effect. As shown in Figure 2, the sample was first deformed into a “s” shape #1, upon exposure to 320~360nm UV source which was applied by a horizontally fixed optical fiber, as shown in C₂, IR image suggested the selected activation of the Zn(Mebip)₂(NTf₂)₂-SMP part while neat SMP part maintain the original temperature. After 15 seconds’ UV irradiation, the SMP change to shape #2, which was subsequently recovered to its permanent shape by immersing the SMP into hot water with 60°C.

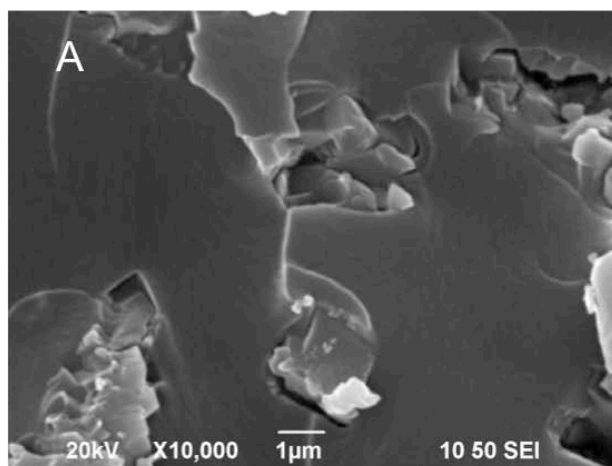


Figure 6.7. SEM images of the SMP composites. A) SEM image of Zn(Mebimpy)₂(NTf₂)₂-SMP at ×10000 magnification.

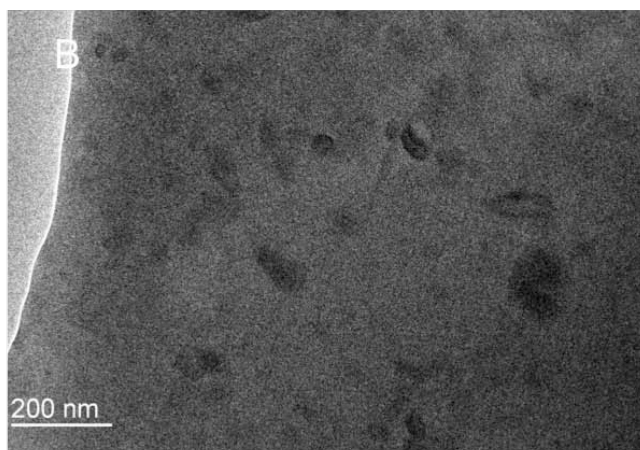


Figure 6.8. TEM image of Zn(Mebimpy)₂(NTf₂)₂-SMP.

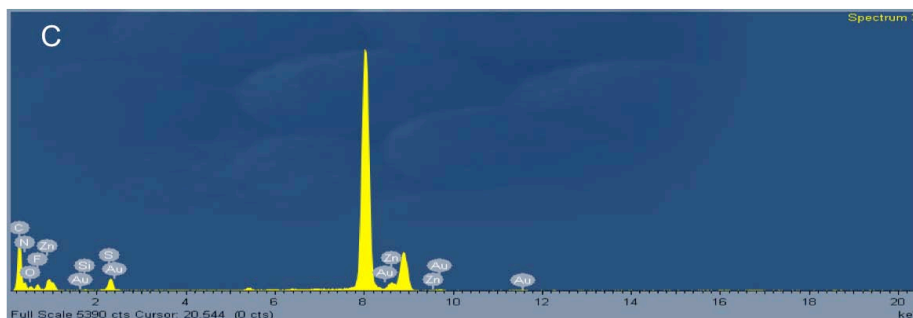


Figure 6.9. EDX image of composite.

The nanoparticulate dispersion and morphologies of the SMP composites were further characterized using scanning electron microscopy (SEM) and transmission electron microscopy (TEM). As shown in **Figure 6.7**, the fracture surface of the epoxy is relatively rough at low magnification of SEM. This may be caused by imperfect compatibility of epoxy matrix and the $\text{Zn}(\text{Mebip})_2(\text{NTf}_2)_2$. Although some projections may be regarded as $\text{Zn}(\text{Mebip})_2(\text{NTf}_2)_2$ clusters, unlike carbon nanotubes, they didn't display specific microstructure. Thus their dispersion can not be proved by simply SEM. To further study the dispersion of $\text{Zn}(\text{Mebip})_2(\text{NTf}_2)_2$ in epoxy matrix, the TEM was employed as the Zinc is the only heavy element available in the composite system. As shown in **Figure 6.8**, the dark spots, which may be considered as Zinc, are dispersed relatively normally in the polymer matrix at high magnification. The energy-dispersive X-ray spectroscopy (EDX) (**Figure 6.9**) further supported the existence of Zn in the matrix. The TEM proved that the $\text{Zn}(\text{Mebip})_2(\text{NTf}_2)_2$ can be dispersed relative normally at high magnification. The compatibility may be further improved by modify the p-C on the pyridine with additional aliphatic branch.

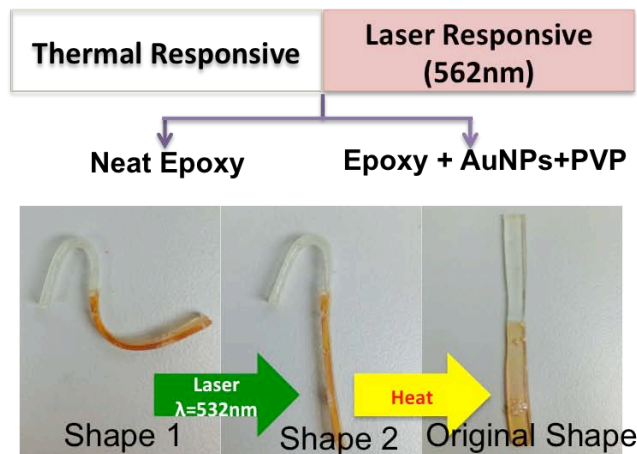


Figure 6.10. Illustration of molecular structure of AuNPs composites

To further enrich the category of light induced triple shape memory effect, gold nanoparticles (average diameter = 10 nm) were partially embedded into part of epoxy resin with Polyvinylpyrrolidone as dispersant. AuNPs are commonly utilized light-heat transfer units, which displayed maximum absorption at visible light region, has already been employed in many fields, for example, selectively kill cancer cells. Zhao et al. introduced functionalized AuNPs into the cross-linked polyethylene glycol to realize the visible light triggered shape recovery and self-healing. The laser source employed here was generated from Optlaser model G2000 532nm laser module. The sample surface temperature during heating was recorded with IR camera. In this work, similar molecular strategy was employed to fabricate vis-light/heat dual sensitive triple shape memory polymer. (see **Figure 6.10**) The polymeric composite also displayed well selective responsive recovery. (see **Figure 6.11**) Also as shown in **Figure 6.12**, TEM figure prove that the AuNPs are well dispersed in epoxy resin.

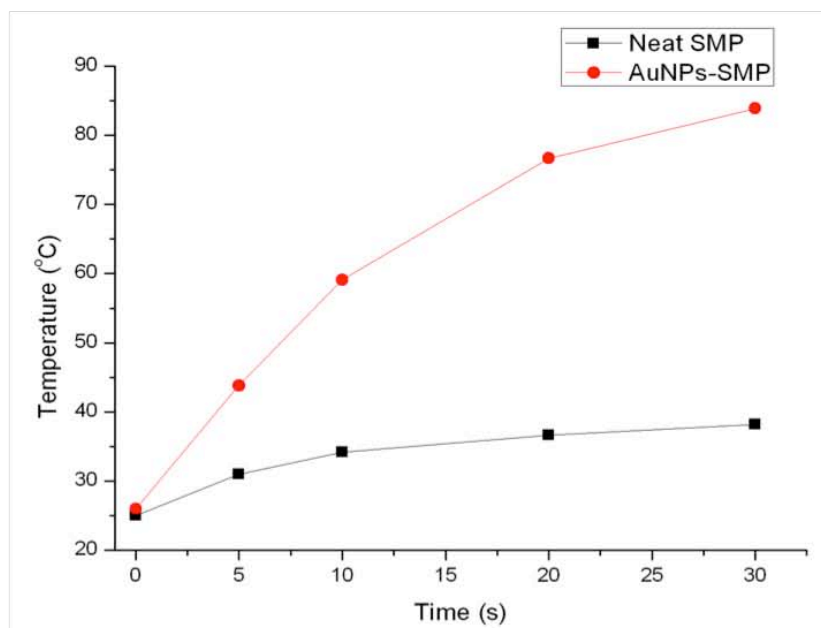


Figure 6.11. The temperature-time relationship the SMP composite.

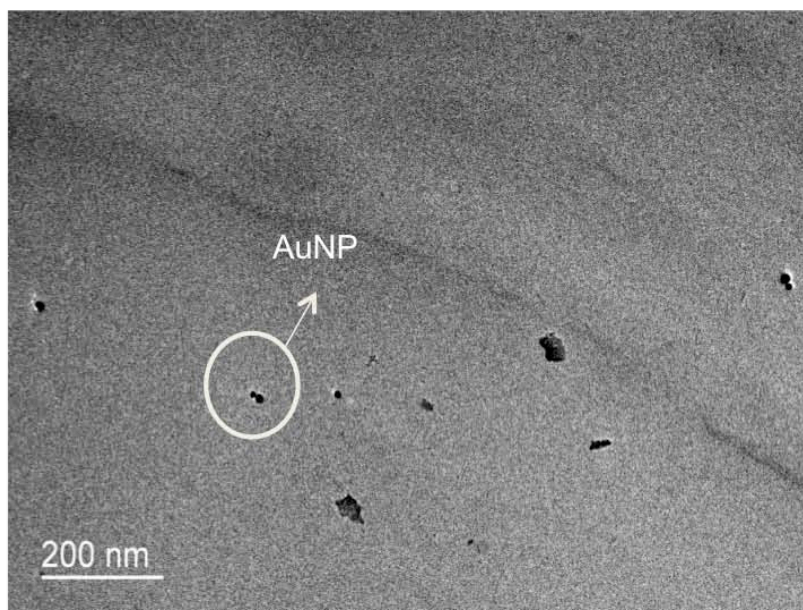


Figure 6.12. TEM of AuNPs part of composite.

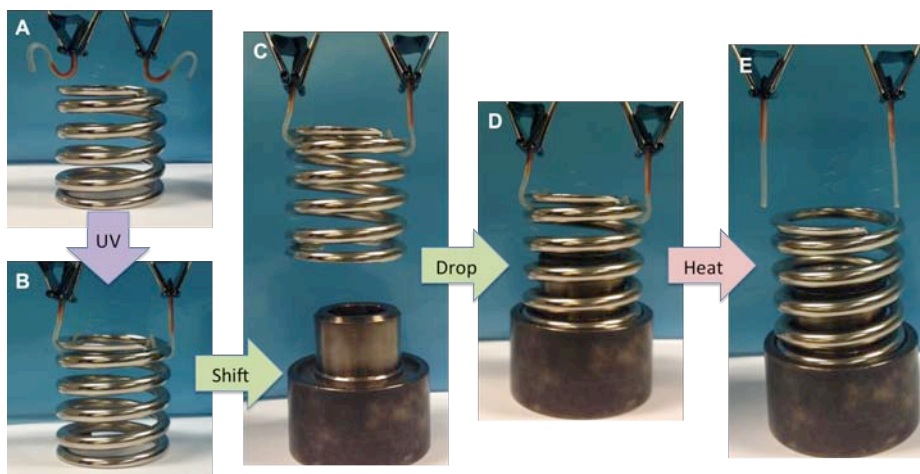


Figure 6.13. The demonstration of a practical application of the outcome SMP as robot hands.

One practical application was demonstrated by employing SMP as robot hands. As shown in **Figure 6.13**, A) initial state of robot hand was fabricated into S shape and exposed to UV source, resulting that B) the metal spring was hold by SMP. C) Then the spring was shifted above the metal base and D) installed on the base. E) The robot hands were further released by heat.

6.4 Summary

In summary, this work concerns a facile approach to UV/heat dual-responsive triple shape memory polymer. The molecular strategy of fabricating such polymer composite was realized by mixing $\text{Zn}(\text{Mebip})_2(\text{NTf}_2)_2$ partially into epoxy resin (10wt%). Unlike other reported UV-sensitive SMP where a sophisticated polymer structure is required and which displayed relatively poor mechanical properties, the advantage of this approach is that UV-sensitivity can be simply introduced to SMP by simply employing $\text{Zn}(\text{Mebip})_2(\text{NTf}_2)_2$ into any polymer matrix without significant sacrifice of thermal and mechanical properties. Also thanks to the light-heat transfer nature from

Zn(Mebip)₂(NTf₂)₂ segmented material structure, the outcome polymer displayed UV sensitivity to composite part, while leaving the shape of neat SMP part unchanged. Thus the outcome composite displayed excellent UV and heat selective localized triple shape memory effect.

CHAPTER 7 SUPRA-MOLECULAR SHAPE MEMORY POLYMER FILM FOR MOISTURE MANAGEMENT

7.1 Introduction

Shape memory polymers (SMPs) are a kind of smart materials whose geometry will (reversibly) recover to pre-defined shape upon proper stimuli.[3, 151, 162] This unique property has been employed in fabricating different prototypes like biomedical device, nano-wrinkles, aerospace applications, optical devices, actuators and smart textiles.[16, 88, 178-180] General thermal induced one-way dual shape memory polymers (1WDSMPs) are realized by introducing cross-links to polymers with proper phase transition temperature (T_{trans}), forming a net-points and switches structure.[76, 181, 182] Despite phase change, supra-molecular units, which processes intrinsic stimuli-responsive association-dissociation and thus act more like a real switch, were also incorporated into (pseudo-) elastic polymers to develop novel functional SMPs such as SMPs with additional thermal switch, light sensitivity, moisture/water sensitivity and self-healing SMPs.[3, 183, 184] Typical supra-molecular switches are metallo coordination bondings or strong intra-molecular hydrogen bondings. Kumpfer et al[171] modified branched poly(butadiene) with end-capped metal-chelating ligand 4-oxy-2,6-bis(N-methylbenzimidazolyl)pyridine (Mebip). After mixtion with metal salts and curing agent, they realized a SMP with metallo supra-molecular switch. Thanks to the intrinsic UV-heat transfer property and coordination bondings of

the metallo-organic unit, the outcome SMP displays a multi-responsiveness to UV, heat and chemical. Later, Wu et al[183] fabricated UV/heat dual responsive SMPs by simply blending $\text{Zn}(\text{Mebip})_2(\text{NTf}_2)_2$ into part of epoxy resin. For hydrogen bonding based supra-switches, self-complementary quadruple hydrogen bonding, ureidopyrimidinone (UPy) was probably first reported ones. Li et al[111] synthesized supra-SMPs containing pendent UPy side groups by copolymerization of butyl acrylate, cross-linker and UPy-substituted ethyl methacrylate monomer. Later, Ware et al[113] incorporated UPy-substituted ethyl methacrylate monomer into a polymer network with higher transition temperature, forming a triple shape memory polymer. In our previous paper, inspired from sea cucumbers, cellulose nano-whiskers (CNWs) were employed as skeleton and were blended into commercial thermal plastic polyurethane (TPU) to realize a rapid water responsive SMP. Zhu et al[144] demonstrated that the skeleton in TPU was formed by intra-molecular hydrogen bonding among CNWs, and such skeleton will soon subside and trigger the shape recovery upon immersing into water. Later, Chen et al[147] systematically studied pyridine based heat/moisture bi-sensitive supra-SMPs, where N,N-bis(2-hydroxyethyl) isonicotinamide (BINA) was incorporated into the soft-segment of polyurethane.

Developing textiles with adaptive functions, which are capable of supporting the abrupt microclimate changes, especially during exercise or in extreme environmental conditions, are fueled by technological and practical needs.[185-188] Despite commonly employed Poly-NiPAAm which was coated or grafted on fabric to enable dual responsiveness (pH and temperature),

the phase transition induced mobility change of SMPs has also inspired textile scientists to fabricate functional fabrics whose water vapor permeability (WVP) could sense, react and adapt to the thermal conditions provided by activity level of the wearer and/or environmental conditions.[89, 189-192] Generally, SMPs with adaptive WVP function are attributed to the stimulus sensitive free volume/mobility change in soft-segments (SS).[193] When below T_{trans} , mobility of SS is low and SMP will act as insulator for water vapor, thus enhancing warmth-keeping. When SMP was heated above T_{trans} , the SS will become 'active' and allow water vapor to escape, thus keep body dry. Different impact factors on thermal sensitive WVP, including kind and average length of soft-segments, glass transition temperature, hard-segment content, coating/laminating method, have been widely studied.[10, 193-198] However, the limitation with above mentioned materials is that they are only thermal sensitive while the demand for moisture sensitive textiles, particularly in sportswear, is widespread. Although limited studies on water sensitive SMPs with traditional phase transitions have been reported, few of them are capable of moisture/humidity sensitivity.

Driven by strong industrial demands and inspired by the environmental sensitivity of supra-molecular entities, the non-covalent bond is proposed here as switch units for designing new SMPs with moisture sensitivity for moisture controlling textiles. Considering the nature of bulk production required by textile applications, hydrogen bonding (HB) supra-molecular complexes may be more feasible because of their availability. Such switch units can both stabilize mechanical strain and endow low WVP at low moisture contents

when locked and shape recovery and high WVP at high moisture contents when opened up due to the nature of association and dissociation of non-covalent bonds. The mechanism of proposed supra-SMP is shown schematically in **Figure 7.1a**. In the present work, a series of moisture/heat bi-sensitive shape memory supra-molecular shape memory polyurethane containing large fraction of pyridine moieties as proton-acceptors were synthesized from 2,6-dihydroxymethyl pyridine (DHMP), HDI, MDI and BDO. The proton-donors are realized from the hydrogen on the amine groups of the polymer backbone, or by mixing additional poly(4-vinyl phenol). The thermal mechanical properties, moisture/heat induced shape memory effect and water vapor permeability were studied systematically. Relationships between structures and properties of Supra-SMPs were studied both experimentally and theoretically using modeling and simulation.

7.2 Polymer design

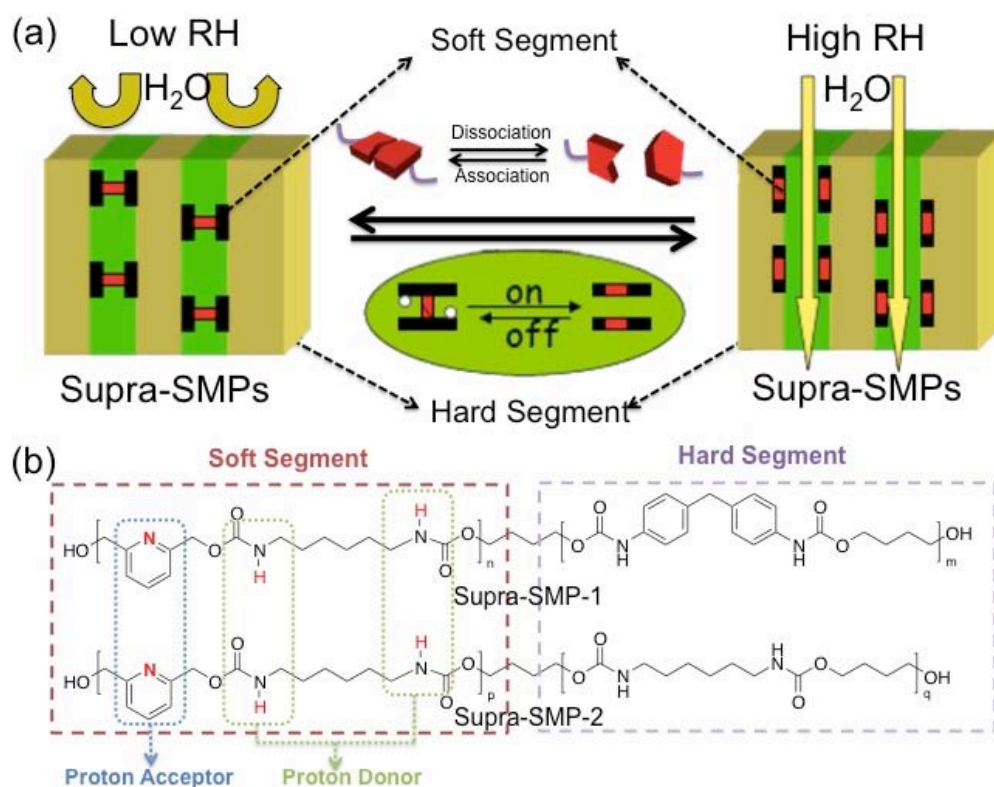


Figure 7.1. Schematic illustration of proposed supra-molecular SMP film as RH sensitive material and the molecular structure.

The supra-SMPs were fabricated by incorporating DHMP into the soft segment of the backbone of the polymer. DHMP was chosen as proton acceptor because of its stronger lewis base nature compared to N,N-bis(2-hydroxyethyl)isonicotinamide (BINA), where the carboxyl group at p-position may compromise the electron density of the nitrogen on the pyridine ring. Thanks to the reaction of NCO with OH group (from HDI and DHMP), the resident hydrogen on the amino group could serve as proton donor. Two types of hard-segment (MDI-BDO and HDI-BDO) was employed to tune the mechanical properties and optimize the performance of moisture management properties of the outcome polymer, because the PU with MDI is more

mechanically strong, hydrophobic and rigid while the PU with HDI is relatively mechanically mild, hydrophilic and flexible. The recipe and hard-segment content is shown in **Table 7.1**.

Table 7.1. Recipes of Supra-SMP 1 &2

	DHMP (g)	HDI (g)	MDI (g)	BDO (g)	HSC (%)
Supra-SMP1-25	2.9	3.34	1.59	0.48	25
Supra-SMP1-35	2.9	3.34	2.53	0.82	35
Supra-SMP1-45	2.9	3.34	3.81	1.29	45

	DHMP (g)	HDI (g)	HDI (g)	BDO (g)	HSC (%)
Supra-SMP2-25	2.9	3.34	1.395	0.684	25
Supra-SMP2-35	2.9	3.34	2.226	1.134	35

7.3 Results and discussions

Introducing supra-molecular switch into the backbone of the polymer enabled the polymer with dual/multiple responsiveness. In our previous reported work, the hydrogen bonding among proton donors and acceptors could be reversibly broken and rebuild by both heat and moisture. The thermal responsive SME of the outcome polymer was tested by bending method. Supra-SMP1 was chosen for their broad tunable dissociation temperature for HB by controlling HSC. The shape fixity and recovery ratio of Supra-SMP1-25 are both around 100%. The moisture/humidity responsive SME of the outcome polymer was also tested by bending method. Interestingly, the moisture responsive time for Supra-SMP2 is much quicker responding compare to Supra-SMP1, on which shape recovery was not observed. This phenomenon may be caused by the

flexibility and relative hydrophilic property (compare to MDI) of HDI in the hard segment, which facilitated the penetration of water vapor. Supra-SMP2 with 25% HSC was chosen for demonstration because of its. As shown in **Figure 7.2**, the dry polymer film was first bended to 180° in the oven and soon get out. After it was fixed in the lab (with temperature of 20°C and relative humidity of 65%) for about 30 seconds, one end of the film was fixed on the instrument. The film soon recovery to 89° in 3mins (**Figure 7.2, b**), suggesting the shape fixation ratio around 52%. Such low shape fixity was attributed to the imperfect cooling. (If the film was cooling for longer time, the moisture may penetrate the film and cause early shape recovery before recording) After 25mins, the film recovered to a total flat form (**Figure 7.2, d**), suggesting a shape recover ratio around 100%.

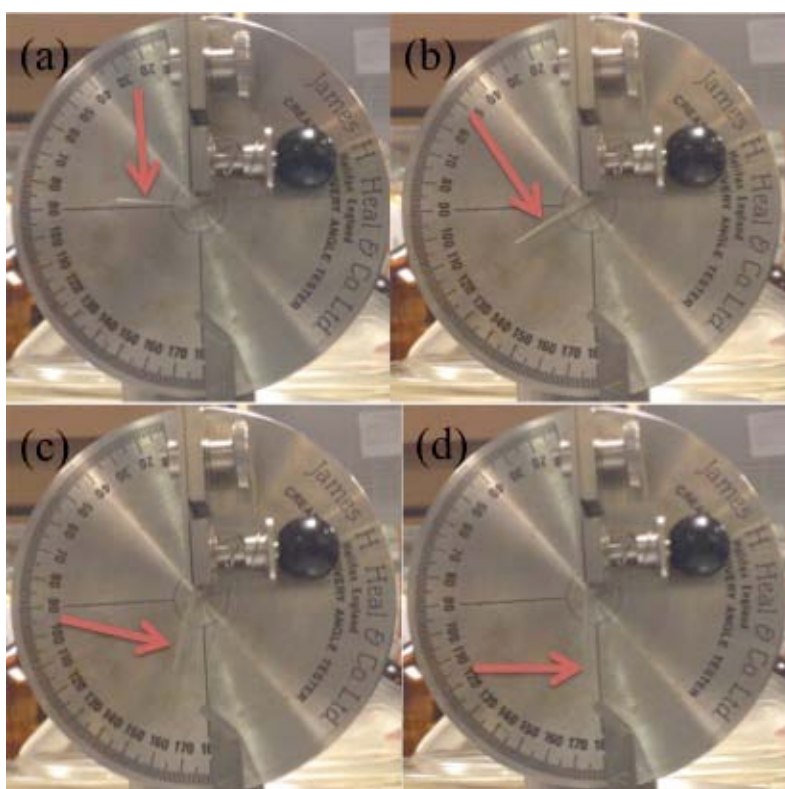


Figure 7.2. Demonstration of moisture induced shape memory effect.

Moisture management property was conducted by measuring the performance of WVP vs RH. Initially, supra-SMP1 with different HSC was chosen and made into film around 0.1mm thickness. As shown in figure 7.3, the WVP increase linearly with increase of RH for all samples with different HSC and ratio of PVP. However, as shown in **Figure 7.3** and **Figure 7.4a**, for Supra-SMP2 (HSC = 25%, thickness~0.1mm) with different ratio of PVP and different type of proton donors, only the one with 90% PVP content showed a slightly RH sensitivity. Interestingly, when we further decrease the thickness of Supra-SMP2, the RH sensitivity got boosted. As shown in **Figure 7.4b** and **7.4c**, when RH is below 65%, the WVP increase slowly, while when RH is above 65%, the WVP of film increase dramatically. Indicating a success moisture management property. The dependence of WVP at 95% relative humidity to film thickness was further fabricated in **Figure 7.4c**, indicates that the thickness has dramatic impact on WVP, indicating that the ideal thickness should be below 25um for industrial applications. Furthermore, by blending external proton donors, say, PMH and PVP, as indicated by **Figure 7.4d**, both Supra-SMP2 itself and Supra-SMP2/PVP could form inter/intra- molecular hydrogen bonding, thus could act as supra-molecular switch for moisture management. While for Supra-SMP2 and PMH, the phenomena may be caused by less hydrogen bonding formed between Supra-SMP2 and PMH, and the hydrophobic property of PMH.

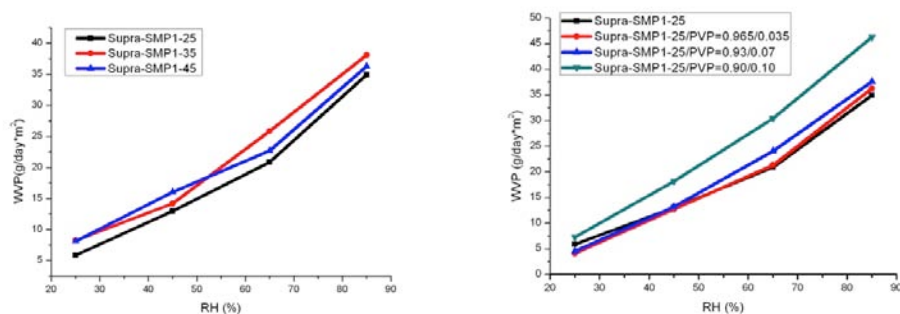


Figure 7.3. WVP of Supra-SMP1 with different hard segment content (left) and different content of PVP (right).

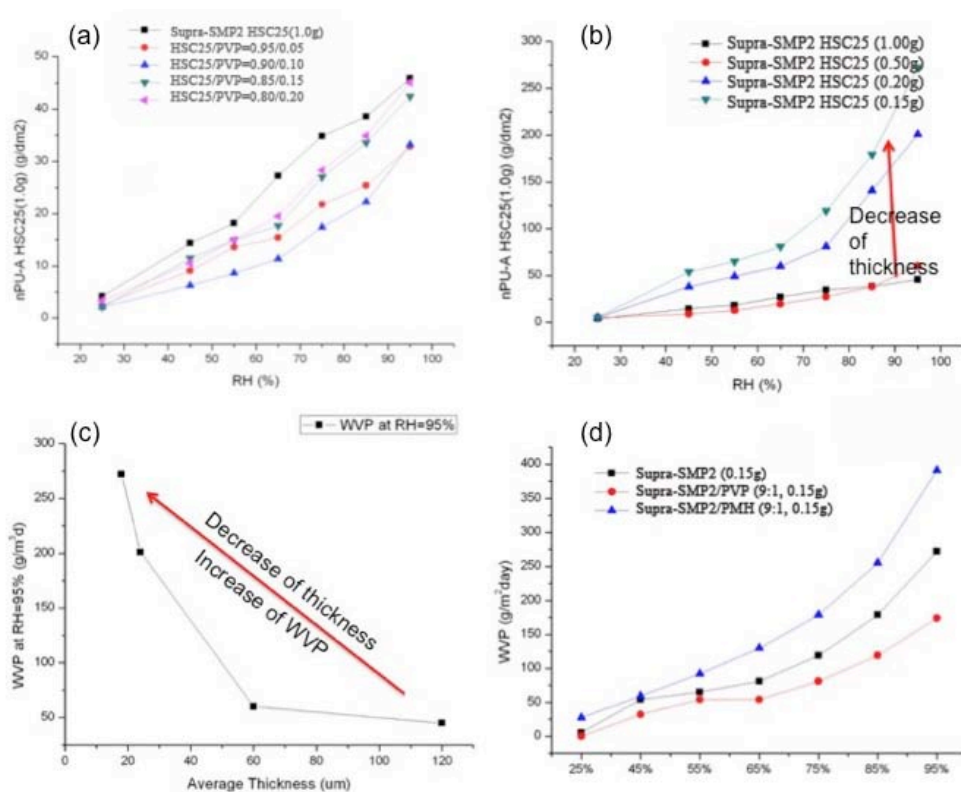


Figure 7.4. WVP vs RH of Supra-SMP2 with (a) different ratio of proton donor, (b, c) different RH thickness of Supra-SMP2 and (d) with different type of proton donor at low thickness.

To further prove the mechanism of RH dependent WVP, FTIR and theoretical study was currently employed to study the film at low moisture state and high

moisture state. FTIR is a common and efficient technic to study hydrogen bonding. To further explore the mechanism of RH dependent WVP, FTIR was employed to study the film at both low moisture state and high moisture state. With increase of the energy of HB, the wavenumber of the peak will move to lower region and vice versa. As shown in **Figure 7.5**, the FTIR of Supra-SMP2 was conducted at both low RH and high RH state. The detailed belongings of related peaks and their shifts were generalized in **Table 7.2**. The shift of peaks can be generalized into two groups, ones related to pyridine ring and ones related to urethane group. According to **Figure 7.5(b,d)**, the peaks related to urethane group (ν_{NH} and $\nu_{\text{C=O}}$) shifts to lower wavenumber, indicating formation of stronger HBs. At the same time, obvious shifts from low wavenumber to high wavenumber were observed for peaks related to pyridine ring. Indicating the breaking (or lower concentration) of hydrogen bonding between DHMP and amino group after the penetration of water vapor. The phenomenon may be further explained the molecular mechanism of moisture management that the pyridine ring formed stable HB with the NH in the urethane group at low RH, while such HB may be broken by the penetration of water vapor at high RH, leading to a higher mobility of SS and thus higher WVP. The dissociated NH on the urethane group may form stronger HB with the carbonyl group, leading to the decrease of wavenumber.

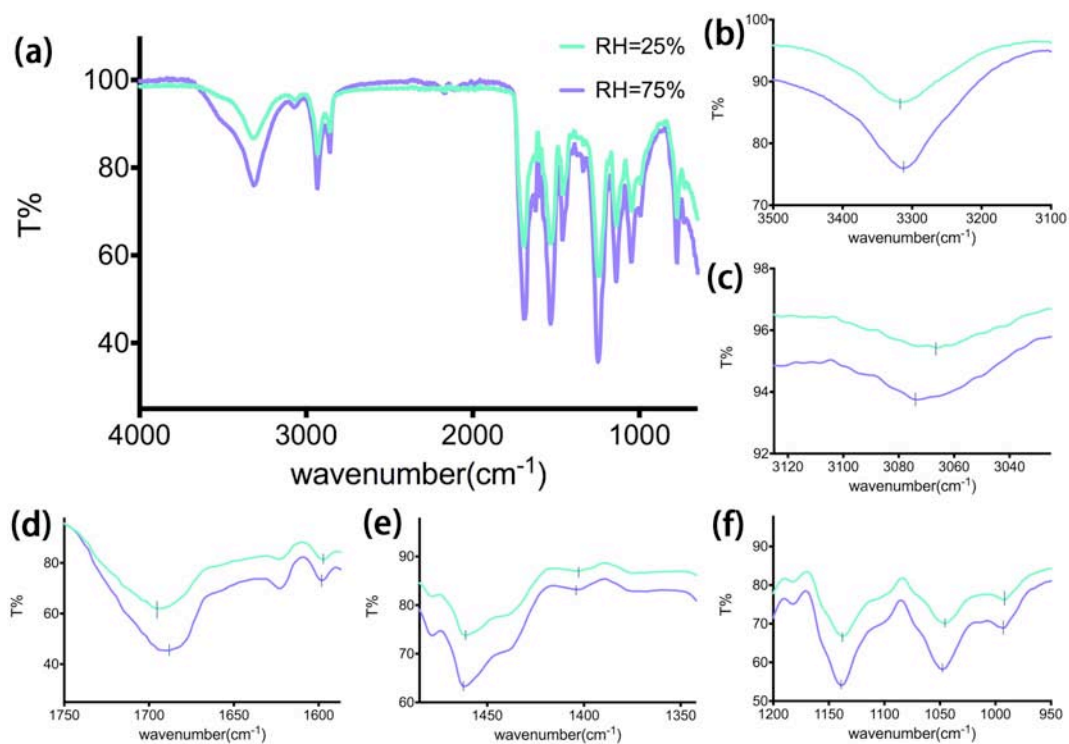


Figure 7.5. Illustration of change of hydrogen bonding in Supra-SMP2 by FTIR at low RH and high RH state.

Table 7.2. Shift of peaks in FTIR and their belonging.

	Supra-SMP2 (RH=25%)/cm ⁻¹	Supra-SMP2 (RH=75%)/ cm ⁻¹
vNH of urethane group	3317	3314
vCH of pyridine ring	3066	3073
vC=O of urethane group	1695	1689
vC-N-C of pyridine ring	1597	1598
vPy stretching vibrations	1461	1462
vPy stretching vibrations	1403	1404
Stretching mode of pyridine	1137	1139
Stretching mode of pyridine	1046	1048

Positron annihilation lifetime spectroscopy (PALS) technique has emerged as a unique and potent probe for detecting the free volume properties of polymers in recent years. The longest-lived component (τ_3) results from the pick-off annihilation of ortho-positronium (o-Ps) in the free volume sites. The o-Ps lifetime (τ_3) is the measure of size of free volume site in polymers (the greater τ_3 , the larger size), and intensities (I_3) is indicative of the number concentration of free volume sites in polymers.[193] In this paper, as shown in **Figure 7.6**, both τ_3 and I_3 of Supra-SMP2 will increase with the increase of RH, indicating larger pore size and concentration at higher RH.

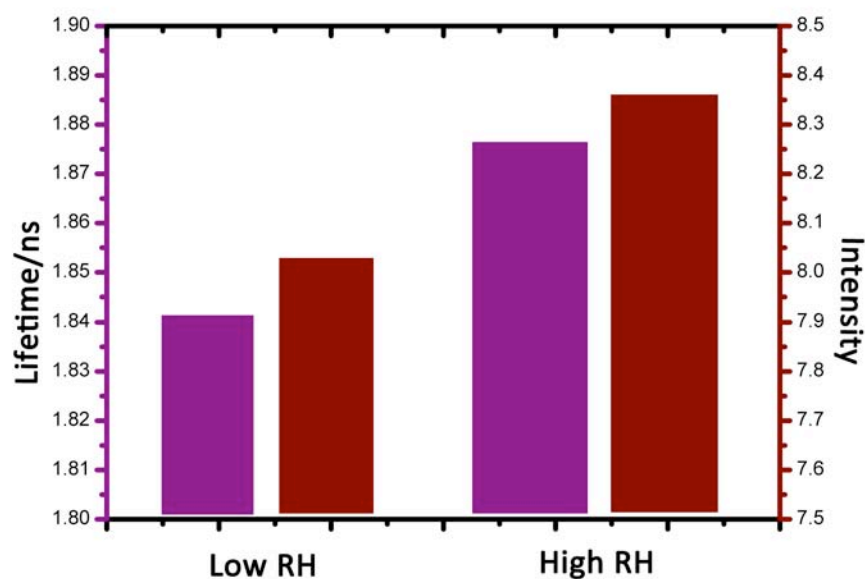


Figure 7.6. Positron annihilation lifetime (τ_3) and intensity (I_3) of Supra-SMP2.

The modelling of HB competition was done by inserting different amount of water molecules in proton donor (PD) and proton acceptor (PA). As shown in

the **Figure 7.7**, the stable state of intra-molecular bondings between/among PD, PA and water were calculated using Gaussian simulation. The pyridine ring will first form HB with PD at dry state. However, with addition of one water molecule (just like the low RH region), the water will firstly participated into the HB in connected with PD and PA, forming a PA...H₂-O...PD structure. When two water molecules was further added (just like the middle or high level of RH), two water molecules will form individual HB with PD and PA. This result may proved the dominant position of water in forming HB in this system and thus mechanism of RH responsive WVP in proposed supra-SMP film may be also ascribed in **Figure 7.7**. The competition of HB in supra-molecular units and water molecules play vital role in realization of moisture management. At low RH, the formation of supra-molecular switches hindered the mobility of SS, thus lead to the low WVP. (left) While with slight increasing of RH, the water molecular participated into the competition of the hydrogen bondings among supra-molecular switches, leading to a PA...H₂-O...PD structure, where the mobility of supra-molecular switches are still locked, leading to a relatively low WVP. Later, at high RH region, the increasing amount of water will form individual HB with PAs/PDs, leading to dissemble of supra-molecular switches and higher mobility of SS, thus higher WVP.

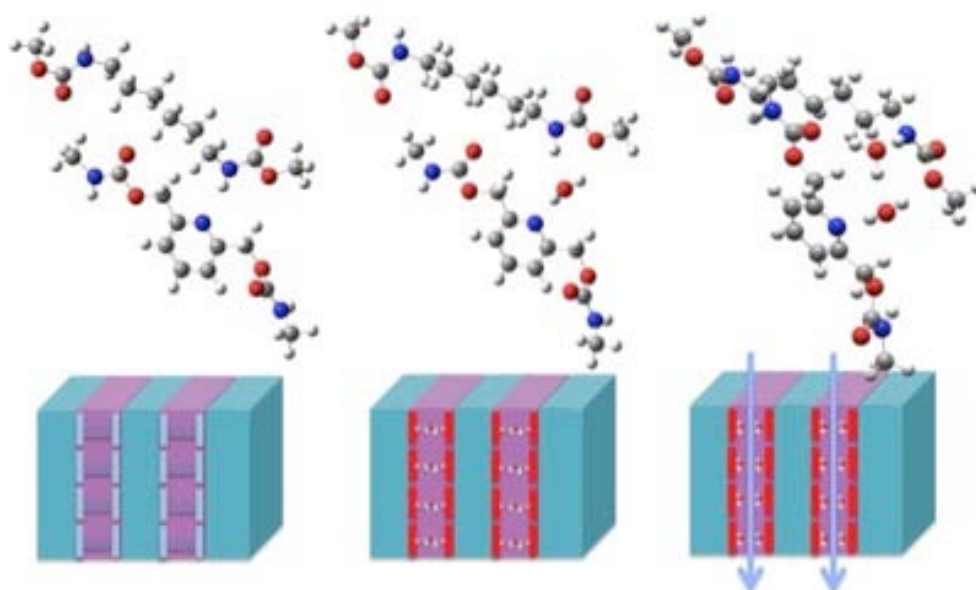


Figure 7.7. Modeling of hydrogen competition and proposed mechanism of RH sensitive WVP.

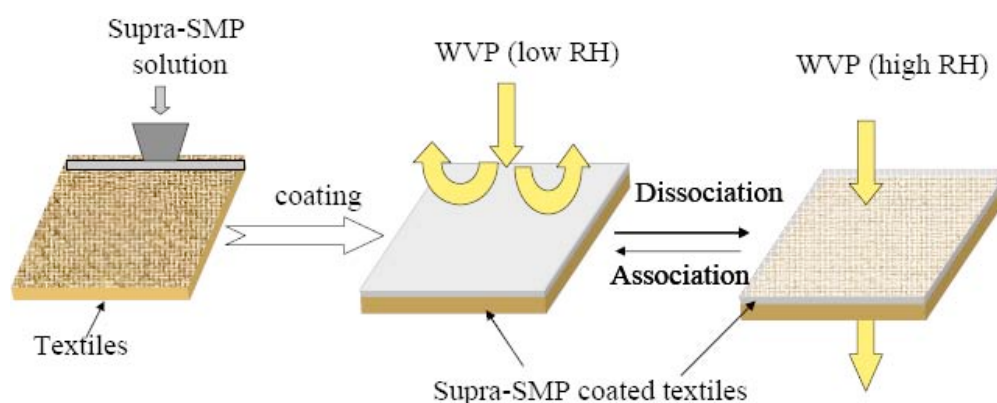


Figure 7.8. Schematic illustration of practical application of Supra-SMP2 as moisture management material in textile industries.

7.4 Summary

In summary, a series of shape memory polymeric film with different supra-molecular switches was fabricated and explored their potential application as moisture management material. After careful study of Supra-SMP with DHMP

as proton acceptor, we found that the thickness of film plays the vital role for moisture management. While the external proton donor like PVP may be beneficial to the performance of moisture management. The molecular mechanism of RH dependent WVP was also proved by FTIR. The outcome polymer displayed strong potential for textiles industrials, especially for sports wears. (As shown in **Figure 7.8**)

CHAPTER 8 CONCLUSIONS AND SUGGESTIONS FOR FUTURE WORK

8.1 Conclusions

8.1.1. General functional SMPs

Recently, functional shape memory polymers are drawing growing research interest. Despite currently reported thermal/athermal stimuli, two-way/triple/multi- shape memory and biological functions, SMPs with multiple functions is no doubt the most promising smart materials for better diversity and adaptability to sophisticate applications. After careful study on current SMPs, this work mainly focus on developing SMPs with novel functions including chromic behavior, reversible shape changing, multi-responsive triple shape memory effect and moisture management functions.

8.1.2. Memory chromic SMPs

In Chapter 4, we reported a chromic polymer which is responsive to its shape memory properties and embrace both the behavior of SMPs and chromic materials. We employed a strategy to fabricate such a smart material which represents a new principle for making chromic materials. This material is made of shape memory polyurethane with tetraphenylethylene units covalently connected to their backbone. The rotation of phenyl groups of the TPE clusters is governed indirectly by the shape memory properties such as original shape, shape deformation and stimuli. We can imagine that when the soft segments

are molten or dissolved in solvent, the switch is open, the AIE units are free from crystal binding and can migrate easily to larger areas, thus reducing the barrier for free rotation for phenyl groups of TPE, the emission intensity reduces or disappears, which leads to no color or pale colors. Such simple approach enabled the material with reversible mechano-, solvato-, thermochromic and SME. Since the switch is a fundamental structural character of SMPs, the shape memory properties have led to the chromism and we call this memory chromic.

8.1.3. Two-way SMPs by interpenetrating polymeric network

Later in Chapter 5, a novel molecular strategy was employed to fabricate a 2WSMP, which is an interpenetrating network (IPN) with elastomeric and crystalline components leading to the switch-spring structure. In this 2WSMP, the switch, crystalline network, is responsible for the reversible shape shrinkage while the spring, the compressed elastomeric network, provides the push force for shape expansion. When heating the outcome IPN to a temperature of 65°C, which is above the melting temperature of the PCL crystalline phase, the switch is open and the polymer will shrink and press the spring, the elastomeric network at the same time. This is the heating induced shrinkage. Then dropping the temperature to around 20°C, room temperature, much below the T_m , the stored energy in the spring, namely, the cross-linked amorphous phase, provides the orientation force to the crystalline segment for recrystallization. This leads to the length expansion. This is the desired 2WSME in a polymer and the DMA proved such 2WSME with a reversible

deformation ratio as high as 5.5%, which is similar to shape memory alloy. We believe that this value can be further improved by replacing PCL with PCO, which displayed relatively higher R_{sc} and T_m . From the result obtained here, it can be seen that it is feasible to construct a tension-free permanent 2WSMP with length change at two different ambient stimuli above and below the melting temperature of the switch phase using an IPN polymer. The synthesis of such IPN is easy and the cost is minimal. This novel and facile method can be applied to many polymers and enhance the performance and add more functions of a shape memory polymer. For example, such polymer could be made into radical fibers of spacer fabrics to make their thickness into a thermal sensitive one, thus resulting in temperature management spacer fabrics. (figure 3) In a word, the material should have great potentials for wide applications like textiles, footwear, packaging, sensors, actuators and artificial muscles.

8.1.4. Light/heat dual sensitive triple shape memory polymer

In Chapter 6, a facile approach to UV/heat dual-responsive triple shape memory polymer. The molecular strategy of fabricating such polymer composite was realized by mixing $Zn(Mebip)_2(NTf_2)_2$ partially into epoxy resin (10wt%). Unlike other reported UV-sensitive SMP where a sophisticated polymer structure is required and which displayed relatively poor mechanical properties, the advantage of this approach is that UV-sensitivity can be simply introduced to SMP by simply employing $Zn(Mebip)_2(NTf_2)_2$ into any polymer matrix without significant sacrifice of thermal and mechanical properties. Also thanks to the light-heat transfer nature from $Zn(Mebip)_2(NTf_2)_2$ segmented material structure, the outcome polymer displayed UV sensitivity to composite

part, while leaving the shape of neat SMP part unchanged. Thus the outcome composite displayed excellent UV and heat selective localized triple shape memory effect.

8.1.5. Supra-molecular shape memory polymer for moisture management

In Chapter 7, a series of shape memory polymeric film with different supra-molecular switches was fabricated and explored their potential application as moisture management material. After careful study of Supra-SMP with DHMP as proton acceptor, we found that the thickness of film plays the vital role for moisture management. While the external proton donor like PVP may be beneficial to the performance of moisture management. The molecular mechanism of RH dependent WVP was also proved by FTIR. The outcome polymer displayed strong potential for textiles industries, especially for sports wears.

8.2. Suggestions for future work

Although a series of work has been done to further study SMPs with novel functions, blank areas in this field are still await to be filled, further optimization are also necessary. Here some comments are listed for the futher suggestion to the related area.

8.2.1. Memory chromic SMPs

So far the memory chromic materials are on the initial stage. By combining the stimuli respond shape memory function with stimuli respond color change

function, the outcome polymer should display better interest in real applications. So far the problems left in this field are 1) shape induced wavelength change; 2) chromic materials in fiber form; 3) non-dye based chromic material and 4) how chromic behavior and shape memory behavior could be truly/dependently connected.

8.2.2. Two-way shape memory fibers

Although two-way shape memory materials have great potential in different application areas, the existing problems are still wait for resolve. So far the problems are 1) how to realize the large shape changing with stress free at low temperature; 2) how to fabricate the two-way shape memory polymers into fiber format and 3) novel two-way shape memory polymers. The first problem may be solved by incorporating polymer network with higher degree of crystalline, while the second problem may request the introduction of physical cross-linking.

8.2.3. Supra-molecular shape memory polymers

Compare with temperature sensitive WVP, moisture sensitive WVP are more attractive for real applications. So far the problem existed in moisture management materials are 1) how to enhance their water vapor permeability at room temperature and 2) how to combine the temperature sensitivity with relative humidity sensitivity.

REFERENCES

REFERENCES

1. Hu, J.L. and S.J. Chen, *A review of actively moving polymers in textile applications*. Journal of Materials Chemistry, 2010. **20**(17): p. 3346-3355.
2. Dong, Y.Q., et al., *Aggregation-induced emissions of tetraphenylethene derivatives and their utilities as chemical vapor sensors and in organic light-emitting diodes*. Applied Physics Letters, 2007. **91**(1).
3. Hu, J.L., et al., *Recent advances in shape-memory polymers: Structure, mechanism, functionality, modeling and applications*. Progress in Polymer Science, 2012. **37**(12): p. 1720-1763.
4. Chen, S.J., et al., *Effect of SSL and HSC on morphology and properties of PHA based SMPU synthesized by bulk polymerization method*. Journal Of Polymer Science Part B-Polymer Physics, 2007. **45**(4): p. 444-454.
5. Chen, S.J., et al., *Effect of molecular weight on shape memory behavior in polyurethane films*. Polymer International, 2007. **56**(9): p. 1128-1134.
6. Chen, S.J., et al., *Supramolecular polyurethane networks containing pyridine moieties for shape memory materials*. Materials Letters, 2009. **63**(17): p. 1462-1464.
7. Chen, S.J., et al., *Fourier transform infrared study of supramolecular polyurethane networks containing pyridine moieties for shape memory materials*. Polymer International, 2010. **59**(4): p. 529-538.
8. Hu, J.L., Y.M. Zeng, and H.J. Yan, *Influence of processing conditions on the microstructure and properties of shape memory polyurethane membranes*. Textile Research Journal, 2003. **73**(2): p. 172-178.
9. Meng, Q.H. and J.L. Hu, *Self-organizing alignment of carbon nanotube in shape memory segmented fiber prepared by in situ polymerization and melt spinning*. Composites Part A-Applied Science And Manufacturing, 2008. **39**(2): p. 314-321.
10. Wang, Z.F., et al., *Effect of temperature and structure on the free volume and water vapor permeability in hydrophilic polyurethanes*. Journal of Membrane Science, 2004. **241**(2): p. 355-361.
11. Ahn, S.K., P. Deshmukh, and R.M. Kasi, *Shape memory behavior of side-chain liquid crystalline polymer networks triggered by dual transition temperatures*. Macromolecules, 2010. **43**(17): p. 7330-7340.
12. Chung, T., A. Rorno-Urbe, and P.T. Mather, *Two-way reversible shape memory in a semicrystalline network*. Macromolecules, 2008. **41**(1): p. 184-192.
13. Chen, S.J., et al., *Two-way shape memory effect in polymer laminates*. Materials Letters, 2008. **62**(25): p. 4088-4090.
14. Yakacki, C.M., *Shape-Memory and Shape-Changing Polymers*. Polymer Reviews, 2013. **53**(1): p. 1-5.
15. Li, J.J., W.R. Rodgers, and T. Xie, *Semi-crystalline two-way shape memory elastomer*. Polymer, 2011. **52**(23): p. 5320-5325.
16. Behl, M., et al., *Reversible Bidirectional Shape-Memory Polymers*. Advanced Materials, 2013. **25**(32): p. 4466-4469.

REFERENCES

17. Lendlein, A., et al., *Light-induced shape-memory polymers*. Nature, 2005. **434**(7035): p. 879-882.
18. Jiang, H.Y., S. Kelch, and A. Lendlein, *Polymers move in response to light*. Advanced Materials, 2006. **18**(11): p. 1471-1475.
19. Yu, Y.L., M. Nakano, and T. Ikeda, *Directed bending of a polymer film by light - Miniaturizing a simple photomechanical system could expand its range of applications*. Nature, 2003. **425**(6954): p. 145-145.
20. Wu, L.B., C.L. Jin, and X.Y. Sun, *Synthesis, properties, and light-induced shape memory effect of multiblock polyesterurethanes containing biodegradable segments and pendant cinnamamide groups*. Biomacromolecules, 2011. **12**(1): p. 235-241.
21. Koerner, H., et al., *Remotely actuated polymer nanocomposites - stress-recovery of carbon-nanotube-filled thermoplastic elastomers*. Nature Materials, 2004. **3**(2): p. 115-120.
22. Leng, J.S., X.L. Wu, and Y.J. Liu, *Infrared light-active shape memory polymer filled with nanocarbon particles*. Journal of Applied Polymer Science, 2009. **114**(4): p. 2455-2460.
23. Liang, J.J., et al., *Infrared-triggered actuators from graphene-Based nanocomposites*. Journal of Physical Chemistry C, 2009. **113**(22): p. 9921-9927.
24. Lendlein, A. and R. Langer, *Biodegradable, elastic shape-memory polymers for potential biomedical applications*. Science, 2002. **296**(5573): p. 1673-1676.
25. Yakacki, C.M., et al., *Unconstrained recovery characterization of shape-memory polymer networks for cardiovascular applications*. Biomaterials, 2007. **28**(14): p. 2255-2263.
26. El Feninat, F., et al., *Shape Memory Materials for Biomedical Applications*. Advanced Engineering Materials, 2002. **4**(3): p. 91 -104.
27. Behl, M., J. Zotzmann, and A. Lendlein, *Shape-Memory Polymers and Shape-Changing Polymers*. Shape-Memory Polymers, 2010. **226**: p. 1-40.
28. Liu, C., H. Qin, and P.T. Mather, *Review of progress in shape-memory polymers*. Journal of Materials Chemistry, 2007. **17**(16): p. 1543-1558.
29. Lee, K.M., et al., *Polycaprolactone-POSS chemical/physical double networks*. Macromolecules, 2008. **41**(13): p. 4730-4738.
30. Xie, T., et al., *Encoding localized strain history through wrinkle based structural colors*. Advanced Materials, 2010. **22**(39): p. 4390-4394.
31. Hribar, K.C., et al., *Light-Induced Temperature Transitions in Biodegradable Polymer and Nanorod Composites*. Small, 2009. **5**(16): p. 1830-1834.
32. Long, K.N., et al., *Photomechanics of light-activated polymers*. Journal Of The Mechanics And Physics Of Solids, 2009. **57**(7): p. 1103-1121.
33. Lendlein, A., H.Y. Jiang, and S. Kelch, *Polymers move in response to light*. Advanced Materials, 2006. **18**(11): p. 1471-1475.
34. Yu, Y.L. and T. Ikeda, *Photodeformable polymers: A new kind of promising smart material for micro- and nano-applications*. Macromolecular Chemistry and Physics, 2005. **206**(17): p. 1705-1708.

REFERENCES

35. Keum, C.D., et al., *Photodeformation behavior of photodynamic polymers bearing azobenzene moieties in their main and/or side chain*. *Macromolecules*, 2003. **36**(13): p. 4916-4923.
36. Seki, T., *Dynamic photoresponsive functions in organized layer systems comprised of azobenzene-containing polymers*. *Polymer Journal*, 2004. **36**(6): p. 435-454.
37. Seki, T., et al., *Nanostructure of a photochromic polymer/liquid crystal hybrid monolayer on a water surface observed by in situ X-ray reflectometry*. *Langmuir*, 2002. **18**(10): p. 3875-3879.
38. Yamamura, M., et al., *Light-tunable solvent drying in photo-responsive solution coatings*. *Drying Technology*, 2008. **26**(1): p. 97-100.
39. Yu, Y.L. and T. Ikeda, *Soft actuators based on liquid-crystalline elastomers*. *Angewandte Chemie-International Edition*, 2006. **45**(33): p. 5416-5418.
40. Ikeda, T., et al., *Precisely direction-controllable bending of cross-linked liquid-crystalline polymer films by light*. *Molecular Crystals and Liquid Crystals*, 2005. **436**: p. 1235-1244.
41. Ikeda, T., J. Mamiya, and Y.L. Yu, *Photomechanics of liquid-crystalline elastomers and other polymers*. *Angewandte Chemie-International Edition*, 2007. **46**(4): p. 506-528.
42. Ikeda, T., et al., *Effect of concentration of photoactive chromophores on photomechanical properties of crosslinked azobenzene liquid-crystalline polymers*. *Journal of Materials Chemistry*, 2010. **20**(1): p. 117-122.
43. Fredin, L.A., *Shape changing polymers*. *Abstracts of Papers of the American Chemical Society*, 2007. **233**: p. 691-691.
44. Yu, Y.L., M. Nakano, and T. Ikeda, *Directed bending of a polymer film by light - Miniaturizing a simple photomechanical system could expand its range of applications*. *nature*, 2003. **425**(6954): p. 145-145.
45. Camacho-Lopez, M., et al., *Fast liquid-crystal elastomer swims into the dark*. *Nature Materials*, 2004. **3**(5): p. 307-310.
46. Zhao, Y., et al., *Photoactive thermoplastic elastomers of azobenzene-containing triblock copolymers prepared through atom transfer radical polymerization*. *Macromolecules*, 2004. **37**(19): p. 7097-7104.
47. Ilnytskyi, J., M. Saphiannikova, and D. Neher, *Photo-induced deformations in azobenzene-containing side-chain polymers: molecular dynamics study*. *Condensed Matter Physics*, 2006. **9**(1): p. 87-94.
48. Endo, T., et al., *Anisotropic photomechanical response of stretched blend film made of polycaprolactone-polyvinyl ether with azobenzene group as side chain*. *Macromolecular Chemistry and Physics*, 2008. **209**(20): p. 2071-2077.
49. Winzek, B., et al., *Recent developments in shape memory thin film technology*. *Materials Science And Engineering A*, 2004. **378**(1-2): p. 40-46.
50. Tobushi, H., et al., *Fabrication and two-way deformation of shape memory composite with SMA and SMP*. *Materials Science Forum*, 2010. **638-642**: p. 2189-2194.

REFERENCES

51. Tobushi, H., et al., *Performance of shape memory composite with SMA and SMP*. Smart Materials for Smart Devices and Structures, 2009. **154**: p. 65-70.
52. Tobushi, H., et al., *Shape Memory Composite with Sma and Smp*. Smst-2007: Proceedings of the International Conference on Shape Memory and Superelastic Technologies, 2008: p. 123-130.
53. Tobushi, H., et al., *Bending actuation characteristics of shape memory composite with SMA and SMP*. Journal Of Intelligent Material Systems And Structures, 2006. **17**(12): p. 1075-1081.
54. Chen, Y.C. and D.C. Lagoudas, *A constitutive theory for shape memory polymers. Part II - A linearized model for small deformations*. Journal Of The Mechanics And Physics Of Solids, 2008. **56**(5): p. 1766-1778.
55. Hu, J.L., S.J. Chen, and H.T. Zhuo, *Properties and mechanism of two-way shape memory polyurethane composites*. Composites Science and Technology, 2010. **70**(10): p. 1437-1443.
56. Qi, H.J., et al., *Two-way reversible shape memory effects in a free-standing polymer composite*. Smart Materials & Structures, 2011. **20**: p. 065010/1-9.
57. Bellin, I., et al., *Polymeric triple-shape materials*. Proceedings Of The National Academy Of Sciences Of The United States Of America, 2006. **103**(48): p. 18043-18047.
58. Luo, X.F. and P.T. Mather, *Triple-shape polymeric composites (TSPCs)*. Advanced Functional Materials, 2010. **20**(16): p. 2649-2656.
59. Zotzmann, J., et al., *Reversible triple-shape effect of polymer networks containing polypentadecalactone- and poly(epsilon-caprolactone)-segments*. Advanced Materials, 2010. **22**(31): p. 3424-3429.
60. Xie, T., X.C. Xiao, and Y.T. Cheng, *Revealing triple-shape memory effect by polymer bilayers*. Macromolecular Rapid Communications, 2009. **30**(21): p. 1823-1827.
61. Bellin, I., S. Kelch, and A. Lendlein, *Dual-shape properties of triple-shape polymer networks with crystallizable network segments and grafted side chains*. Journal of Materials Chemistry, 2007. **17**(28): p. 2885-2891.
62. Behl, M. and A. Lendlein, *Triple-shape polymers*. Journal of Materials Chemistry, 2010. **20**(17): p. 3335-3345.
63. Zotzmann, J., et al., *Copolymer networks based on poly(omega-pentadecalactone) and poly(epsilon-caprolactone) segments as a versatile triple-shape polymer system*. Advanced Functional Materials, 2010. **20**(20): p. 3583-3594.
64. Behl, M., et al., *One-step process for creating triple-shape capability of AB polymer networks*. Advanced Functional Materials, 2009. **19**(1): p. 102-108.
65. Kolesov, I.S. and H.J. Radusch, *Multiple shape-memory behavior and thermal-mechanical properties of peroxide cross-linked blends of linear and short-chain branched polyethylenes*. Express Polymer Letters, 2008. **2**(7): p. 461-473.
66. Chen, S.J., et al., *Triple shape memory effect in multiple crystalline polyurethanes*. Polymers for Advanced Technologies, 2010. **21**(5): p. 377-380.

REFERENCES

67. Pretsch, T., *Triple-shape properties of a thermoresponsive poly(ester urethane)*. *Smart Materials & Structures*, 2010. **19**(1): p. 015006/1-7.
68. Pretsch, T., *Durability of a polymer with triple-shape properties*. *Polymer Degradation And Stability*, 2010. **95**(12): p. 2515-2524.
69. Qin, H.H. and P.T. Mather, *Combined one-way and two-way shape memory in a glass-forming nematic network*. *Macromolecules*, 2009. **42**(1): p. 273-280.
70. Kumar, U.N., et al., *Non-contact actuation of triple-shape effect in multiphase polymer network nanocomposites in alternating magnetic field*. *Journal of Materials Chemistry*, 2010. **20**(17): p. 3404-3415.
71. Luo, H.S., J.L. Hu, and Y. Zhu, *Polymeric Shape Memory Nanocomposites with Heterogeneous Twin Switches*. *Macromolecular Chemistry and Physics*, 2011. **212**(18): p. 1981-1986.
72. Wang, L., et al., *Multi-stimuli sensitive shape memory poly(vinyl alcohol)-graft-polyurethane*. *Polymer Chemistry*, 2013. **4**(16): p. 4461-4468.
73. Wu, Y., et al., *A facile approach to fabricate a UV/heat dual-responsive triple shape memory polymer*. *Journal of Materials Chemistry A*, 2015. **3**(1): p. 97-100.
74. Wang, S.Q., et al., *Hyperbranched Polycoumarates with Photofunctional Multiple Shape Memory*. *Angewandte Chemie-International Edition*, 2013. **52**(42): p. 11143-11148.
75. Zeng, C., et al., *Polymers with Multishape Memory Controlled by Local Glass Transition Temperature*. *Acs Applied Materials & Interfaces*, 2014. **6**(4): p. 2753-2758.
76. Razzaq, M.Y., et al., *Triple-Shape Effect in Polymer-Based Composites by Cleverly Matching Geometry of Active Component with Heating Method*. *Advanced Materials*, 2013. **25**(38): p. 5514-5518.
77. Xie, T., *Tunable polymer multi-shape memory effect*. *Nature*, 2010. **464**(7286): p. 267-270.
78. Yang, X.F., et al., *Triple Shape Memory Effect of Star-Shaped Polyurethane*. *Acs Applied Materials & Interfaces*, 2014. **6**(9): p. 6545-6554.
79. Wang, Y.R., et al., *Relation between temperature memory effect and multiple-shape memory behaviors based on polymer networks*. *Rsc Advances*, 2014. **4**(39): p. 20364-20370.
80. Samuel, C., et al., *Designing Multiple-Shape Memory Polymers with Miscible Polymer Blends: Evidence and Origins of a Triple-Shape Memory Effect for Miscible PLLA/PMMA Blends*. *Macromolecules*, 2014. **47**(19): p. 6791-6803.
81. Nochel, U., et al., *Triple-Shape Effect with Adjustable Switching Temperatures in Crosslinked Poly[ethylene-co-(vinyl acetate)]*. *Macromolecular Chemistry and Physics*, 2014. **215**(24): p. 2446-2456.
82. Hoehner, R., et al., *Tunable Multiple-Shape Memory Polyethylene Blends*. *Macromolecular Chemistry and Physics*, 2013. **214**(23): p. 2725-2732.
83. Shao, Y., C. Lavigueur, and X.X. Zhu, *Multishape Memory Effect of Norbornene-Based Copolymers with Cholic Acid Pendant Groups*. *Macromolecules*, 2012. **45**(4): p. 1924-1930.

REFERENCES

84. Gong, T., et al., *Thermally activated reversible shape switch of polymer particles*. Journal of Materials Chemistry B, 2014. **2**(39): p. 6855-6866.
85. Zhou, J., et al., *Shapeshifting: Reversible Shape Memory in Semicrystalline Elastomers*. Macromolecules, 2014. **47**(5): p. 1768-1776.
86. Wu, Y., et al., *Two-way shape memory polymer with "switch-spring" composition by interpenetrating polymer network*. Journal of Materials Chemistry A, 2014. **2**(44): p. 18816-18822.
87. Bothe, M. and T. Pretsch, *Bidirectional actuation of a thermoplastic polyurethane elastomer*. Journal of Materials Chemistry A, 2013. **1**(46): p. 14491-14497.
88. Yao, X., et al., *Fluorogel Elastomers with Tunable Transparency, Elasticity, ShapeMemory, and Antifouling Properties***. Angewandte Chemie-International Edition, 2014. **53**(17): p. 4418-4422.
89. Mondal, S. and J.L. Hu, *Water vapor permeability of cotton fabrics coated with shape memory polyurethane*. Carbohydrate Polymers, 2007. **67**(3): p. 282-287.
90. Takashima, K., et al., *Pneumatic artificial rubber muscle using shape-memory polymer sheet with embedded electrical heating wire*. Smart Materials and Structures, 2014. **23**(12).
91. Rossiter, J., et al., *Shape memory polymer hexachiral auxetic structures with tunable stiffness*. Smart Materials and Structures, 2014. **23**(4).
92. Chen, C.M. and S. Yang, *Directed Water Shedding on High-Aspect-Ratio Shape Memory Polymer Micropillar Arrays*. Advanced Materials, 2014. **26**(8): p. 1283-1288.
93. Sarwate, P., et al., *Controllable strain recovery of shape memory polystyrene to achieve superhydrophobicity with tunable adhesion*. Journal of Micromechanics and Microengineering, 2014. **24**(11).
94. Kunzelman, J., et al., *Shape memory polymers with built-in threshold temperature sensors*. Journal of Materials Chemistry, 2008. **18**(10): p. 1082-1086.
95. Ecker, M. and T. Pretsch, *Multifunctional poly(ester urethane) laminates with encoded information*. Rsc Advances, 2014. **4**(1): p. 286-292.
96. Torbati, A.H., et al., *Fabrication of a light-emitting shape memory polymeric web containing indocyanine green*. Journal of Biomedical Materials Research Part B-Applied Biomaterials, 2014. **102**(6): p. 1236-1243.
97. Wu, Y., et al., *Memory Chromic Polyurethane with Tetraphenylethylene*. Journal of Polymer Science Part B-Polymer Physics, 2014. **52**(2): p. 104-110.
98. Li, J., et al., *Switching periodic membranes via pattern transformation and shape memory effect*. Soft Matter, 2012. **8**(40): p. 10322-10328.
99. Zheng, Y.W., et al., *Light-induced shape recovery of deformed shape memory polymer micropillar arrays with gold nanorods*. Rsc Advances, 2015. **5**(39): p. 30495-30499.
100. Espinha, A., et al., *Shape-memory effect for self-healing and biodegradable photonic systems*. Photonic Crystal Materials and Devices Xi, 2014. **9127**.

REFERENCES

101. Xu, H.X., et al., *Deformable, Programmable, and Shape-Memorizing Micro-Optics*. *Advanced Functional Materials*, 2013. **23**(26): p. 3299-3306.
102. Espinha, A., et al., *Thermoresponsive Shape-Memory Photonic Nanostructures*. *Advanced Optical Materials*, 2014. **2**(6): p. 516-521.
103. Alteheld, A., et al., *Biodegradable, amorphous copolyester-urethane networks having shape-memory properties*. *Angewandte Chemie-International Edition*, 2005. **44**(8): p. 1188-1192.
104. Zhang, X.M., et al., *Biodegradable shape memory nanocomposites with thermal and magnetic field responsiveness*. *Journal of Biomaterials Science-Polymer Edition*, 2013. **24**(9): p. 1057-1070.
105. Gong, T., et al., *Remotely actuated shape memory effect of electrospun composite nanofibers*. *Acta Biomaterialia*, 2012. **8**(3): p. 1248-1259.
106. Zhang, H.J., H.S. Xia, and Y. Zhao, *Optically triggered and spatially controllable shape-memory polymer-gold nanoparticle composite materials*. *Journal of Materials Chemistry*, 2012. **22**(3): p. 845-849.
107. Han, J.J., et al., *High Intensity Focused Ultrasound Triggered Shape Memory and Drug Release from Biodegradable Polyurethane*. *Macromolecular Chemistry and Physics*, 2013. **214**(11): p. 1195-1203.
108. Wang, L., et al., *Tunable Temperature Memory Effect of Photo-Cross-Linked Star PCL-PEG Networks*. *Macromolecules*, 2014. **47**(5): p. 1828-1836.
109. Zhu, Y., J. Hu, and K. Yeung, *Effect of soft segment crystallization and hard segment physical crosslink on shape memory function in antibacterial segmented polyurethane ionomers*. *Acta Biomaterialia*, 2009. **5**(9): p. 3346-3357.
110. Zhuo, H.T., J.L. Hu, and S.J. Chen, *Coaxial electrospun polyurethane core-shell nanofibers for shape memory and antibacterial nanomaterials*. *Express Polymer Letters*, 2011. **5**(2): p. 182-187.
111. Li, J.H., et al., *Shape-memory effects in polymer networks containing reversibly associating side-groups*. *Advanced Materials*, 2007. **19**(19): p. 2851-2855.
112. Zhu, Y., J.L. Hu, and Y.J. Liu, *Shape memory effect of thermoplastic segmented polyurethanes with self-complementary quadruple hydrogen bonding in soft segments*. *European Physical Journal E*, , 2009. **28**: p. 3-10.
113. Ware, T., et al., *Triple-Shape Memory Polymers Based on Self-Complementary Hydrogen Bonding*. *Macromolecules*, 2012. **45**(2): p. 1062-1069.
114. Luo, H.Y., et al., *Novel Biodegradable Shape Memory Material Based on Partial Inclusion Complex Formation between alpha-Cyclodextrin and Poly(epsilon-caprolactone)*. *Biomacromolecules*, 2008. **9**: p. 2573-2577.
115. Zhang, S., et al., *A Novel Supramolecular Shape Memory Material Based on Partial alpha-CD-PEG Inclusion Complex*. *Polymer*, 2008. **49**: p. 3205-3210.
116. Luo, H.Y., et al., *Preparation and Properties of Degradable Shape Memory Material Based on Partial alpha-Cyclodextrin-Poly(epsilon-*

REFERENCES

- caprolactone) Inclusion Complex*. *Macromolecular Chemistry and Physics*, 2009. **210**: p. 669-676.
117. Fan, M.M., et al., *Supramolecular network based on the self-assembly of gamma-cyclodextrin with poly(ethylene glycol) and its shape memory effect*. *Macromolecular Rapid Communications*, 2009. **30**: p. 89-903.
 118. Barry Van Gemert, M., M. Anu Chopra, and P. Anil Kumar, all of Pa, *polymerizable polyalkoxylated naphthopyrans*, U.S. Patent, Editor. 2000, Transitions Optical, Inc., Pinellas Park, Fla.
 119. Burnworth, M., et al., *Optically healable supramolecular polymers*. *Nature*, 2011. **472**(7343): p. 334-U230.
 120. Coulibaly, S., et al., *Reinforcement of Optically Healable Supramolecular Polymers with Cellulose Nanocrystals*. *Macromolecules*, 2014. **47**(1): p. 152-160.
 121. Yang, W.W., et al., *Tuning of Redox Potentials by Introducing a Cyclometalated Bond to Bis-tridentate Ruthenium(II) Complexes Bearing Bis(N-methylbenzimidazolyl)benzene or -pyridine Ligands*. *Inorganic Chemistry*, 2012. **51**(2): p. 890-899.
 122. Pardinan-Blanco, I., et al., *Control on the dispersion of gold nanoparticles in an epoxy network*. *Journal of Non-Crystalline Solids*, 2007. **353**(8-10): p. 826-828.
 123. Luo, N., D.N. Wang, and S.K. Ying, *Crystallinity of Hard and Hydrogen Bonding Segments in Segmented Poly(urethane urea) Copolymers*. *Polymer*, 1996. **37**: p. 3577-3583.
 124. Seymour, R.W., A.E.A. Jr., and S.L. Cooper, *Segmental Orientation Studies of Block Polymers. I. Hydrogen-Bonded Polyurethanes*. *Macromolecules*, 1973. **6**: p. 896-902.
 125. Luo, N., D.N. Wang, and S.K. Ying, *Hydrogen-Bonding Properties of Segmented Polyether Poly(urethane urea) Copolymer*. *Macromolecules*, 1997. **30**: p. 4405-4409.
 126. He, Z.W., et al., *Remote Controlled Multishape Polymer Nanocomposites with Selective Radiofrequency Actuators*. *Advanced Materials*, 2011. **23**(28): p. 3192-3196.
 127. Cheng, K.H., et al., *Fabrication of and Ultraviolet Lasing in TPE/PMMA Polymer Nanowires*. *Journal of Physical Chemistry C*, 2008. **112**(45): p. 17507-17511.
 128. Hu, J.L., et al., *Recent Advances in Shape-Memory Polymers: Structure, Mechanism, Functionality, Modeling and Applications*. *Progress in Polymer Science*.
 129. Meng, Q.H. and J.L. Hu, *A poly(ethylene glycol)-based smart phase change material*. *Solar Energy Materials and Solar Cells*, 2008. **92**(10): p. 1260-1268.
 130. Yan, X.Z., et al., *A Multiresponsive, Shape-Persistent, and Elastic Supramolecular Polymer Network Gel Constructed by Orthogonal Self-Assembly*. *Advanced Materials*, 2012. **24**(3): p. 362-+.
 131. Neffe, A.T., et al., *Polymer Networks Combining Controlled Drug Release, Biodegradation, and Shape Memory Capability*. *Advanced Materials*, 2009. **21**(32-33): p. 3394-3398.
 132. Behl, M., M.Y. Razaq, and A. Lendlein, *Multifunctional shape-memory polymers*. *Advanced Materials*, 2010. **22**(31): p. 3388-3410.

REFERENCES

133. Cho, S.Y., J.G. Kim, and C.M. Chung, *A fluorescent crack sensor based on cyclobutane-containing crosslinked polymers of tricinnamates*. *Sensors and Actuators B-Chemical*, 2008. **134**(2): p. 822-825.
134. Loh, K.J., et al., *Carbon Nanotube Sensing Skins for Spatial Strain and Impact Damage Identification*. *Journal of Nondestructive Evaluation*, 2009. **28**(1): p. 9-25.
135. Chung, D.D.L., *Damage in cement-based materials, studied by electrical resistance measurement*. *Materials Science & Engineering R-Reports*, 2003. **42**(1): p. 1-40.
136. Zhao, Z.J., et al., *Full emission color tuning in luminogens constructed from tetraphenylethene, benzo-2,1,3-thiadiazole and thiophene building blocks*. *Chemical Communications*, 2011. **47**(31): p. 8847-8849.
137. Zhao, Z.J., et al., *Aggregation-induced emission, self-assembly, and electroluminescence of 4,4'-bis(1,2,2-triphenylvinyl)biphenyl*. *Chemical Communications*, 2010. **46**(5): p. 686-688.
138. Zhao, Z.J., et al., *Creation of highly efficient solid emitter by decorating pyrene core with AIE-active tetraphenylethene peripheries*. *Chemical Communications*, 2010. **46**(13): p. 2221-2223.
139. Qin, A., J.W.Y. Lam, and B.Z. Tang, *Luminogenic polymers with aggregation-induced emission characteristics*. *Progress in Polymer Science*, 2012. **37**(1): p. 182-209.
140. Upamali, K.A.N., L.A. Estrada, and D.C. Neckers, *Selective detection of Cr(VI) in aqueous media by carbazole-based fluorescent organic microcrystals*. *Analytical Methods*, 2011. **3**(11): p. 2469-2471.
141. Zhang, X.Q., et al., *Piezofluorochromism of an Aggregation-Induced Emission Compound Derived from Tetraphenylethylene*. *Chemistry-an Asian Journal*, 2011. **6**(3): p. 808-811.
142. Wang, J., et al., *Hyperbranched polytriazoles with high molecular compressibility: aggregation-induced emission and superamplified explosive detection*. *Journal of Materials Chemistry*, 2011. **21**(12): p. 4056-4059.
143. Yuan, W.Z., et al., *Towards high efficiency solid emitters with aggregation-induced emission and electron-transport characteristics*. *Chemical Communications*, 2011. **47**(40): p. 11216-11218.
144. Zhu, Y., et al., *Rapidly switchable water-sensitive shape-memory cellulose/elastomer nano-composites*. *Soft Matter*, 2012. **8**(8): p. 2509-2517.
145. Kumar, U.N., et al., *Shape-Memory Nanocomposites with Magnetically Adjustable Apparent Switching Temperatures*. *Advanced Materials*, 2011. **23**(36): p. 4157-+.
146. Razzaq, M.Y., M. Behl, and A. Lendlein, *Magnetic Memory Effect of Nanocomposites*. *Advanced Functional Materials*, 2012. **22**(1): p. 184-191.
147. Chen, S.J., et al., *Novel moisture-sensitive shape memory polyurethanes containing pyridine moieties*. *Polymer*, 2009. **50**(19): p. 4424-4428.

REFERENCES

148. Ebara, M., et al., *Shape-Memory Surface with Dynamically Tunable Nano-Geometry Activated by Body Heat*. *Advanced Materials*, 2012. **24**(2): p. 273-278.
149. Ji, F.L., J.L. Hu, and S.S.Y. Chui, *Influences of phase composition and thermomechanical conditions on shape memory properties of segmented polyurethanes with amorphous reversible phase*. *Polymer Engineering and Science*, 2012. **52**(5): p. 1015-1026.
150. Tosin, M., F. Degli-Innocenti, and C. Bastioli, *Detection of a toxic product released by a polyurethane-containing film using a composting test method based on a mineral bed*. *Journal of Environmental Polymer Degradation*, 1998. **6**(2): p. 79-90.
151. Leng, J.S., et al., *Shape-memory polymers and their composites: Stimulus methods and applications*. *Progress in Materials Science*, 2011. **56**(7): p. 1077-1135.
152. Ratna, D. and J. Karger-Kocsis, *Shape memory polymer system of semi-interpenetrating network structure composed of crosslinked poly (methyl methacrylate) and poly (ethylene oxide)*. *Polymer*, 2011. **52**(4): p. 1063-1070.
153. Liu, G.Q., et al., *Shape-memory behavior of poly (methyl methacrylate-co -N-vinyl-2-pyrrolidone)/poly (ethylene glycol) semi-interpenetrating polymer networks based on hydrogen bonding*. *Journal of Polymer Research*, 2011. **18**(6): p. 2109-2117.
154. Liu, G.Q., et al., *Novel shape-memory polymer with two transition temperatures*. *Macromolecular Rapid Communications*, 2005. **26**(8): p. 649-652.
155. Feng, Y.K., et al., *Degradable depsipeptide-based multiblock copolymers with polyester or polyetherester segments*. *International Journal of Artificial Organs*, 2011. **34**(2): p. 103-109.
156. Park, Y.H., K.Y. Kim, and M.H. Han, *Preparation and properties of highly functional copolyetheresters*. *Journal of Applied Polymer Science*, 2003. **88**(1): p. 139-145.
157. Pandini, S., et al., *One-way and two-way shape memory behaviour of semi-crystalline networks based on sol-gel cross-linked poly(epsilon-caprolactone)*. *Polymer*, 2013. **54**(16): p. 4253-4265.
158. Chen, E.C. and T.M. Wu, *Isothermal crystallization kinetics and thermal behavior of poly(epsilon-caprolactone)/multi-walled carbon nanotube composites*. *Polymer Degradation and Stability*, 2007. **92**(6): p. 1009-1015.
159. Bontempi, E., et al., *Laboratory two-dimensional X-ray microdiffraction technique: a support for authentication of an unknown Ghirlandaio painting*. *Applied Physics a-Materials Science & Processing*, 2008. **92**(1): p. 155-159.
160. Zhao, Y., D. Keroack, and R. Prud'homme, *Crystallization under strain and resultant orientation of poly(epsilon-caprolactone) in miscible blends*. *Macromolecules*, 1999. **32**(4): p. 1218-1225.
161. Raquez JM, V.S., Meyer F, Verge P, Alexandre M, Thomassin JM, and e. al., *Chem Eur J*, 2011. **17**: p. 10135-43.
162. Xie, T., *Recent advances in polymer shape memory*. *Polymer*, 2011. **52**(22): p. 4985-5000.

REFERENCES

163. Wu, Y.H., J.L.; Han, J.; Zhu, Y.; Huang, H.; Li, J.; Tang, B. Z., *J. Mater. Chem. A*, 2014: p. DOI: 10.1039/C4TA03640A.
164. Chen, S.J., et al., *Development of liquid-crystalline shape-memory polyurethane composites based on polyurethane with semi-crystalline reversible phase and hexadecyloxybenzoic acid for self-healing applications*. *Journal of Materials Chemistry C*, 2014. **2**(21): p. 4203-4212.
165. Bai, Y.K., et al., *Poly(vinyl butyral) based polymer networks with dual-responsive shape memory and self-healing properties*. *Journal of Materials Chemistry A*, 2014. **2**(24): p. 9169-9177.
166. Bai, Y.K., et al., *A tough shape memory polymer with triple-shape memory and two-way shape memory properties*. *Journal of Materials Chemistry A*, 2014. **2**(13): p. 4771-4778.
167. Liu, Y.J., et al., *Shape memory polymers and their composites in aerospace applications: a review*. *Smart Materials and Structures*, 2014. **23**(2).
168. Iqbal, D. and M.H. Samiullah, *Photo-Responsive Shape-Memory and Shape-Changing Liquid-Crystal Polymer Networks*. *Materials*, 2013. **6**(1): p. 116-142.
169. Zhang, H.J. and Y. Zhao, *Polymers with Dual Light-Triggered Functions of Shape Memory and Healing Using Gold Nanoparticles*. *ACS Applied Materials & Interfaces*, 2013. **5**(24): p. 13069-13075.
170. Zhang, H.J., H.S. Xia, and Y. Zhao, *Light-Controlled Complex Deformation and Motion of Shape-Memory Polymers Using a Temperature Gradient*. *ACS Macro Letters*, 2014. **3**(9): p. 940-943.
171. Kumpfer, J.R. and S.J. Rowan, *Thermo-, Photo-, and Chemo-Responsive Shape-Memory Properties from Photo-Cross-Linked Metallo-Supramolecular Polymers*. *Journal of the American Chemical Society*, 2011. **133**(32): p. 12866-12874.
172. Wang, W.X., et al., *Sodium dodecyl sulfate/epoxy composite: water-induced shape memory effect and its mechanism*. *Journal of Materials Chemistry A*, 2014. **2**(15): p. 5441-5449.
173. Xie, T. and X.C. Xiao, *Self-peeling reversible dry adhesive system*. *Chemistry of Materials*, 2008. **20**(9): p. 2866-2868.
174. Rousseau, I.A. and T. Xie, *Shape memory epoxy: Composition, structure, properties and shape memory performances*. *Journal of Materials Chemistry*, 2010. **20**(17): p. 3431-3441.
175. Meng, Q.H., et al., *Polycaprolactone-based shape memory segmented polyurethane fiber*. *Journal of Applied Polymer Science*, 2007. **106**(4): p. 2515-2523.
176. Baker, R.M., J.H. Henderson, and P.T. Mather, *Shape memory poly(epsilon-caprolactone)-co-poly(ethylene glycol) foams with body temperature triggering and two-way actuation*. *Journal of Materials Chemistry B*, 2013. **1**(38): p. 4916-4920.
177. Wagermaier, W., et al., *Characterization Methods for Shape-Memory Polymers*. *Shape-Memory Polymers*, 2010. **226**: p. 97-145.
178. Sambe, L., et al., *Programmable Polymer- Based Supramolecular Temperature Sensor with a Memory Function***. *Angewandte Chemie-International Edition*, 2014. **53**(20): p. 5044-5048.

REFERENCES

179. Wang, Z., et al., *Programmable, pattern-memorizing polymer surface*. *Advanced Materials*, 2011. **23**(32): p. 3669-3373.
180. Wu, Y., Hu, J.L.; Han, J.; Zhu, Y.; Huang, H.; Li, J.; Tang, B. Z., *Two-way shape memory polymer with "switch-spring" composition by interpenetrating polymer network*. *J. Mater. Chem. A*, 2014. **2**.
181. Luo, Y.W., et al., *A General Approach Towards Thermoplastic Multishape-Memory Polymers via Sequence Structure Design*. *Advanced Materials*, 2013. **25**(5): p. 743-748.
182. Wischke, C., M. Schossig, and A. Lendlein, *Shape-Memory Effect of Micro-/Nanoparticles from Thermoplastic Multiblock Copolymers*. *Small*, 2014. **10**(1): p. 83-87.
183. Wu Y., H.J.L., Zhang C., Han J., Wang Y. and Bipin K., *A facile approach to fabricate a UV/heat dual-responsive triple shape memory polymer*. *J. Mater. Chem. A*, 2015: p. DOI: 10.1039/C4TA04881D.
184. Chen, H.M., et al., *Use of intermolecular hydrogen bonding to synthesize triple-shape memory supermolecular composites*. *Rsc Advances*, 2013. **3**(19): p. 7048-7056.
185. Chen, Y., et al., *The polyurethane membranes with temperature sensitivity for water vapor permeation*. *Journal of Membrane Science*, 2007. **287**(2): p. 192-197.
186. Duan, Z., N.L. Thomas, and W. Huang, *Water vapour permeability of poly(lactic acid) nanocomposites*. *Journal of Membrane Science*, 2013. **445**: p. 112-118.
187. Lavric, P.K., M.M.C.G. Warmoeskerken, and D. Jovic, *Functionalization of cotton with poly-NiPAAm/chitosan microgel. Part I. Stimuli-responsive moisture management properties*. *Cellulose*, 2012. **19**(1): p. 257-271.
188. Lin, C.Y., et al., *Smart temperature-controlled water vapor permeable polyurethane film*. *Journal of Membrane Science*, 2007. **299**(1-2): p. 91-96.
189. Lomax, G.R., *Breathable polyurethane membranes for textile and related industries*. *Journal of Materials Chemistry*, 2007. **17**(27): p. 2775-2784.
190. Ding, X.M., et al., *Preparation of temperature-sensitive polyurethanes for smart textiles*. *Textile Research Journal*, 2006. **76**(5): p. 406-413.
191. Ding, X.M., et al., *Free volume and water vapor transport properties of temperature-sensitive polyurethanes*. *Journal of Polymer Science Part B-Polymer Physics*, 2005. **43**(14): p. 1865-1872.
192. Zhuo, H.T., J.L. Hu, and S.J. Chen, *Study of water vapor permeability of shape memory polyurethane nanofibrous nonwovens*. *Textile Research Journal*, 2011. **81**(9): p. 883-891.
193. Mondal, S., J.L. Hu, and Z. Yong, *Free volume and water vapor permeability of dense segmented polyurethane membrane*. *Journal of Membrane Science*, 2006. **280**(1-2): p. 427-432.
194. Mondal, S. and J.L. Hu, *Structural characterization and mass transfer properties of nonporous-segmented polyurethane membrane: Influence of the hydrophilic segment content and soft segment melting temperature*. *Journal of Membrane Science*, 2006. **276**(1-2): p. 16-22.

REFERENCES

195. Mondal, S. and J.L. Hu, *Structural characterization and mass transfer properties of nonporous segmented polyurethane membrane: Influence of hydrophilic and carboxylic group*. Journal of Membrane Science, 2006. **274**(1-2): p. 219-226.
196. Mondal, S. and J.L. Hu, *Influence of hard segment on thermal degradation of thermoplastic segmented polyurethane for textile coating application*. Polymer-Plastics Technology and Engineering, 2007. **46**(1): p. 37-41.
197. Wang, Z.F., et al., *Water-vapor permeability of hydrophilic polyurethanes studied by positron annihilation*. Chemical Journal of Chinese Universities-Chinese, 2004. **25**(10): p. 1953-1957.
198. Wang, Z.F., et al., *Free volume and water vapor permeability properties in polyurethane membranes studied by positrons*. Materials Chemistry and Physics, 2004. **88**(1): p. 212-216.